

Control of steel flow through the casting nozzle and within the mould is an important determinant of steel cleanliness and surface quality. Techniques including visualisation of steel flow in the nozzle using electromagnetic, ultrasonic and thermal sensors in combination with the measurement of steel flow velocities and distribution in the mould allow project partners Corus RD & T, Sidenor I + D, BFI, Saarstahl and MEFOS to develop a physical picture of the steel flow behaviour during the casting process, including effects such as nozzle clogging and flow asymmetry/biased flow.

In addition, a full-scale physical model of a slab caster has been designed and manufactured using a low-temperature liquid metal to simulate the casting process.

Work has been carried out using these techniques to correlate with existing data, product grading schemes and both product cleanliness and surface quality. An assessment has been made of the influence of flow pattern in the SEN and mould on solidification.

A study was made of reasons for changes observed in flow patterns, including determination of why flow patterns change during stable casting. An investigation into the influence of casting parameters on clogging and wear has been carried out, including criteria for monitoring the condition of the nozzle during casting.

From these assessments recommendations have been made for process optimisation. These include the control of flow pattern in the SEN, optimisation of SEN immersion depth and online monitoring of clogging.

A comparison was made between the various techniques, indicating their capability and limitations.

Price (excluding VAT) in Luxembourg: EUR 7



Publications Office

ISBN 978-92-79-14429-5



9 789279 144295

KI-NA-24205-EN-C

EC



EUROPEAN  
COMMISSION

European  
Research Area

Flowvis: measurement, prediction and control of steel flows in the casting nozzle and mould

EUR 24205

# Flowvis: measurement, prediction and control of steel flows in the casting nozzle and mould



## Interested in European research?

**RTD info** is our quarterly magazine keeping you in touch with main developments (results, programmes, events, etc.). It is available in English, French and German. A free sample copy or free subscription can be obtained from:

Directorate-General for Research  
Information and Communication Unit  
European Commission  
B-1049 Brussels  
Fax (32-2) 29-58220  
E-mail: [research@ec.europa.eu](mailto:research@ec.europa.eu)  
Internet: [http://ec.europa.eu/research/rtdinfo/index\\_en.html](http://ec.europa.eu/research/rtdinfo/index_en.html)

## How to obtain EU publications

### Free publications:

- via EU Bookshop (<http://bookshop.europa.eu>);
- at the European Commission's representations or delegations.  
You can obtain their contact details by linking <http://ec.europa.eu> or by sending a fax to +352 2929-42758.

### Publications for sale:

- via EU Bookshop (<http://bookshop.europa.eu>);
- Priced subscriptions (Official Journal of the EU, Legal cases of the Court of Justice as well as certain periodicals edited by the European Commission) can be ordered from one of our sales agents.  
You can obtain their contact details by linking <http://bookshop.europa.eu>, or by sending a fax to +352 2929-42758.

EUROPEAN COMMISSION  
Directorate-General for Research  
Research Fund for Coal and Steel Unit

Contact: *RFCS publications*  
Address: *European Commission, CDMA 0/124, B-1049 Brussels*  
Fax (32-2) 29-65987; e-mail: [rtd-steel@ec.europa.eu](mailto:rtd-steel@ec.europa.eu)

European Commission

# Research Fund for Coal and Steel

## Flowvis: measurement, prediction and control of steel flows in the casting nozzle and mould

S. R. Higson, P. Drake, M. Lewus

**Corus UK Ltd**

Teesside Technology Centre, PO Box 11, Grangetown, Middlesbrough, TS6 6US, UNITED KINGDOM

T. Lamp, H. Köchner

**Betriebsforschungsinstitut (BFI), Stahlinstitut VDEh**

Postfach 105145, 40042 Düsseldorf, GERMANY

P. Valentin, C. Bruch

**Saarstahl AG**

Bismarckstraße 57-59, 66333, Völklingen, GERMANY

J. Ciriza, J. J. Lauraudogoitia

**Sidenor I + D)**

Barrio Ugarte s/n, 48970 Basauri, SPAIN

J. Björkvall, L. Bergman

**MEFOS**

Box 812, SE-971 25, Luleå, SWEDEN

Contract No RFSR-CT-2004-00011

1 July 2004 to 30 June 2008

**Final report**

Directorate-General for Research

## LEGAL NOTICE

Neither the European Commission nor any person acting on behalf of the Commission is responsible for the use which might be made of the following information.

***Europe Direct is a service to help you find answers  
to your questions about the European Union***

**Freephone number (\*):  
00 800 6 7 8 9 10 11**

(\* Certain mobile telephone operators do not allow access to 00 800 numbers or these calls may be billed.

A great deal of additional information on the European Union is available on the Internet. It can be accessed through the Europa server (<http://europa.eu>).

Cataloguing data can be found at the end of this publication.

Luxembourg: Publications Office of the European Union, 2010

ISBN 978-92-79-14429-5

doi:10.2777/85987

ISSN 1018-5593

© European Union, 2010

Reproduction is authorised provided the source is acknowledged.

*Printed in Luxembourg*

PRINTED ON WHITE CHLORINE-FREE PAPER

## CONTENTS

	<b>Page</b>
<b>FINAL SUMMARY REPORT</b>	<b>5</b>
<b>SCIENTIFIC AND TECHNICAL DESCRIPTION OF RESULTS</b>	<b>15</b>
<b>1. OBJECTIVES OF THE PROJECT</b>	<b>15</b>
<b>2. COMPARISON OF INITIALLY PLANNED ACTIVITIES AND WORK ACCOMPLISHED</b>	<b>15</b>
<b>3. DESCRIPTION OF ACTIVITIES AND DISCUSSION</b>	<b>16</b>
<b>4. CONCLUSIONS</b>	<b>96</b>
<b>5. EXPLOITATION AND IMPACT OF THE RESULTS</b>	<b>97</b>
<b>6. TECHNICAL AND ECONOMIC POTENTIAL FOR THE USE OF THE RESULTS</b>	<b>97</b>
<b>7. PATENT FILING</b>	<b>98</b>
<b>8. PUBLICATIONS/CONFERENCE PRESENTATIONS RESULTING FROM THE PROJECT</b>	<b>98</b>
<b>9. REFERENCES</b>	<b>99</b>
<b>10. LIST OF FIGURES AND TABLES</b>	<b>99</b>



# **FLOWVIS: MEASUREMENT, PREDICTION AND CONTROL OF STEEL FLOWS IN THE CASTING NOZZLE AND MOULD**

RFCS Contract No. RFSR-CT-2004-00011

## **FINAL SUMMARY REPORT**

Control of steel flow, through the casting nozzle and within the mould, is an important determinant of steel cleanliness and surface quality. Techniques under development such as the visualisation of steel flow in the nozzle using electromagnetic, ultrasonic, thermal and vibration sensors in combination with the measurement of steel flow velocities and distribution in the mould, allow a physical picture to be developed of the steel flow behaviour during the casting process, including effects such as nozzle clogging and flow asymmetry/biased flow.

The overall objectives of the project were:

1. The improvement of steel surface and internal quality by the development of measuring and predictive tools for use in the tundish nozzle and casting mould. This will involve the correlation and application of the developed tools with plant data to generate guidelines for quality improvement.
2. The correlation of measured quantities within the tundish nozzle and casting mould with existing product grading schemes.
3. The development of continuous on-line ultrasonic systems for monitoring casting conditions within the casting nozzle and the prediction and control of casting conditions and product quality.
4. Measurement of the degradation of flow patterns with time with the aim of correlation with casting nozzle condition. This may lead to developing criteria for changing the SEN during casting or on-line measurement, to indicate wear of refractory components.
5. Comparison of the relative merits of the various flow measurement techniques.

In order to fulfil these main objectives the secondary objectives are:

6. Improvement of existing sensors in terms of suitability for plant application and extension of capability.
7. Observations on how actual measured flow regimes compare with the established idealised situation.

### **Work Package 1 - Sensor Development**

The objectives of Work Package 1 were to improve existing sensors in terms of suitability for plant application and extension of capability and the development of a physical model of the nozzle using low temperature liquid metal.

#### *Task 1.1 Development of electromagnetic sensor (Corus, MEFOS)*

Work has been carried out to develop two types of electromagnetic sensor.

The first was the electromagnetic Steel Flow Visualisation (SFV) sensor used by Corus. The SFV sensor uses transmitter and receiver coils mounted on either side of the Submerged Entry Nozzle (SEN) to detect the flow pattern in the nozzle between the tundish and mould. A new sensor was developed which was more robust, compact and easier to handle. To extend the potential functionality of the

sensor, the enhancement was designed to give three independent views each operating on a different frequency. Although it was not possible to produce opposing views, an array was successfully developed which has three channels spread over an angle of approximately 60°. The new sensor was designed and manufactured by the University of Manchester and then further developed for use in plant trials.

The second electromagnetic sensor was designed to measure flow velocity of steel in the SEN in approximately the same location as the SFV sensor. The sensor was developed by Metals Process Control AB (MPC) for MEFOS. The sensor was successfully calibrated in the laboratory.

#### *Task 1.2 Development of nozzle ultrasonic sensor (BFI)*

The work was focused on the development and improvement of a remote controlled ultrasonic sensor system for application at the SEN. A system was developed that used a sensor head fitted with transducers used for transmitting and receiving the ultrasound signal. The transducers were connected to the SEN using new optimised coupling rods which focused the sound energy at the tip. The total height of the system was reduced from 150 mm to 80 mm and a spring-loaded system was used to apply the sensor head to the SEN.

To allow trial data to be collected remotely by BFI a data acquisition system was installed to replace the mobile system which enabled the steel plant to perform ultrasonic measurements without external support. The system is equipped with a remote access to enable BFI to monitor and evaluate the ultrasonic data during the plant trials.

#### *Task 1.3 Development of nozzle inner pressure method (Sidenor)*

A method for pressure assessment at two different points along the pouring line was developed within the project 7215.PP/045<sup>(1)</sup> located at the stopper rod tip and at the nozzle inner wall and further refined in this project. The first measuring point is available using the gas feeding system through the stopper. The second measuring point is measured by using experimental nozzles with a small hole in the lateral wall. The test configuration used a multi-channel data logger connected to a laptop.

Due to the critical importance of the air-tight condition of the gas feeding circuit through the stopper for the reliability of the inner pressure measurements an experimental pin-bolt stopper was used during the pressure trials in order to guarantee an optimum tightness condition.

#### *Task 1.4 Development of nozzle refractory temperature method (Sidenor)*

At Sidenor, characterisation of the nozzle refractory temperature pattern throughout casting time was carried out by means of using thermocouples to try to correlate that thermal pattern with the nozzle inner clogging conditions and obtain additional information about the steel flow pattern inside the nozzle. A new fixing method was designed based on a steel belt accommodated in the nozzle outer face in order to provide the required pressure for the achievement of a reliable contact between thermocouples and nozzle refractory material by means of using cone sealing couplings. The experimental arrangement was designed to allow the use of up to four thermocouples simultaneously.

#### *Task 1.5 Development of mould flow measurement devices (Corus, MEFOS)*

The Karmen Vortex flow measurement sensor used at Corus is a commercially available system purchased from Heraeus Electro-nite. The system uses a probe consisting of an instrumented refractory rod dipped into a steel flow which uses vibration frequency to measure flow velocity.

The meniscus velocity sensor used by MEFOS, along with its SEN flow velocity sensor, operate using the principle of the Lorentz force which is generated when a conductor is moving in a magnetic field. This electromagnetic induction of current and its interaction with the magnetic field render the possibility to measure the steel velocity. The sensor was also developed by MPC. MPC has developed the different sensors without any funding from the RFCS. MEFOS can therefore not present any

details on the mechanical systems incorporated in the sensors. A fully functioning prototype was not successfully produced.

A calibration device was developed using a spinning disc to simulate steel flow and used for calibration and development of the Lorentz force devices.

#### *Task 1.6      Adaptation of ultrasonic sensor at caster (Saarstahl)*

The development of the ultrasonic system discussed in Task 1.2 included the installation of a permanent data acquisition system on the caster at Saarstahl. The adaptation of the ultrasonic sensor at the Saarstahl AG caster was performed in several steps. The hardware in the area of the SEN (sensor, coupling rods etc) for an automatic ultrasonic measurement system has been developed and BFI's automatic stationary ultrasonic system was installed on one strand of the continuous caster no. 4 of Saarstahl AG (SAG).

During the development of the stationary ultrasonic system, plant trials in collaboration with BFI continued in the form of campaigns using BFI's mobile measurement system.

#### *Task 1.7      Design and construction of physical model of casting nozzle using circulating low temperature liquid metal (MEFOS)*

The physical model was a full-scale model of a submerged entry nozzle and a mould based on the actual continuous caster used at SSAB Tunnpålar in Luleå for the production of slabs. A low melting alloy, MCP-137, was chosen to simulate the liquid steel in the model. The model was constructed in stainless steel as one of the requests was to use non-magnetic material to prevent the influence on the different sensors. Extensive functionally tests of the model were performed using water before the low melting point alloy was charged into the model. Once commissioned it was possible to run the model with a constant metal height in the tundish at different volume flows for several hours.

#### *Task 1.8      Physical model trials, simulation of a variety of flow conditions (MEFOS)*

Three campaigns of trials were carried out using the low melting point alloy. Problems with air leakage led to extensive formation of dross which impaired the correct operation of the model. The potential sources of air leakage were identified and sealed. Another problem occurred related to the mechanical toughness of the whole model. The model displayed oscillations which were overcome by mechanically stabilising the model and mounting a hydraulic damper.

*Campaign 1.* The height of metal in the tundish and the immersion depth in the mould were kept constant at 0.86 and 0.3 m respectively. The casting speed has been varied between 0.3-1.1 m/min. Both the SEN flow sensor and the meniscus velocity sensor did not give any conclusive results due to low intensity of the signals. A combined measurement with SEN flow sensor and the compact laser vibrometer, CLV was also carried out during this first campaign. Unfortunately the poor performance of the SEN flow sensor prevented any comparison between the two different measuring techniques. However, the CLV sensor provided some interesting results.

*Campaign 2.* A totally new SEN flow sensor was delivered by MPC. In the physical model the meniscus velocity sensor gave an insignificant signal change. However, the results from the SEN flow sensor were more promising.

*Campaign 3.* During this campaign one of the main objectives was to improve results from the meniscus velocity sensor. MEFOS prepared the physical model for trials with both sensors from MPC and trials were planned to be executed. Unfortunately MPC informed MEFOS at short notice that it did not have the possibility to provide any sensors for the planned trials. The main reason for this may have been that MPC AB was purchased by Agellis AB thereby changing the commercial motivation in the development of the sensors. This resulted in that no results could be obtained during this campaign.

## **Work Package 2 - Plant Trials**

The objective of Work Package 2 was to carry out extensive production plant trials to gather data from all available sources.

*Task 2.1 to 2.6 Trials using electromagnetic SFV, nozzle and mould flow sensors, the ultrasonic and pressure sensors, SEN thermocouples, instrumented moulds.*

Extensive plant trials were carried out by Corus, Sidenor BFI, Saarstahl and MEFOS.

Plant trials were performed at SSAB Tunnpått in Luleå by MEFOS. Problems were encountered with both the meniscus velocity sensor and the SEN flow sensor and they were returned to MPC. However, as mentioned earlier the purchase of MPC by Agellis resulted in no further sensors being delivered to MEFOS after these plant trials.

## **Work Package 3 - Assessment of Trial Data**

The objective of Work Package 3 was to assess all trials data from diverse sources including sensor data, instrumented moulds, steel flow measurement and different casting parameters.

*Task 3.1 Product quality assessment - surface (Corus)*

Details have been obtained of all surface quality issues in finished plate which can be linked to casting defects which have led to the finished product being rejected or dressed for all trial casts processed at the plate mill. From these defect maps have been generated for comparison to trial data.

The most significant defects found were long crack. It was not possible to correlate the occurrence of long crack to SFV sensor data, Mould Thermal Monitoring (MTM instrumented mould) or mould surface velocity flow measurements. Defects tended to be concentrated in the earlier ladles of sequences and did not appear to be generated when the flow patterns being monitored began to degrade after prolonged casting. It has not been possible to find clear links between product defects and the trends in electromagnetic sensor output and other casting parameters other than a majority of long crack defects being generated during periods of controlled raising of the mould level.

*Task 3.2 Product quality assessment - cleanness (Saarstahl)*

To provide the inclusion length values needed for the calibration and verification of the on-line signal analysis an extensive assessment of product quality concerning the cleanness in the semi-finished material has been done at Saarstahl. Two methods were used, blue brittle and ultrasonic immersion technique. Inclusion analyses were also made to obtain information concerning the inclusions passing BFI's ultrasonic sensors at the submerged entry nozzle and possibly influencing the measured signal.

*Task 3.3 Characterise steel flow pattern as a function of casting conditions (Sidenor)*

Observations during the plant trials have confirmed the theory that the pouring duct between stopper rod tip and nozzle exit does not run full of steel, and that the "steel level" within the nozzle is determined by the inner pressure value. According to the industrial trials, and for no clogging and no wear conditions, the inner pressure will be around 0.6 bar. "Steel level" within the nozzle can be estimated at around 580 mm above meniscus. The higher the gas flow rate, the higher the back-pressure, that is to say, the lower the vacuum. Therefore, according to this theory, the larger the gas flow rate, the lower the "steel level" will be within the nozzle.

#### *Task 3.4 Development of improved signal analysis (BFI)*

Plant trial data were used by BFI to develop improved ultrasonic signal analysis with special regard to propagation time and phase shift of the ultrasonic pulses within the SEN system. The initial work was carried out using a simple static water model in the laboratory.

It was noted that data from plant trials exhibited high variability and that was not leading to the desired prediction of the steel cleanliness. The acquired data were used to redesign and test the analysis routines off-line. A multivariate regression analysis approach was chosen in the form of a Partial Least Squares (PLS-) algorithm. The result is a prediction of the inclusion length for the volume of liquid steel scanned by the ultrasound.

### **Work Package 4 - Correlation with Existing Data, Product Grading Schemes and Product Quality**

The objectives of Work Package 4 were to correlate measured data with cast product grading schemes and product quality. This included observations on how actual flow regimes compared with the established idealised situation.

#### *Task 4.1 Correlation of measured data with product grading schemes (Corus)*

Direct correlation with product grading schemes was unsuccessful. However direct correlation with process parameters used as trigger variables by the product grading scheme were examined in great detail in other Work Packages.

#### *Task 4.2 Correlation of measured data with product quality (BFI, Saarstahl)*

Based on the PLS-algorithm developed in Task 3.4 a new process model for on-line prediction of product quality was developed. Data from production plant trials (WP 2) were applied to investigate the interactions between different continuous casting parameters and product quality, mainly in terms of cleanliness. Overall, a good agreement of the on-line ultrasonic inclusion length index prediction as measured during casting with the inclusion length index as measured by immersion technique at the semi-finished product was observed.

With regard to clogging a theoretical consideration of the steel flow through the air-tight casting system reveals a negative pressure at the stopper rod tip since the SEN's inner diameter is bigger than required for the actual steel flow<sup>(1)</sup>. Clogging would reduce the outlet diameter of the SEN leading to a build up in back pressure which will reduce the negative pressure above. The change of the SEN's inner pressure may have an influence on the flow in the region of the on-line ultrasonic measurement which is located approximately in the middle between SEN inlet and SEN outlet. Verification of this is not easy to gain since clogging occurred very seldom during the production plant trials. Data gathered during a trial where clogging was found in the SEN showed no unusual signals or inclusion length predictions. This indicates that the occurring of a light clogging has no influence on the flow condition inside the SEN.

#### *Task 4.3 Assess influence of flow pattern on mould solidification (Sidenor)*

Work concerning this task focused on the assessment of the effect of the steel flow patterns on the in-mould solidification, i.e. mould level stability, mould heat flux and friction between billet and mould because of their well-known influence on as-cast surface quality.

Taking these results into account, it could be stated that a 'Partly full nozzle' compared with an 'Empty nozzle' gives rise in general to worse in-mould solidification conditions, i.e. worse mould level stability, worse mould thermocouples stability, lower thermal flux and less stable friction.

Additionally, a high variability in the steel jet position gives rise to higher mould thermocouples variability, higher mould thermal flux variability and higher friction variability.

## **Work Package 5 - Reasons for Changes Observed in Flow Patterns**

The objectives of Work Package 5 were to measure the degradation of flow patterns with time with the aim of correlation with casting nozzle condition and to assess the feasibility of developing criteria for changing the SEN during casting or on-line measurement, to indicate wear of refractory components.

### *Task 5.1 Determination of reasons for flow pattern changes during stable casting (Corus, Sidenor)*

*Electromagnetic Steel Flow Visualisation Sensor.* Examination of the relationships between flow patterns measured using the SFV sensor and casting variables have shown two basic flow states. A "full" SEN and a "not full" SEN which has three components: The steel stream, the steel level in the SEN and a void. The transition between these two occurs on the Corus caster studied when the stopper gas pressure rises above -0.15 bar. There are exceptions to this but these are discussed in Task 5.3. In the "not full" state when the flow pattern is reasonably stable there is a connection between sensor signal and stopper gas pressure.

Clear indication of shifting flow conditions with respect to stopper position have been previously reported in the project 7215.PP/045<sup>(1)</sup>. The phenomenon is especially linked to alumina flushes.

*Multiple frequency sensor.* Assessment of the logged data confirmed that the output from the new sensor is directly comparable to the original single frequency system. The multiple frequency sensor does not provide much additional information regarding the actual flow pattern than the signal "noise" or variability of a single channel.

*Mould symmetry.* The mould symmetry index is generated from the instrumented mould. There is no apparent link between the symmetry and SFV sensor measurements. However observations have noted that shifts in symmetry are associated with major disturbances to stable casting, e.g. ladle changes etc. There are however, notable changes in symmetry which are not connected to such occurrence.

*Karmen Vortex Mould Velocity Measurements.* Mould surface velocity measurements were carried out simultaneously on either side of the SEN. During a transition between "full" and "not full" there is a significant drop in mould surface velocity on both sides of the SEN and visa versa.

Clear links have been found between SFV measurement, Karmen vortex surface flow and symmetry index for certain conditions.

*Statistical analysis of electromagnetic sensor signals.* An in depth statistical analysis of Corus data has confirmed the qualitative observations concerning the primary process variable affecting the stability of flow in the SEN as being the stopper argon pressure and that stopper position although significant has a less marked influence. Other parameters considered do not have a statistically significant influence on SFV signal and hence flow pattern.

The most influential parameters over the steel flow pattern condition at Sidenor CCM2 are the air-tight condition of the gas injection circuit through the stopper, gas flow rate, the extent of clogging at the nozzle exit and stopper rod position changes.

### *Task 5.2 Study of the influence of casting parameters on clogging/wear (Sidenor)*

Clogging and wear may lead to steel flow changes in the mould and to the subsequent inhomogeneous heat transfer in the mould, mould powder entrapment or defects in the cast product due to non-uniform shell growth. Nozzle thermal characterisation by means of using thermocouples is a method able to assess the extent of clogging at the nozzle inner body. Additionally, a good correlation was observed between stopper back-pressure variation (vacuum level) and nozzle outlet restriction due to clogging.

### *Task 5.3 Investigate criteria for changing casting nozzle during casting (Corus)*

The degree of clogging is directly related to the total casting time. However certain grades are more susceptible than others. The SFV sensor can only indicate that there is significant clogging when combined with other process parameters. There appears to be a link with stopper pressure and stopper position. There is some evidence that build up of alumina in the SEN exit ports is changing the flow pattern within the mould. This can be seen in changes in mould surface velocity.

### *Task 5.4 On-line evaluation of flow pattern, clogging and wear within SEN (BFI, Saarstahl)*

The results of the extensive plant trials showed stable casting conditions and very low inclusion length indices. This is a strong indication that no sudden changes of flow patterns had occurred.

## **Work Package 6 - Recommendations for Process Optimisation**

The objective of Work Package 6 was to recommend criteria for optimisation of both nozzle design and casting parameters, based on the results of the research work.

### *Task 6.1 Optimisation of casting parameters (Corus, BFI, Sidenor, MEFOS)*

Although there has been no strong evidence at Corus to indicate that product surface quality is affected by the flow pattern within the SEN, stable casting conditions are preferable. The SEN designed to run "full". This is the most stable condition as it removes the potential for transient conditions caused by fluctuation of steel level and steel stream position within the SEN.

Trials to investigate surface defects have hinted that the occurrence of long crack in slab material is in part related to the active level control used to spread wear in the SEN by ramping mould level. This ramping is necessary to prolong SEN life.

Inclusions show a very low level at Saarstahl steelworks and clogging related to this occurs very seldom. A potential for optimisation of the casting process at Saarstahl might be given in diminishing the outer diameter of the SEN which has a positive effect on the spatial conditions in the mould.

Most of the recommendations for optimisation of the casting parameters and conditions for the billet caster of Basauri Plant are applicable for any caster and these include:

- Air-tight quality of the stopper gas injection circuit.
- Optimum nozzle immersion depth
- Use of the stopper-gas back-pressure for on-line assessment of clogging at the nozzle exit.
- Use of thermocouples as a method for the on-line assessment of the extent of clogging at the nozzle inner body.

The promising results from the trials in the physical model at MEFOS imply that the SEN flow sensor could be developed to a working sensor at industrial conditions both for velocity measurements as well as for determination of clogging problems. However, the lack of result means that no optimisation of casting parameters may be reported from MEFOS.

### *Task 6.2 Optimisation of casting nozzle design (Corus, Sidenor)*

There has been no strong evidence indicating that the flow condition within the SEN at Corus has an effect on product surface quality. As a result of trials using the electromagnetic sensor with mould flow measurements there are no recommendations for design changes in the casting nozzle.

It has been highlighted that a large vacuum level in the SEN at Sidenor can give rise to a clear worsening of the mould level stability. Casting speed and gas flow rate are fixed. Increasing gas flow rate could give rise to pinhole problems. Therefore either the nozzle outlet diameter could be reduced, although not recommended as it would promote clogging or the nozzle immersion depth could be increased.

#### *Task 6.3 Application and testing of optimisation criteria (All partners)*

A trial has been successfully carried out to test whether the stopper gas flow rate can be used to stimulate the transition to a "full" SEN at Corus. Results of the trial also indicated that when the SEN is "not full" there was a reduction in stability of both stopper position and mould level.

The results of this project demonstrate that the inner geometry of the pouring system of Saarstahl is near to the optimum with special regard to the cleanliness in terms of inclusion length. If the outer diameter of the SEN is to be reduced the only way is to diminish the wall thickness. But this is demanding to the mechanical stability, the chemical stability especially at the meniscus area and the air tightness since air ingress must be avoided. The design and application of a new SEN is far beyond the outline of this project since this will lead into questions regarding the inner structure of the refractory material.

During the project, the recommendations and conclusions were properly tested at plant and applied to the industrial practice. In this respect, the following recommended practices have been already standardised at the CCM2 of Basauri Plant:

- Optimised stopper rods and gas injection circuit.
- The nozzle immersion depth at the Basauri billet caster was increased from 105 mm to 115 mm.

Concerning the new techniques or signals able to give helpful information for the process control and optimisation:

- On-line assessment of the clogging extent at the nozzle inner body by thermal characterisation using thermocouples is recommendable only on a trial basis because of the complexity of the technique.
- On-line assessment of the clogging at the nozzle exit has been incorporated as a process control signal.

#### *Task 6.4 Compare and contrast different measurement techniques (All partners)*

In order to compare and contrast the different measurement techniques first we need to be clear what the different techniques are capable of, what their limitations are and how they interact with normal operation of a casting plant.

There is a clear use for the nozzle pressure technique in process control and relatively small investment cost involved. This is probably the most generally useful and easily transferable technology. The ultrasonic technique provides a clear indication of product quality and could be directly used for product grading, and for tracking quality critical product for high grade application. There are disadvantages in that it is quite invasive in terms of plant operation and requires significant effort to prepare. The electromagnetic SFV sensor does provide a potential control signal for the SEN flow condition especially if it was decided to actively control the SEN to its "full" condition but there is a need to balance cost against benefit. The remaining techniques are useful diagnostic tools which are each useful in targeted specific requirements on a trial basis but it is unlikely that a permanent plant installation would be considered either in terms of cost or reliance as an ongoing plant control device.

## **Conclusions**

The conclusions of the project are presented as part of the results of Work Package 6.

1. As a result of measurement trials recommendations have been made to improve steel surface and internal quality
  - To maintain "ideal" SEN flow pattern on Corus Scunthorpe slab caster, stopper gas pressure should be maintained below -0.15 bar.
  - Surface defects on Corus Scunthorpe slab caster appear to be linked with active level control. Consideration should be given to alternative method of spreading SEN wear.
  - Recommendations for optimisation of the casting parameters and conditions for the billet caster of Basauri Plant are applicable for any caster these include:
    - Air-tight quality of the stopper gas injection circuit.
    - Optimum nozzle immersion depth.
    - Use of the stopper-gas back-pressure for on-line assessment of clogging at the nozzle exit.
    - Use of thermocouples as a method for the on-line assessment of the extent of clogging at the nozzle inner body.
  
2. The correlation of measured quantities within the tundish nozzle using the SFV sensor and in the casting mould with existing product grading schemes has been unsuccessful. The BFI/Saarstahl ultrasonic technique could be used to track product internal quality in terms of inclusions.
  
3. An ultrasonic on-line measurement system was developed and tested for monitoring the product quality in terms of cleanliness immediate during continuous casting. Based on the PLS-algorithm developed in Task 3.4 a new process model for on-line prediction of product quality was developed.
  
4. Measurement of the degradation of flow patterns with time has been studied.
  - The degree of clogging is directly related to the total casting time.
  - The SFV sensor can only indicate that there is significant clogging when combined with other process parameters.
  - The stopper back pressure method developed at Sidenor can detect clogging and wear in the SEN and could be used as an indicator.
  
5. New sensor developments were successfully completed, commissioned and used in experimental trials:
  - Multiple frequency electromagnetic Steel Flow Visualisation sensor.
  - Nozzle ultrasonic sensor including remote data acquisition system which allows trials to be monitored from a different site.
  - Nozzle inner pressure method.
  - Nozzle refractory temperature method which allow up to four thermocouples to be embedded in the SEN.

New sensor developments were attempted but led to limited success:

  - Electromagnetic SEN flow velocity sensor. Partial success but no plant results
  - Meniscus velocity sensor.
  
6. A low temperature liquid metal model has been designed, manufactured and used.

### **Patent filing**

The supplier of the single frequency electromagnetic SFV sensor (MPC AB) holds a patent for the technology which predates the project. Corus has an agreement allowing use and development of the system.

No patents have been derived from the research in the case of Sidenor, BFI, Saarstahl and MEFOS.

## **Publications / conference presentations resulting from the project**

5<sup>th</sup> European Continuous Casting Conference, Nice, France. June 2005: Visualisation of Steel Flow in the Continuous Casting Nozzle using an Electromagnetic Technique. S R Higson, P Drake (Corus R, D & T, UK), A Lyons (MPC AB, Sweden), A Peyton, B Lionheart (University of Manchester, UK)

2nd International Workshop on Measuring Techniques for Liquid Metal Flows, Dresden, Germany. April 2007: An electromagnetic technique to measure steel flow patterns within the continuous casting nozzle. S R Higson, P Drake (Corus R, D & T, UK), A Lyons (MPC AB, Sweden), A Peyton (University of Manchester, UK)

Sensors for non-contact velocity measurements for continuous casting of steel. U Sjöström (MEFOS, Sweden)

5th World Congress on Industrial Process Tomography, Bergen, Norway. September 2007: Developments of multiple frequency electromagnetic induction system for steel flow visualization. X Ma, A J Peyton (University of Manchester, UK), S R Higson, P Drake (Corus R, D & T, UK).

SMEA Conference, Sheffield June 2007: Electromagnetic Visualisation of Steel Flow in Nozzles during Continuous Casting. A Peyton (University of Manchester, UK), S R Higson (Corus R, D & T, UK), A Lyons (AGELLIS Group AB Sweden)

No publications were made by Saarstahl, BFI Sidenor.

## **References**

1. Higson et al: 'Improvement in cast product quality by the visualisation and control of the steel flow pattern in the tundish pouring nozzle (SEN/SES)', ECSC Contract Number 7215.PP/045

## SCIENTIFIC AND TECHNICAL DESCRIPTION OF RESULTS

### 1. OBJECTIVES OF THE PROJECT

The objectives of the work proposed were:

1. The improvement of steel surface and internal quality by the development of measuring and predictive tools for use in the tundish nozzle and casting mould. This involved the correlation and application of the developed tools with plant data to generate guidelines for quality improvement.
2. The correlation of measured quantities within the tundish nozzle and casting mould with existing product grading schemes.
3. The development of continuous on-line ultrasonic systems for monitoring casting conditions within the casting nozzle and the prediction and control of casting conditions and product quality.
4. Measurement of the degradation of flow patterns with time with the aim of correlation with casting nozzle condition. This may lead to developing criteria for changing the SEN during casting or on-line measurement, to indicate wear of refractory components.
5. Comparison of the relative merits of the various flow measurement techniques.

In order to fulfil these main objectives the secondary objectives were:

6. Improvement of existing sensors in terms of suitability for plant application and extension of capability.
7. Observations on how actual measured flow regimes compared with the established idealised situation.

### 2. COMPARISON OF INITIALLY PLANNED ACTIVITIES AND WORK ACCOMPLISHED

Overall the majority of planned work was completed as planned.

Corus - When the FLOWVIS project was originally proposed it was planned that plant trials would be carried out at the slab casters at Corus UK Port Talbot and Scunthorpe Works. Due to circumstances within Corus beyond the control of R, D & T it is not possible to perform trials at Port Talbot so all trials have been concentrated on the Caster at Scunthorpe. The technical annex states that: *"If feasible, trial data will be compared with down stream product quality data."* The original concept when proposed was that an attempt would be made to correlate product quality data measured in a strip mill which used an automated strip surface evaluation system with the trials data gathered at the caster. This is not feasible. However, to fulfil this aspect of the project, plant trials have been performed on a slab caster which supplies steel for plate production. Final quality data from the plate mill was processed for correlation with caster measurements.

Work to correlate measured data with product grading schemes have been similarly effected. Initially the caster at Scunthorpe had no formal grading system. However, this caster underwent significant upgrading during the project which included the introduction of a grading scheme. The system is new and yielded limited results due to lack of historical.

Sidenor - No significant deviation from plan.

BFI/Saarstahl - No significant deviation from plan.

MEFOS – The major part of the project work, the development of a low temperature liquid metal model was completed to plan. The development of sensors was impaired by a third party supplier who was not part of the project. Despite encouraging results when using the model, when plant trials were carried out no usable results were generated. The third party failed to deliver updated sensors which prevented further the industrial plant trials.

### **3. DESCRIPTION OF ACTIVITIES AND DISCUSSION**

#### **Work Package 1 - Sensor Development**

The objectives of Work Package 1 were to improve existing sensors in terms of suitability for plant application and extension of capability and the development of a physical model of the nozzle using low temperature liquid metal.

#### **Task 1.1 - Development of the electromagnetic sensor**

##### **Corus**

##### *Multiple frequency sensor*

The existing prototype electromagnetic Steel Flow Visualisation (SFV) sensor is constructed of several discrete components: sensor head, conditioning electronics, waveform generator, signal amplifier, data logger and logging computer. The system is cumbersome and vulnerable in a plant environment. The equipment has not proven reliable and is susceptible to partial or total failure. One of the objectives of the sensor development was to produce a more rugged, dedicated and simplified system.

It was decided that the feasibility of changing the operating principle of the electromagnetic steel flow visualisation (SFV) sensor from a single view to multiple view sensor would be investigated. The original sensor, used in the steel flow visualisation project ECSC Contract Number 7215.PP/045<sup>(1)</sup>, employed a single electromagnetic transmitter to generate three fundamentally similar signals for the receiver coils. The proposed enhancement would give three independent and opposing views. Previous work has indicated that the variation of signal level cannot only be linked to metal volume, but also to proximity to the receiver. By placing the transmitters on opposite sides of the target SEN, the system could potentially be used to distinguish preferential flow within the nozzle.

To investigate the feasibility of this approach a laboratory test rig was designed and manufactured. This equipment replaced the sensor head and could be used in conjunction with the existing conditioning electronics. The test rig consisted of three transmitters and corresponding receiver coils mounted to allow their position around a central target to be altered easily. Each transmitter could be driven at a different frequency. The existing frequency filters in the conditioning electronics were altered to receive the separate signals and allow them to be analysed independently.

The experiments showed that the frequency filters were not capable of distinguishing between the signals. The conclusions of these tests were that it will not be possible to use the existing amplifiers and processing electronics for a multiple frequency device. In addition to this it was noted that when the transmitters were energised in the test rig the proximity of the receiver coils to the transmitters of the other channels meant that the signals were saturated before the backing off stage even if the frequency difference exceeded operating width of the filters.

The combination of these two problems meant that it was not be possible to modify the existing electromagnetic sensor electronics for multiple channel operation. These results were discussed both with MPC, the system manufacturer, and the University of Manchester School of Electrical Engineering. They both agreed with the conclusions.

The University of Manchester suggested that it would be possible to overcome these problems by designing a new electronic signal processing package with PC based processing. It was agreed that this would be pursued and work was initiated at Manchester in collaboration with Corus.

The new sensor system was designed to use the existing "mark 2" sensor body with new coils. An array of three transmitter and three receiver coils were specified.

A design was produced for the new system. It consisted of five main components:

- Sensor body.
- Transmitter excitation electronics.
- Receiver electronics.
- PC based data acquisition card.
- PC with data processing and logging software.

A multifunction data acquisition card mounted in the logging computer handled all signals into and out of the PC. Separate custom electronic excitation and receiver detection circuit boards were designed and manufactured at Manchester. Data processing and logging software was controlled by a graphical user interface created using LabView software.

The electronics system was tested using the laboratory test rig. Titanium bars were placed in the field of view and the results were recorded. Unacceptable parasitic oscillatory signals were observed which were a function of the excitation frequency. Real signal changes, for small titanium bars, were not recognised. A series of modifications were carried out including shielding, grounding, coil orientation and isolating 50 Hz sources where possible. The most significant improvement was achieved by changing the CRT monitor to an LCD monitor, although at 450 Hz and 750 Hz the problem persisted. A minimum frequency separation of 100 Hz between the excitation frequencies was also required.

It was agreed that the parasitic frequencies were still present but at acceptably low amplitudes. It was found that the signal amplitudes of these parasitic frequencies could change dramatically with a small change of only one of the excitation frequencies. Further experimentation, revealed that mathematically unrelated combinations of three frequencies did not induce the problem. Frequencies of 601.632, 701.387 and 801.722 Hz are problem free and have been set as default frequencies.

The low signal amplitude changes caused by the presence of a titanium bar were queried. To maximise signal strength the electromagnetic field strength had to be increased or the number of turns needed to be increased on the receiver coil. The latter was optimised but was ultimately constrained by the internal dimensions of the sensor head. The transmitter field strength was a function of the current and the number of turns. Coil turns were removed from the transmitter coils to maximise the current flowing through them. To allow the maximum current capacity of the current drivers to be used the inadequate heat sinks used in the mounting frame were replaced by a large heat sink fitted to the front cover of the sub-rack with the current drivers removed from the electronic cards and fitted to it.

However the problem with signal saturation if transmitters and receivers from different channels were placed together was not resolved by this system. It was not possible to position transmitters facing each other to provide opposing views. The optimum configuration was found to be three independent views spread over an angle of approximately 60°.

In parallel with this, a second sensor head was commissioned from MPC, Sweden. The aim of this was to allow the new system to be developed and tested leaving the original system available for plant trial work to continue. The new sensor head was manufactured with slotted location holes to allow the coil positions to be altered if necessary. The new system and its LabVIEW user interface screen can be seen in Fig. 1. Thermocouples were strategically fixed inside the sensor to allow temperatures to be monitored during operation on the continuous casting machine. The complete plant system was successfully tested in the laboratory using titanium bars to simulate liquid steel.

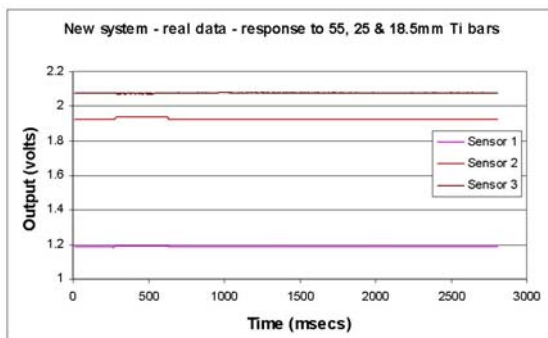


Fig. 1a: New multi-frequency electromagnetic steel flow visualisation sensor (Corus)

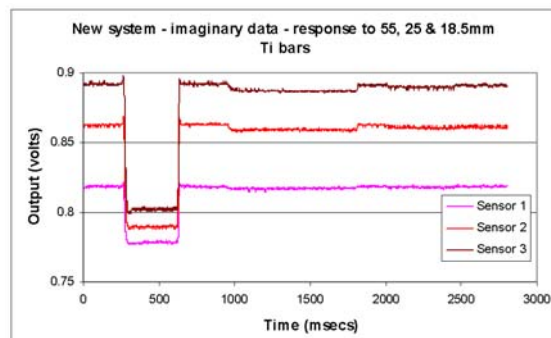


Fig. 1b: New multi-frequency electromagnetic SFV sensor user interface screen (Corus)

The new sensor control software stores and files data on demand. Plots of receiver coil voltages are shown in Fig. 2 in response to various round titanium bars placed in the SEN region of the sensor. The signal processing produces two types of output as a result of complex filtering, a "real" signal and a phase shifted "imaginary" signal. The real data show a poor response to the bars whilst the imaginary data shows a good response. An 18.5 mm bar was undetectable with the old sensor. The imaginary data will be used as the output for plant trials.



(a)



(b)

Fig. 2: Graphs showing sensor response to titanium bars for real and imaginary voltage (Corus)

One pilot plant trial was carried out at Teesside Technology Centre using the new sensor to hot commission the system. The trial used conditions representative of a production caster with the aim of hot testing the prototype sensor. The experimental casting arrangement consists of a stoppered ladle, a stoppered tundish which contains the pouring nozzle and a pseudo casting mould to enable submerged pouring to be practised. A transparent quartz glass tube was used to contain a steel stream of known diameter within a standard submerged entry nozzle. This was to investigate whether the sensor would be able to register a steel stream within the SEN. Steel supply for the trial was via Teesside Technology Centre's Electric Arc Furnace.

During the trial the steel flow was interrupted to generate step changes in steel volume in the sensor view. The sensor performed well and these breaks were clearly visible in the output traces, see Fig. 3. The sensor was successfully hot commissioned.

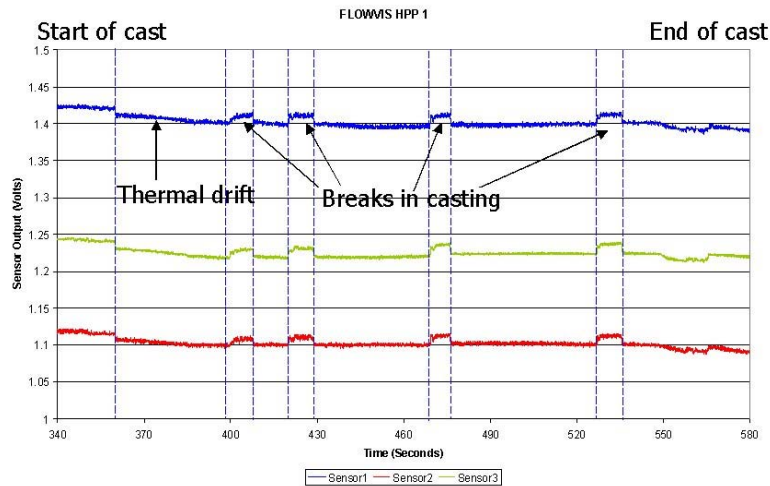


Fig. 3: Output from the new electromagnetic sensor during pilot plant trial (Corus)

During the pilot plant trial sensor temperatures were monitored manually. To facilitate data logging during future trials an eight channel thermocouple data logger was purchased which allowed the internal sensor temperatures to be logged and monitored independently of the sensor software using the same data logging PC.

The sensor head was made more rugged for use in the plant environment. The coils were coated in a resin material to prevent the individual coils moving relative to each other. The cables within the sensor head were fixed in place as it was found that movement of the signal cables between the sensor coils and signal amplifiers caused significant signal noise. Disposable thermal shielding was applied to the sensor head (see Fig. 1a) as well as air cooling.

The existing prototype electromagnetic Steel Flow Visualisation (SFV) sensor is constructed of several discrete components: Sensor head, conditioning electronics, waveform generator, signal amplifier, data logger and logging computer. The system is cumbersome and vulnerable in a plant environment. The equipment has not proven reliable and is susceptible to partial or total failure. One of the objectives of the sensor development was to produce a more rugged, dedicated and simplified system.

#### *Sensor support*

To facilitate the trials a new support bracket was designed for the electromagnetic sensor. The design was significantly simpler than the existing system and allowed the sensor to be positioned around the SEN during casting. The new bracket consists of a simple arm, which bolts around the body of the sensor. A tongue at the top of the arm is inserted into a small block welded to the base of the tundish. The arm is adjustable for height and angle. This adjustment must be done off line before the tundish is preheated. This design allows the sensor to be inserted easily once the tundish is in position over the mould. This can be done either just before casting begins or during casting. In the event of a deviation from normal casting operations, the sensor can swiftly be removed by simply pulling the handle on the rear of the bracket. Figure 4 shows the new bracket and sensor in situ during casting at Corus UK, Scunthorpe slab caster. A total of seven tundishes were modified to accept the new support bracket.



Fig. 4: New sensor support bracket (Corus)

## MEFOS

The principle with the non-contact electromagnetic velocity sensors used by MEFOS within the current project relied on the well known fact that when a conductor moves in a magnetic field a force related to the velocity of the conductor will act on the magnetic field. This is the Lorentz force. This approach was used during a previous RFCS project<sup>(2)</sup> where flow velocities in the mould meniscus were investigated. The results from the previous project were determined to be most interesting. During the current project further development of the measuring technique has been undertaken.

Another important task within the current project has been the development of an electromagnetic sensor to determine the velocities in the submerged entry nozzle (SEN). The SEN flow sensor relies on the same principle as the previously used meniscus velocity sensor<sup>(2)</sup> and is a non-contact velocity sensor.

Both the development of the new SEN flow sensor and the further development of the meniscus velocity sensor have been completed in co-operation with Metal Process Control AB (MPC). The further development of the meniscus velocity sensor is described in more detail in Task 1.5, which relates to development of mould flow measurement devices. The theory for both the electromagnetic sensors is presented in that section.

It needs to be clarified that the biggest difference between the two electromagnetic sensors is that when measuring the velocity in the casting nozzle the distance between the metal flow and the sensor will be constant which may not be the case in the mould. The SEN flow sensor is located in the horizontal plane contrary to meniscus velocity sensor which is placed in vertical plane. In conjunction with the measurement with the newly developed SEN flow sensor it was thought that it would be of great interest to combine these measurements with the compact laser vibrometer, CLV.

The CLV sensor is an existing unit that already has been used in water modelling and in a continuous casting machine in an earlier ECSC-funded project<sup>(1)</sup>. Originally it was planned to use the CLV sensor as a complement to the SEN flow sensor during the trials in the physical model as well as plant trials.

The CLV sensor is used for non-contact measurement of surface vibration velocities. It consists of a controller and a sensor head. The working principle of the CLV measurements is vibrational velocities on the basis of laser interferometry. The beam of a helium-neon laser is pointed at the vibrating object and scattered back from it. The object beam is thereby subjected to a small frequency shift which is described as the Doppler frequency. The Doppler frequency is a function of the velocity component in

the direction of the object beam and the laser wavelength. The resulting signal is decoded and a voltage is generated which is proportional to the instantaneous velocity of the vibrating object.

## Task 1.2 - Development of nozzle ultrasonic sensor

### BFI

The work was focused on the development and improvement of a remote controlled ultrasonic sensor system for application at the SEN. Figure 5 exhibits the principal layout of the ultrasonic sensor system. The ultrasonic transducers used for transmitting and receiving the ultrasound signal were separated from the up to 1000 °C hot SEN surface by coupling rods. Both, transducers and coupling rods, were located in a sensor head which is cooled with compressed air. Based on previous experience the cooling system was optimised during the project in a way to avoid high frequency disturbances of the measurement signal induced by the cooling flow. Due to this measure the signal to noise ratio was improved up to 40 dB.

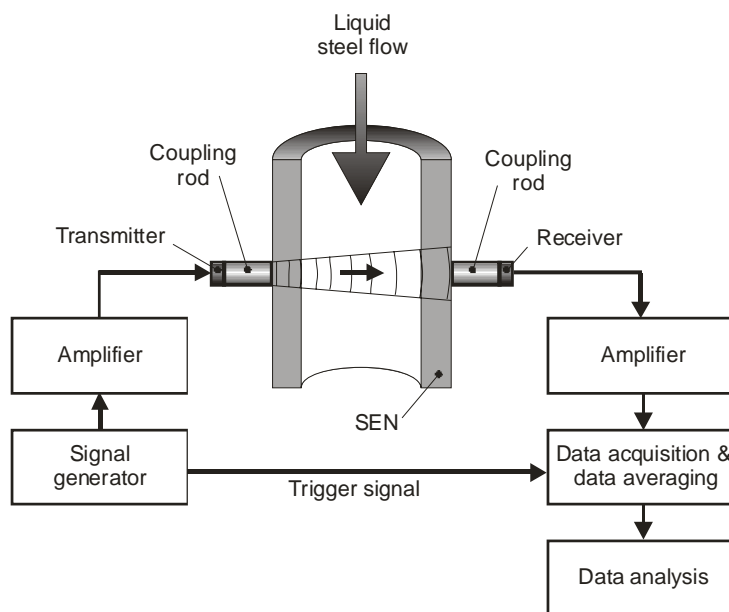


Fig 5: Working principle of ultrasonic sensor system (BFI)

One major drawback of the existing ultrasonic system was the need for machined areas at the SEN where the coupling rod was connected to the SEN surface. During the first four plant trials these machined areas caused severe interference with the production process because the modified SEN had to be rotationally adjusted during preparation of the tundish. To avoid the need for machined areas an adapted coupling rod was developed. The coupling rod tip was tapered with a screw driver like profile. In order to optimise the taper of the coupling rods to focus the sound energy at the tip of the coupling rod numerical simulations trials were made. In Fig. 6 the calculated distribution of the ultrasonic energy throughout the whole ultrasound charged system is shown. The upper part demonstrates the displacement of the solid parts for the SEN filled with water and, second filled with liquid steel. This system was developed for implementation at Saerstahl AG. The casters at Saerstahl do not use gas injection in the SEN which means that interpretation of the ultrasonic signal is more straight forward as there is only a liquid phase. In the lower part of Fig. 6 the distribution of the acoustic pressure inside the two liquid fillings is plotted.

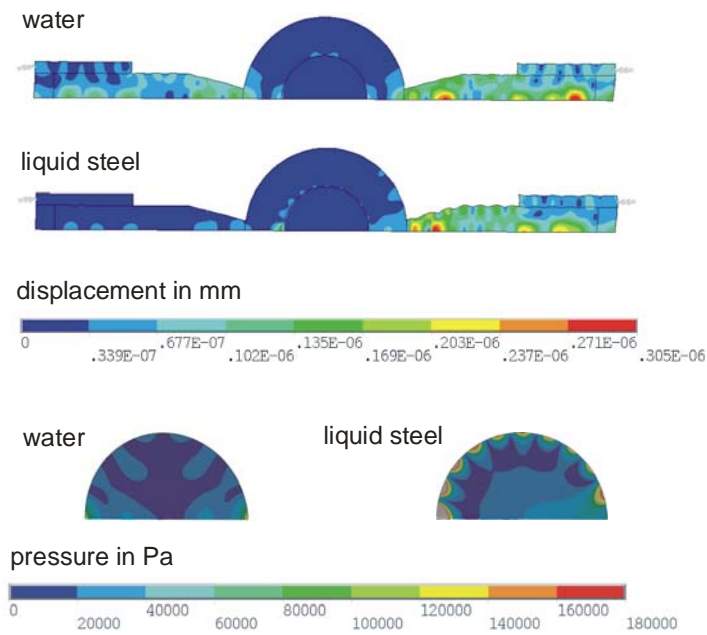


Fig. 6: Numerical model trial of the new automated ultrasonic sensor system (BFI)

The taper of the coupling rod was optimised for the coupling of a liquid steel filled SEN. A comparison was made with a water filled nozzle to validate the numerical results using physical water model trials. With both water and metal filling the SEN, the ultrasonic energy is not only transported directly through the system but also through the wall of the SEN. This gives a total excitation of the liquid section inside the SEN with no "dead areas" and this will allow all alterations of the conditions inside to be monitored.

During the project an automated flux addition unit was installed on the caster. Because of the physical height of the original ultrasonic sensor heads the new flux addition could not be positioned correctly during the ultrasonic trials. Due to the altered flux addition position casting conditions were not representative and it was decided to redesign the ultrasonic sensor heads and the sensor head holder.

The total height of the system was reduced from 150 mm to 80 mm. A spring loaded anchor system was used to fix the sensor head inside the sensor head holder. With this measure the twisting of the former round sensor heads was eliminated. This twisting was found to be adversely affecting the coupling of the new tapered coupling rods. Figure 7a shows the redesigned sensor head holder which was manufactured by Sairstahl AG after mounting at the tundish bottom. Figure 7b shows the complete ultrasonic system during casting operation.



Fig. 7a: Sensor holder before tundish preheating (Saarstahl)



Fig. 7b: Measurement device during operation (BFI/Saarstahl)

During the redesign of the sensor heads many construction details were altered. These alterations caused problems during the subsequent plant trials and significant time was spent in setting up the redesigned system for operation.

To allow trial data to be collected remotely by BFI a data acquisition system was installed to replace the mobile system. The permanent data acquisition system enables the steel plant to perform ultrasonic measurements without external support. The permanent data acquisition system is equipped with a remote access by virtual personal network (vpn) to enable BFI to monitor and evaluate the ultrasonic data during the plant trials. The installation of this is discussed in Task 1.6.

### Task 1.3 - Development of nozzle inner pressure method

#### Sidenor

A method for pressure assessment at two different points along the pouring line was developed within the project 7215.PP/045<sup>(1)</sup> (see Fig. 8). Those points are located at the stopper rod tip (point 1) and at the nozzle inner wall (point 2). This technique makes it possible to study the pressure evolution at both points throughout casting time including non-steady periods such as start-up.

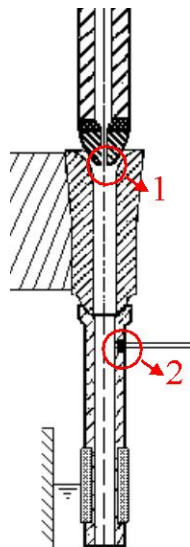


Fig. 8: Location of the pressure measuring points (Sidenor)

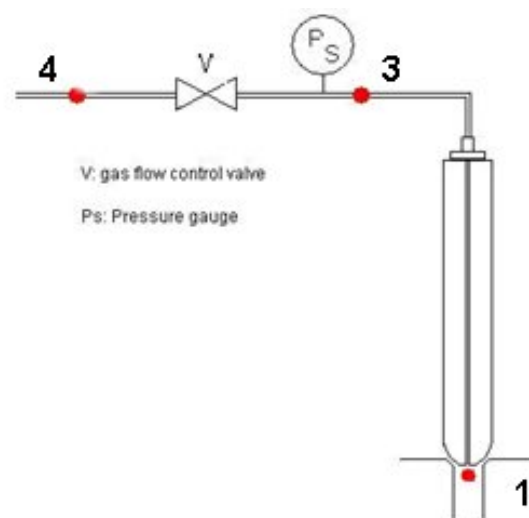


Fig. 9: Pressure at the stopper rod tip. Back-pressure measuring procedure (Sidenor)

The first measuring point (Point 1: Pressure at the stopper rod tip), is available using the gas feeding system through the stopper. Figure 9 shows the place where the pressure is measured (Ps). The bore diameter of the stopper rod tip is 5 mm, and the normal gas flow rate is very low ( $\leq 0.81$  l/min); therefore, it is possible to assume that the pressure at the stopper rod tip (point 3) is equal to the back-pressure measured in Ps (point 3). The second measuring point (Point 2: Pressure at the nozzle inner wall), is measured by using experimental nozzles with a small hole in the lateral wall (see Fig. 10).

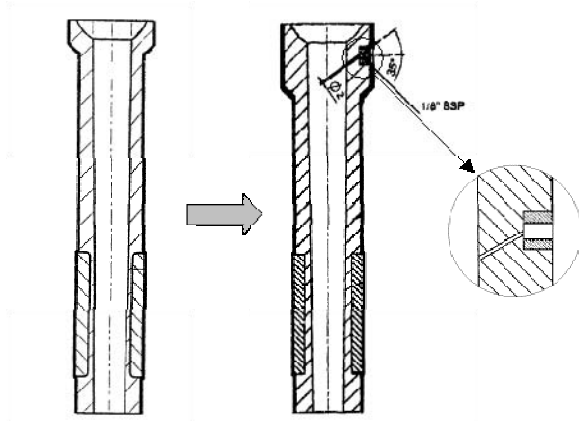


Fig 10: Pressure at the nozzle inner wall. Standard and experimental SES nozzle with a small hole (diameter: 2 mm) in the lateral wall for pressure measurements (Sidenor)

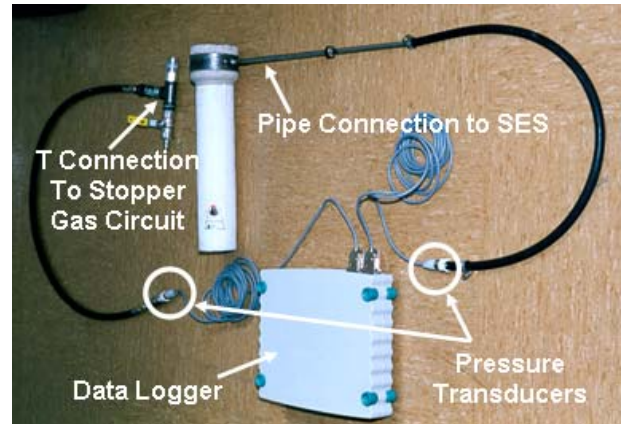


Fig. 11: Nozzle inner pressure tests devices (Sidenor)

Figure 11 shows the test configuration used for the pressure tests; and it is composed of a multi-channel data logger connected to a laptop, a pressure transducer to measure the pressure at the stopper rod tip (gauge type, nominal measuring range of absolute pressure in bar: 0 bar to 10 bar), a T connection with a tap in order to be able to switch off the gas injection through the stopper at any time during the trials and a stainless steel connector pipe screwed to the experimental nozzle wall and sealed with refractory cement to avoid air infiltration through the junction.

Due to the critical importance of the air-tight condition of the gas feeding circuit through the stopper for the reliability of the inner pressure measurements already presented, an experimental pin-bolt stopper was used during the pressure trials in order to guarantee an optimum tightness condition. Figure 12 shows a sketch of the experimental stopper rod. This experimental stopper presents an improved tightness quality with regard to the standard one. That tightness improvement is basically achieved by means of using graph-oil joints at the most critical points of the stopper rod structure, and by this way the thermal expansion effects on the tightness quality are counteracted.

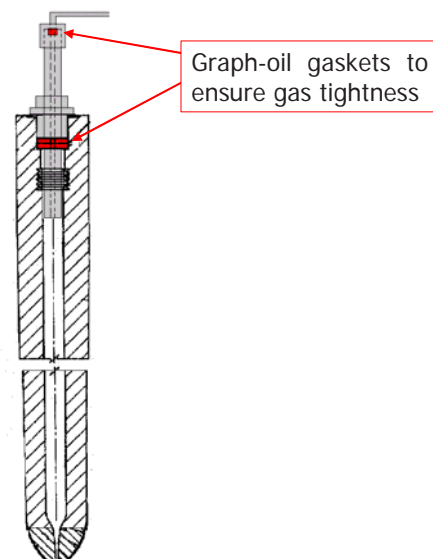


Fig. 12: Experimental pin-bolt stopper for improved gas tightness (Sidenor)

## Task 1.4 - Development of nozzle refractory temperature method

### Sidenor

At Sidenor, characterisation of the nozzle refractory temperature pattern throughout casting time was carried out by means of using thermocouples. The purpose was to try to correlate that thermal pattern with the nozzle inner clogging conditions, as well as to obtain additional information about the steel flow pattern inside the nozzle.

In project 7215.PP/045<sup>(1)</sup>, trials were carried out using two type K thermocouples as shown in Fig. 13. They were located at 340 mm from the nozzle exit. Nozzle wall refractory thickness at that position is 16 mm, and the thermocouples were inserted into the nozzle to approximately 11 mm from inner face. Once the thermocouples were inserted, they were sealed with refractory cement in order to guarantee a good contact between them and the refractory material.

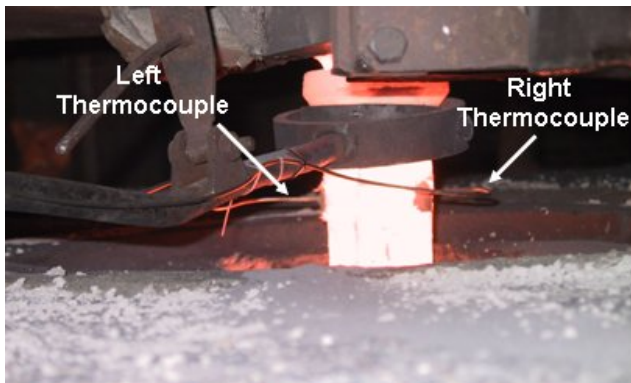


Fig. 13: Thermocouple location at the nozzle wall for the trials with two thermocouples (Sidenor)



Fig. 14: New fixing method to guarantee a good contact between the thermocouples and the refractory nozzle body (Sidenor)

In order to avoid the contact deterioration problem between thermocouple tip and refractory material a new method was designed. This new fixing method was based on a steel belt accommodated in the nozzle outer face in order to provide the required pressure for the achievement of a reliable contact between thermocouples and nozzle refractory material by means of cone sealing couplings (see Fig. 14). Additionally, this experimental arrangement was designed to allow the use of up to four thermocouples simultaneously.

## Task 1.5 - Development of mould flow measurement devices

### Corus

The Karmen Vortex flow measurement sensor is a commercially available system purchased from Heraeus Electro-nite. The system uses a probe consisting of an instrumented refractory rod dipped into a steel flow, which measures the frequency that vortices shed around the probe from the vibration, they impart. Computer software then converts this measured frequency into a flow velocity.

The equipment is bulky and difficult to transport. A simple modification has been made to the support arms allowing them to be split into shorter sections. The sensor was proven during the asymmetric flow project ECSC Contract Number 7210.PR/142<sup>(2)</sup> and will not be further modified.

## MEFOS

### Working principle of sensors

As previously mentioned the principle with the SEN flow sensor and the meniscus velocity sensor are closely correlated to the measurement of the Lorentz force which is introduced when a conductor is moving in a magnetic field. This electromagnetic induction of current and its interaction with the magnetic field render the possibility to measure the steel velocity. The Lorentz force describes the interaction between the sensor and the liquid metal. The theory is explained below, see Fig. 15.

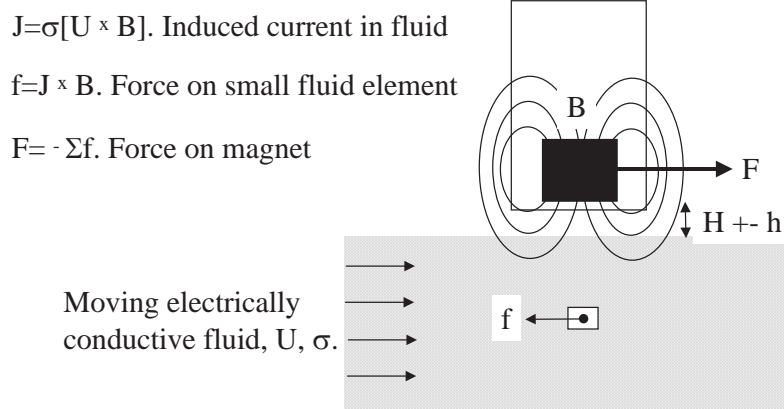


Fig. 15: Theory of the electromagnetic sensors exemplified by a schematic description of the meniscus velocity sensor (MEFOS)

If a permanent magnet or a coil emits a magnetic field,  $\mathbf{B}$ , and an electrically conducting fluid moves in a magnetic field eddy currents,  $\mathbf{J}$ , are created in the fluid as presented in Equation 1.

$$\bar{\mathbf{J}} = \sigma[\bar{\mathbf{U}} \times \bar{\mathbf{B}}] \quad (1)$$

Where  $\sigma$  is the electrical conductivity of the fluid and  $\bar{\mathbf{U}}$  is the velocity vector of the fluid. From this equation it is clearly shown that the electrical conductivity of the fluid as well as the velocity of the fluid and the amplitude of the magnetic field has an important effect of the eddy current. A force directed against the fluid motion is created in a small volume element as seen in Fig. 15. This force may be described according to Equation 2.

$$\mathbf{f} = (\bar{\mathbf{J}} \times \bar{\mathbf{B}}) \quad (2)$$

This force will also act on the magnet and will be directed parallel to the motion of the fluid. The total force acting on the magnet may be calculated by integration of the sum of the volume penetrated by the magnetic field according to Equation 3 which is also clearly illustrated in Fig. 15.

$$\mathbf{F} = -\int \mathbf{f} \partial v \quad (3)$$

Theory states that there is a direct proportionality between the velocity, electrical conductivity and the total force. Special calibration equipment was used in conjunction with the development of the different electromagnetic sensors. The calibration equipment consists of a rotating disc where the actual velocities may be calculated at different radii thereby facilitating a factor to recalculate the sensor output to a velocity. The calibrating rig is presented in Fig. 16. Originally this calibration rig was constructed in the previous project<sup>(5)</sup> to be used with a rotating aluminium disc. In this project some modifications of the calibration rig were performed facilitating the use of an especially cast disc of MCP-137. MCP-137 is a low melting point material used in the physical model described in Task 1.7.



Fig. 16: Calibration rig set up for calibration of the meniscus velocity sensor with a rotating disc of MCP-137 (MEFOS)

Figure 17 shows the impact of the electric conductivity of the conductor on the eddy current,  $\bar{J}$ , which has a strong impact on the signal response of the sensor. Solid aluminium has a significantly higher conductivity than the alloy MCP-137. It needs to be pointed out that the solid MCP-137 has approximately the same electrical conductivity as liquid steel.

#### Comparison between output signal from the sensor

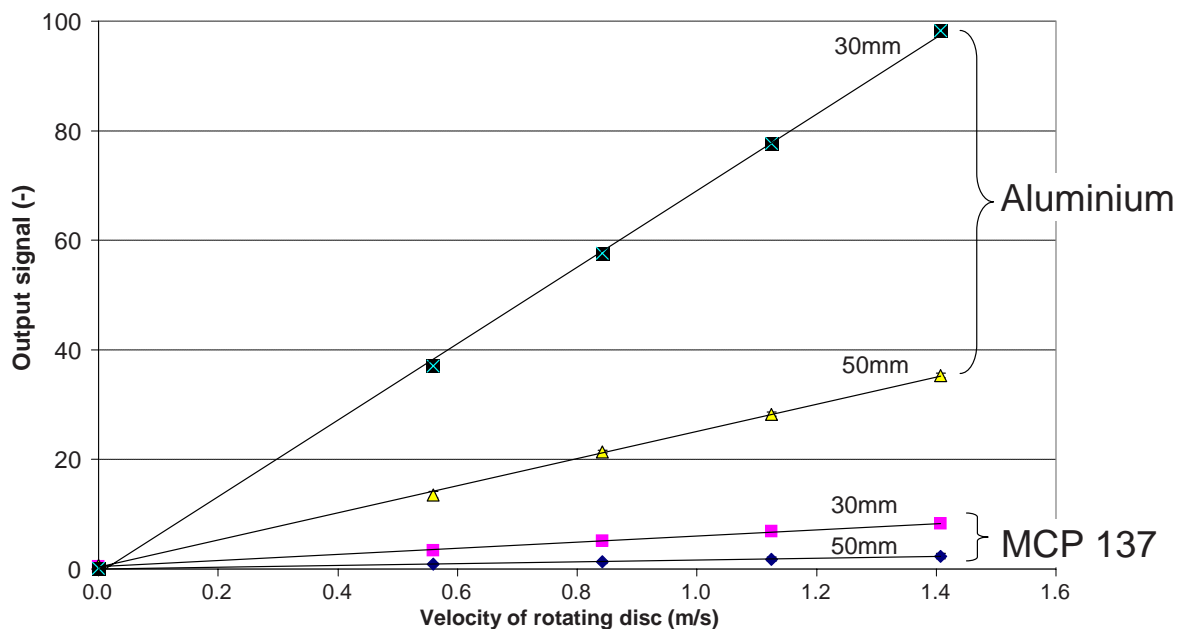


Fig. 17: Difference in signal response between a rotating aluminium disc and a rotating disc of alloy MCP-137 (MEFOS)

From Equation 3 it is also shown that the distance between the magnetic field and the conductor is an important parameter since an increase in distance will decrease the magnetic field strength which will decrease the force. This fact is clearly illustrated in Fig. 17 as well as in Fig. 18 from the calibrations of

one of the meniscus velocity sensors. It needs to be pointed out that the actual forces were not accessible by MEFOS as MPC only provided the signal strength from the sensor.

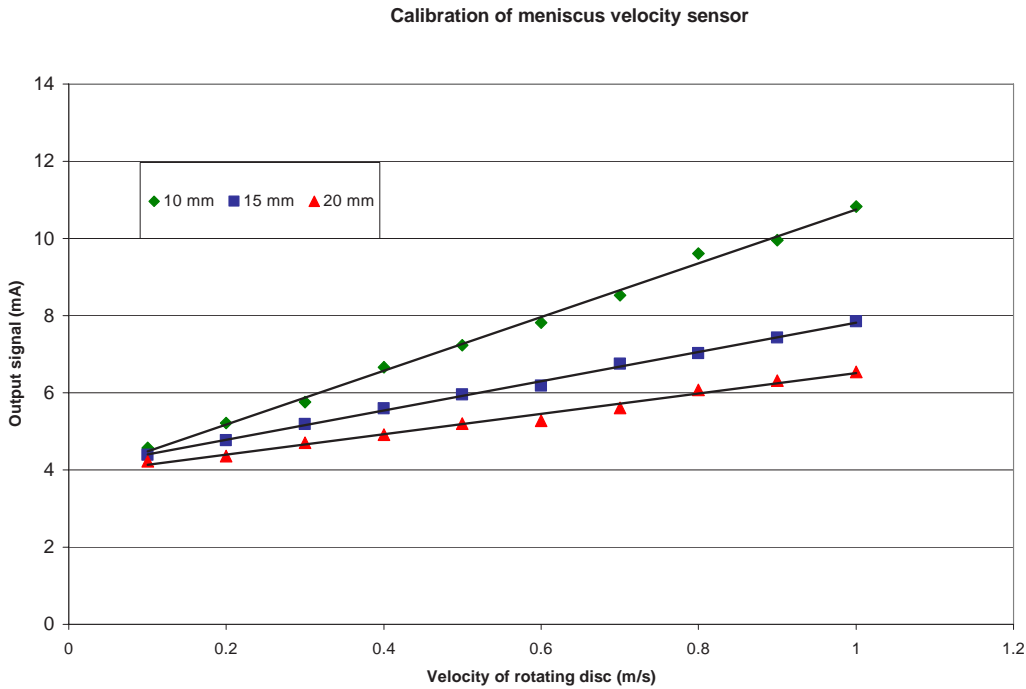


Fig. 18: Calibration of meniscus velocity sensor using a rotating plate of alloy MCP-137 in the calibration rig at MEFOS (MEFOS)

From Fig. 15 it may be shown that the meniscus velocity sensor would give both information of direction and velocity of the steel flow in the mould in contrast to the SEN flow sensor which only provides the vertical steel velocity in the SEN.

In the present study MPC has not provided any detailed information on how the force is actually measured inside the SEN flow sensor as well as the meniscus velocity sensor. It may be noted that MPC has developed the different sensors with the purpose of making the sensors commercially attractive to the market. Further, it may be mentioned that MPC did not have any financing from the present project. MEFOS can therefore not present any details on the mechanical systems incorporated in the sensors. From Figs. 17 and 18 it is clearly seen that the recorded signal from the different sensors are a function of the magnetic field, the velocity, the electrical conductivity as well as the distance between the sensors and the measured conductor. One important task for MEFOS together with the assistance of MPC in the current project was to improve the signal strength from the different sensors. During the scope of the work different factors were addressed.

As mentioned earlier the electrical conductivity has a great impact on the measured forces attained in the sensors, see Equation 1. This is also clearly illustrated in Figs. 17 and 18 from the calibration trials where the signal ratio is much higher for aluminium than for the selected alloy, MCP-137. This is mostly due to the electric conductivity of aluminium being much higher than the alloy. The values for both solid and liquid aluminium, MCP-137 and steel are presented in Table 1. It is evident that the electric conductivity is in the same order of magnitude for liquid steel and MCP-137, as shown in Equation 4. It was therefore assumed that the alloy would be suitable to represent liquid steel in the physical model with respect to the electrical conductivity.

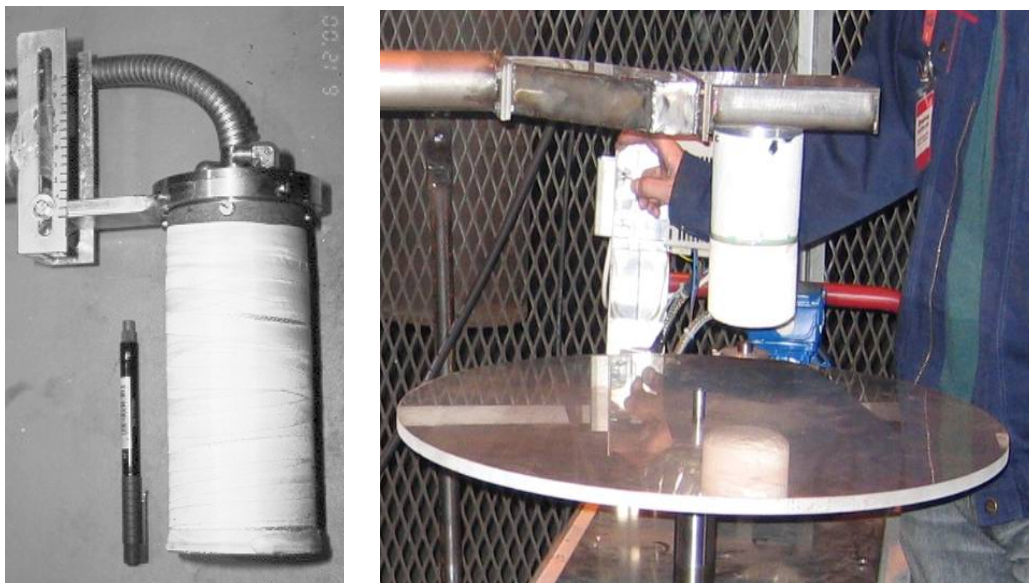
$$\sigma_{\text{alloy, liquid}} \approx 1.4 \sigma_{\text{steel, liquid}} \quad (4)$$

Table 1: Electrical conductivity (MEFOS)

	$\sigma$ (1/ $\Omega$ m)	Reference
Al (solid)	$9.2 \cdot 10^6$	6
Al (liquid)	$4.5 \cdot 10^6$	6
MCP-137 (solid)	$1.7 \cdot 10^6$	7
MCP-137 (liquid)	$1.0 \cdot 10^6$	7
Steel (solid)	$0.8 \cdot 10^6$	6
Steel (liquid)	$0.7 \cdot 10^6$	6

It is clear that the velocity of the fluid in the mould and the electrical conductivity of liquid steel cannot be changed, thus the efforts for improving the signal strength must be by increasing the magnetic field and decreasing the distance between the sensor and liquid steel or alloy. MPC has stated that it uses one of the strongest magnetic materials available in the new sensors. As a consequence, the most important factor that could be addressed during the present study was the distance between the sensors and the fluid. When the distance between the sensor and the liquid steel decreases cooling of the sensor becomes critical.

The use of a physical model with a low melting alloy, MCP-137, has been employed for the basic design of the different sensors thereby drastically reducing the demand of cooling during the development. The development and construction of the physical model is thoroughly presented in Task 1.7. Figure 19a shows the original meniscus velocity sensor<sup>(2)</sup>. Figure 19b shows the enhanced meniscus velocity sensor developed by MPC.



Figs. 19a and 19b: Original and enhanced meniscus velocity sensors (MEFOS)

## Task 1.6 - Adaptation of ultrasonic sensor at caster

### Saarstahl

The development of the ultrasonic system discussed in Task 1.2 included the installation of a permanent data acquisition system on the caster at Saarstahl.

Two major layouts for adaptation of ultrasonic sensor at the caster have been intensively discussed:

1. Mounting of the sensor at a movable support mounted at the casting platform, or
2. Mounting of the sensor at the bottom of the tundish at both sides of the SEN.

These are shown in Fig. 20 together with a schematic plot of the data acquisition and control system developed by BFI.

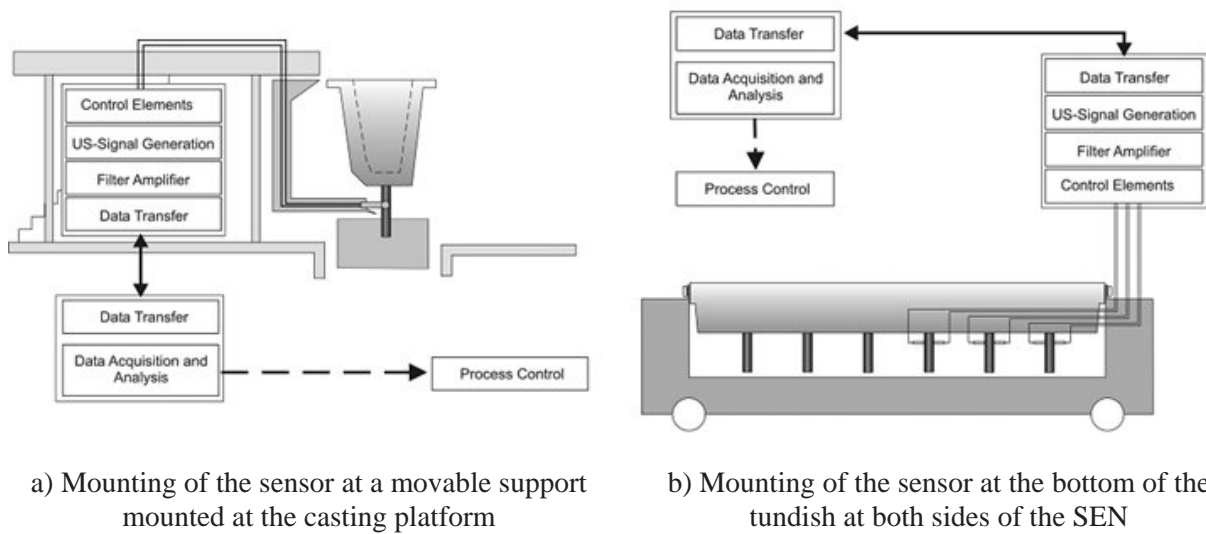


Fig. 20: Possible layouts of the ultrasonic sensor system (Saarstahl)

The preferred layout, b, provides the benefit of more precise alignment of the sensor heads to the SEN and the working conditions in front of the tundish will not be affected during casting by a movable support structure. However, this will mean that the sensor system will have to be mounted prior to tundish preheating. The insulation and cooling must be capable of withstanding conditions during the preheating phase.

The adaptation of the ultrasonic sensor at the Saarstahl AG caster was performed in several steps, partially to take into account the experience derived from the first plant trials, and partially because of the need to react to alterations at the continuous casting machine which resulted in changes in the geometric conditions. The hardware in the area of the SEN (sensor, coupling rods etc.) for an automatic ultrasonic measurement system has been developed; some problems had to be solved concerning the electrical supply including the data transfer and handling. The BFI's automatic stationary ultrasonic system was installed on one strand of the continuous caster no. 4 of Saarstahl AG (SAG). An appropriate position of the data acquisition system at the casting platform was chosen near the strands and all preparations to connect it with the supply lines in the steel plant were done by SAG's Construction Department. The necessary switchboard was designed and built as shown in Fig. 21.



Fig. 21: Data acquisition system (Saarstahl)

Independent of these preparations new sensor heads were constructed by BFI as described in Task 1.2. To fit these new sensors to SAG's casting machine, modified sensor holders were built in SAG's workshop to fix the sensors on both sides of the submerged entry nozzles underneath the tundish bottom. These were shown in Fig. 7.

During the development of the stationary ultrasonic system, plant trials in collaboration with BFI continued in the form of campaigns with BFI's mobile measurement system.

### **Task 1.7 - Design and construction of physical model of casting nozzle using circulating low temperature liquid metal**

#### **MEFOS**

The design of the physical model was a full-scale model of a submerged entry nozzle and a mould based on the actual continuous caster used at SSAB Tunplåt in Luleå for the production of slabs. When a physical model is used to investigate any industrial phenomena or process it is important to assure that the similitude of the model matches the real system.

As previously mentioned a low melting alloy, MCP-137, was chosen to simulate the liquid steel in the model. The alloy has the eutectic composition of the bismuth (58 wt-%) and tin (42 wt-%) system with a melting point of 137 °C. The density of the alloy is 8580 kg/m<sup>3</sup>. This alloy was chosen over other low melting alloys containing cadmium and/or lead, which have an even lower melting point due to the toxicity of these alloys. By choosing an alloy with a melting point of 137 °C a great deal of effort had to be carried out with respect to electric heating and the insulation of the physical model. The total amount of the low melting alloy in the model is approximately 2.2 tons which corresponds to a volume of 0.25 m<sup>3</sup> liquid metal.

The model was constructed in stainless steel as one of the requests was to use non-magnetic material to prevent the influence on the different sensors.

The cross-sectional area of the mould was chosen to correspond to the smallest actual width in the caster at SSAB, 800 mm. During the design it was also decided that actual submerged entry nozzles used at SSAB should be used in the model. Further, the height of the liquid metal in the tundish would

be the same as in the tundish used at the caster; however, the volume of the tundish in the model was much less than the actual tundish. The total volume of the model tundish is 42 dm<sup>3</sup> and the metal height can be varied between 700 to 900 mm in the current configuration. The model tundish was also equipped with an overflowing controlled system at the height 920 mm which would activate an automatic emergency stop of the whole model.

This results to a geometrical scaling factor of 1:1 between the physical model and the actual caster. This was one of the main goals during the design and construction of the model. However, the most common way to assure that the physical model describes the real system in an accurate way is by investigating dimensionless number between the model and the real system.

The Froude number is a function of the geometrical set up of the model with comparison with the real system and the scale ratio 1:1, which implies that Froude number is satisfied, see Equation 5.

$$Fr = \frac{V^2}{gd} \quad (5)$$

V: velocity (m/s)

g: acceleration due to gravity (m/s<sup>2</sup>)

d: diameter (m)

Dynamic similarities may also be of interest when comparing a physical model with a real system. Generally we are balancing force ratios between the model and the prototype to maintain similitude. Dynamic similarity ensures that the interactions between the forces which occur in the model will occur in the same fashion in the actual system. This analysis is normally used by analysing the Reynolds number, see Equation 6.

$$Re = \frac{Vd\rho}{\mu} \quad (6)$$

V: velocity (m/s)

d: diameter (m)

$\rho$ : density (kg/m<sup>3</sup>)

$\mu$ : viscosity (Ns/m<sup>2</sup>)

Due to the lack of experimental information of the viscosity of the MCP-137 alloy at low temperatures it is difficult to use the Reynolds number in the present case. MEFOS initiated contact with a number of laboratories in Sweden and Finland to make viscosity measurements of MCP-137 thereby rendering the possibility to include the Reynolds similarity in the analysis. Unfortunately, none of the laboratories were able to attain reliable and reproducible results. The Reynolds similarity will be further discussed in connection with the flow rate determination of the fluid in the model.

In Fig. 22 the model is shown during the construction work without the electric heating elements and insulation. In the physical model the SEN is mounted to the tundish with the help of a flange from below in contrast to normal practice in the SSAB continuous caster where the SEN is mounted from the top of the tundish. It was therefore important to attain a tight coupling between the SEN and the model. In Fig. 23 the fully constructed model is presented with a mounted SEN from SSAB.



Fig. 22: Physical model during construction (MEFOS)

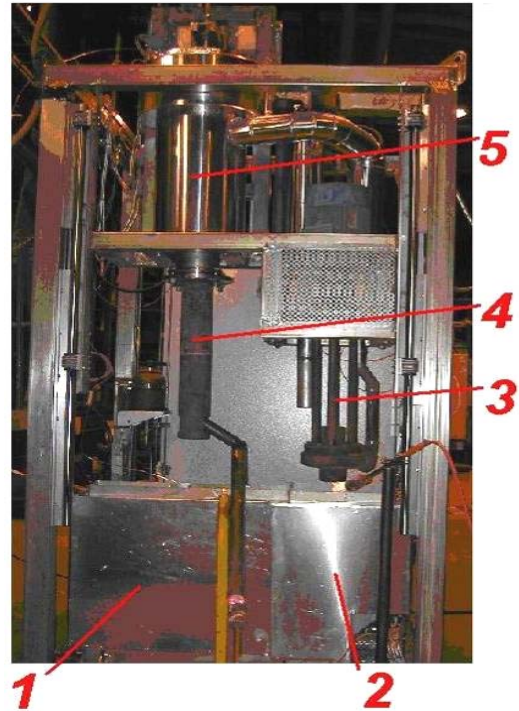


Fig. 23: Physical model. (MEFOS)  
 1: Mould, 2: Pump section, 3: Centrifugal pump, 4: Casting nozzle, 5: Tundish

Extensive functionally tests of the model were performed using water. Initially a specially adapted SEN with an inspection window were planned to be used during the trials. However, extensive air leakage between the SEN and the mounted inspection glass prevented the use of a casting nozzle with an inspection window, as illustrated in Figs. 24a and 24b. During this stage of the model development it was thought that air leakage from the mounted inspection glass was the major air leakage into the SEN. An actual casting nozzle from SSAB was mounted in the model for the duration of all further trials.



Figs 24a and 24b: The inspection window of the casting nozzle without (8a) and with (8b) flowing water (MEFOS)

However, during the further development of the model several sources of air leakages were found both in the manufactured stainless steel stopper rod as well as between the SEN and the model. These air leakages were not detected during the initial functionality tests using water. The different air leakages

detected were addressed during the trial campaigns in the model and will be further discussed in connection with the trials.

The greatest difference between the physical model and an actual casting machine is as previously mentioned the volume of the tundish. The volume flow of the liquid metal in the physical model corresponds to the volume flow of steel in the actual caster at different casting speeds. To achieve a controlled volume flow in the model a pump, originally designed for pumping lead, was used as showed in Fig. 23 item 3.

The metal or water is transported continuously from the mould up to the tundish using the pump. The flow rate of the fluid is controlled by the pump velocity in contrast to the situation in an industrial caster where the steel flow is controlled by the stopper position. Every pump has special characteristics regarding the pump efficiency depending on the fluid in question. The pump characteristics are normally investigated by producing a so-called pumping curve for each related fluid. In order to achieve this, the volume flow has to be measured at a number of different pump velocities. The pump curve is necessary to have a control of the continuously circulated fluid in the physical model. However, as there is no measurement device to measure the volume flow of the liquid metal this had to be achieved by measuring the filling time of a predetermined volume of metal for different pumping speeds. This method of determination of volume flow was developed during the functional tests using water. The controlled volume for determination of the volume flow was chosen at a tundish level of 860 mm thereby avoiding any unnecessary activation of the overflow control system. This was a total volume of  $33.5 \text{ dm}^3$ .

The filling rate of the controlled volume was relatively fast due to the small tundish. The short filling time of the control volume prevented an accurate manual determination of filling time. Therefore the height of metal in the tundish was measured using a laser based system, measuring distances with accuracy on the millimetre scale.

The pump curve for the volume flow of water is presented in Fig. 25 and the corresponding pump curve for MCP-137 is shown in Fig. 26. From these figures it is clearly seen that the pump works more efficiently for the MCP-137 alloy than for water which is what would be expected as the pump originally was designed for pumping lead. The results from these volume flow investigations also show that the method of using a controlled volume combined with a filling time seems to provide accurate descriptions of the pump capacity.

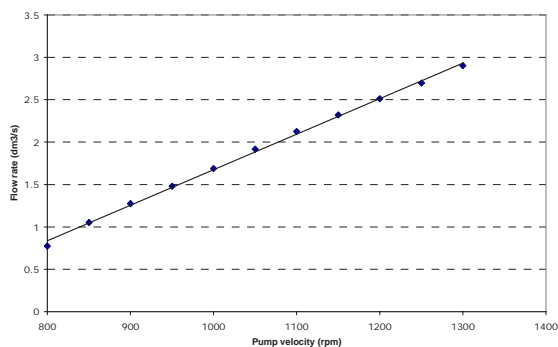


Fig. 25: Volume flow rate of water in the model as a function of pump velocity (MEFOS)

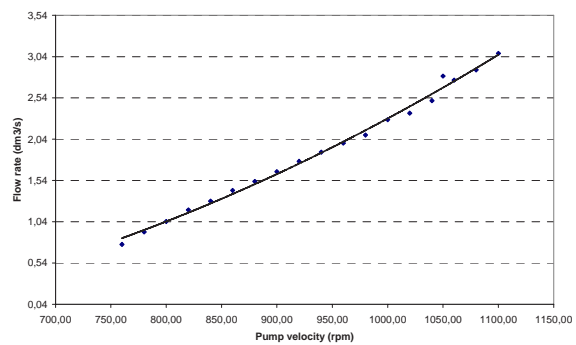


Fig. 26: Volume flow rate of the liquid alloy, MCP-137, in the model as a function of pump velocity (MEFOS)

It may be assumed that the flow of metal through the SEN may be regarded as turbulent due to the high volume rate as showed in both Figs. 25 and 26. As mentioned earlier the normal approach when constructing any physical model includes an analysis of different dimensionless numbers. Due to the lack of experimental information of the viscosity of MCP-137 the similarity in Reynolds number was left out of the design of the model. It may be noted that the similarity in Reynolds number is most important in laminar flow and becomes less important in turbulent flow<sup>(3)</sup> and therefore not considering the Reynolds number would not greatly influence the design of the physical model.

Normally the volume flow rate of liquid metal is not used as a parameter in continuous casting at the steel plant and therefore the flow rate was recalculated to casting speed using the geometry of the mould, see Fig. 27.

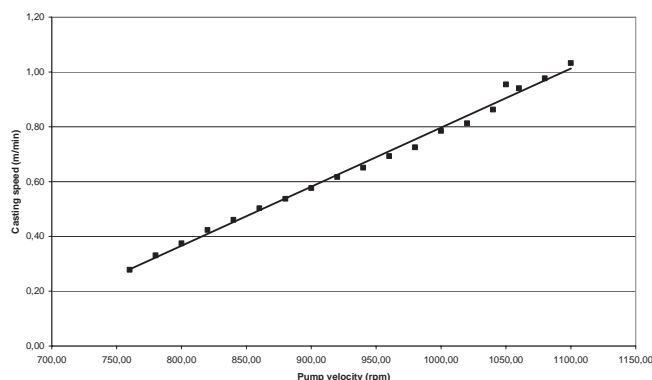


Fig. 27: Casting speed of the liquid alloy in the model as a function of pump velocity (MEFOS)

As seen from Figs. 26 and 27 a disturbance of the pumps performance is seen at ~1050 rpm which corresponds to a casting speed at approximately 1.0 m/min. This may be due to some mechanical problems with the pump as the disturbance is not shown in Fig. 25. The disturbance may be related to the density of the fluid. However, as the disorder of the pump performance occurred in a narrow range no further attention was addressed to this issue.

As mentioned earlier, in an industrial caster the flow rate of the fluid is controlled by the stopper position and in the physical model is the flow rate controlled by the pump velocity. In order to simulate the real situation in a full-scale caster the height of metal in the model tundish needs to be constant at a specified pump velocity, corresponding to a real casting speed. It is also necessary to have the same height of metal in the model tundish as in the real tundish; the height of steel in the tundish at SSAB has an average value between 850-900 mm. During the model trials it was decided to have a constant metal height in the tundish of 860 mm thereby facilitating the possibility to test the reproducibility of the results. This height was not changed for the remainder of the project.

As mentioned above, a laser based system was developed to measure the upper surface of the fluid in the tundish with an accuracy on the millimetre scale. This system was employed to ensure that the height of the fluid in the tundish was kept constant over time using the stopper rod system. During the initial trials with water the stopper rod position was controlled with an accuracy of 0.1 mm to assure a constant height in the tundish. The system showed a higher sensitivity during the trials with the liquid alloy. In the beginning of the trials with liquid alloy it was not possible to sustain a constant height of metal in the tundish for any longer time period with the stopper rod system used for the water trials. It was necessary to further improve the accuracy of the stopper controlling system to a scale of 0.01 mm. After this improvement no problems were encountered to have a constant metal height in the tundish at different volume flows for several hours.

### Task 1.8 - Physical model trials, simulation of a variety of flow conditions

#### MEFOS

After successful water trials the model was filled with the alloy and the function tests were repeated. The process starts by melting the metal in the mould and pumping section. At the same time the pump and submerged entry nozzle were preheated using burners to a temperature of 180-200 °C. As the metal is molten, the upper section, which consists of a tundish and a centrifugal pump, is submerged into the bath. The pump is started by a process operator and as soon as the section is in position, it can be regulated at specific velocities. Molten metal will thereby be transported up to the tundish by the pump and continuously delivered into the mould through a submerged entry nozzle and thereby

simulate the sequence of continuous casting. Heating elements in the bottom of the mould prevent the metal from being solidified.

The problem with the air leakage was more severe during the initial trials with MPC-137 as this led to an extensive formation of dross. The dross consisted of approximately 10 percent of oxide phase and the remaining amount of MPC-137. This was concluded after remelting the dross in a stainless steel bucket. During the first trial of the model with MPC-137 the dross formation was 60 kg after running the model for 30 minutes.

The potential sources of air leakage were identified during a systematic investigation. Each of the air leakage problems were addressed separately. This led to an unexpected delay of the physical model trials. It was concluded that the greatest impact on the air leakage were problems with the manufactured stainless steel stopper rod. The stopper rod is a hollow pipe with the exact outer dimensions as the stopper rod used at SSAB which is illustrated in Fig. 28. From the figure it is seen that the stopper rod is equipped with an inner tube facilitating gas injection during casting. This inner tube was plugged as no experiments using gas injection were planned to be performed. The welding at position A and B were not sufficiently performed and air leakage occurred at these positions. After adjustment of the welding, the problem with the dross formation was reduced. However, the performance of the model was not sufficient with respect to the dross formation.

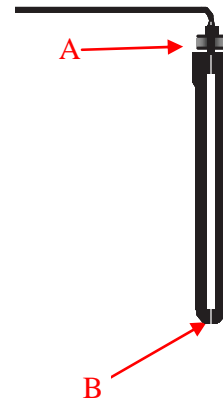


Fig. 28: Schematic illustration of the manufactured stopper rod with the weak welding points marked as A and B (MEFOS)

Another problem occurred related to the mechanical toughness of the whole model. The model displayed a longitudinal oscillation which may have been caused by the difference in pressure through the stopper opening. The model was mechanically stabilised and a hydraulic damper was mounted. This reinforced construction in combination with the damper solved the problem with the oscillation of the model.

The SEN from SSAB which was used in the model is made of ceramic material and during actual casting the SEN was preheated before use in the caster. During preheat, the ceramic material will sinter and thereby become air-tight. It was not practical to use a preheated SEN during model trials. Instead the SENs used during the model trials were treated with water glass to prevent air leakages through any porosity in the ceramic material. The treatment of the SEN with the water glass gave a small improvement regarding the dross formation.

Finally the flange between the SEN and the model was identified as the most significant source of air leakage to address. After an extensive analysis of the problems related to the flange, three major factors were identified as the main sources for the air leakage. The tightening of the flange was limited to the mechanical resistance of the ceramic SEN. Secondly it was found out that the mounting of the head of the casting nozzle was not absolutely circular in the model. It was therefore necessary to modify the head of the casting nozzles used during the trials to get the optimal fit in the model. The last problem that needed to be addressed was to find a suitable sealing material between the casting nozzle and the model in the flange.

Finding a suitable sealing material was the most time consuming part of the functional tests of the model. Different sealing materials and different gasket types were tried out in the model to get an air-tight connection between the SEN and the foundation surface at the bottom of the tundish. It was

somewhat difficult to find a material with an optimal performance at the operational temperature throughout the operation of the model.

By using a special gasket, originally designed for sterilisation of medical equipment an air-tight seal was obtained. With the use of this gasket the dross formation during operation of the model was negligible.

### **Campaign 1**

During the first campaign the height of metal in the tundish and the immersion depth in the mould were kept constant at 0.86 and 0.3 m respectively. The casting speed has been varied between 0.3-1.1 m/min. MPC came to MEFOS with its newly developed sensors which it had calibrated at its own facilities. Both the SEN flow sensor and the meniscus velocity sensor did not give any conclusive results due to low intensity of the signals. Throughout the measurement sequence the dross formation related to air leakages may have been too extensive. This might have influenced the signal intensity of the meniscus velocity sensor. However, the dross formation could not affect the signal output from the SEN flow sensor.

MEFOS and MPC decided that a final calibration of any new sensors would be conducted at MEFOS using the MCP-137 alloy to insure the signal response from the different sensors. Examples of the calibrations have been discussed earlier in conjunction with the development of the sensors, Task 1.5. These calibrations were conducted using the meniscus velocity sensor.

As mentioned earlier a combined measurement with the newly developed SEN flow sensor and the compact laser vibrometer, CLV was also carried out during this first campaign. The working principle of this sensor was presented earlier. Unfortunately the poor performance of the SEN flow sensor prevented any comparison between the two different measuring techniques. However, the CLV sensor provided some interesting results.

The CLV sensor was mounted on a rack and directed towards the surface of the submerged entry nozzle during the experiments. As the motor of the pump creates vibrations, separate measurements were also conducted on the motor during the measurements facilitating compensation for this background noise in the further analysis.

The signal intensity of the laser beam was logged over a frequency spectrum, reaching from zero to 120 Hz, for a total of eight specific flows in the model. The mean signal intensity was calculated as a function of frequency at the different flows to enable detection of which frequencies that provided the clearest intensities. This analysis showed that the clearest signals refer to a frequency span of 0-30 Hz and therefore the higher frequency spans were not used in the further analysis.

One example of the signal output from the CLV sensor at a casting speed of 0.8 m/min for both the SEN and the engine of the pump is presented in Fig. 29.

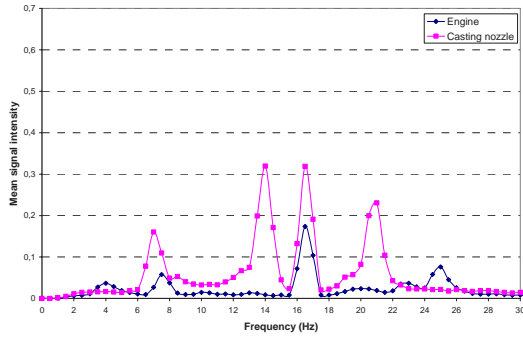


Fig. 29: Measured signal output from the CLV sensor as a function of the frequency at the casting speed of 0.8 m/min. (MEFOS)

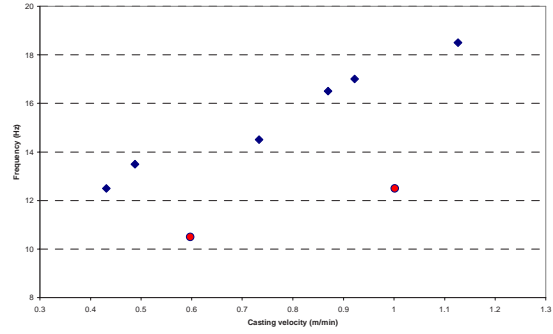


Fig. 30: The frequency of the maximum peak, as a function of casting speed, at the corrected signal from the flow with background noise excluded (MEFOS)

A simplified treatment of the signal intensity was employed by investigating the difference in signal between the CLV and the engine of the pump. For each of the investigated casting speeds the peak with the highest mean signal intensity was identified to study the correlation between the results of the CLV as a function of casting speed, see Fig. 30. A trend of higher frequency at higher casting speeds may be observed in Fig. 30 except for two casting speeds.

The discrepancy observed between the frequency and the casting speed has not been further investigated as the investigations of the current project are focused on the development of electromagnetic sensors. No further trials were performed using the CLV sensor.

## Campaign 2

During the second campaign a totally new SEN flow sensor was delivered by MPC as the previous version of the sensor could not give any useful information. The meniscus velocity sensor had not been altered in any fundamental way according to MPC. MPC informed MEFOS that it had mostly addressed the treatment of the signal output of the sensor in comparison with the equipment used during the first campaign.

The poor results during the first campaign showed the importance of calibration of the sensors before any trials in the physical model was performed. As previously discussed, calibration of the sensors on a rotating disc of MCP-137 was conducted. The results from the calibration of the meniscus velocity sensor have been presented earlier when the development of the electromagnetic sensors was discussed. Three different standoff distances from the sensor to the plate have been investigated, ranging from 10-20 mm, see Fig. 18. With constant distance the output signal becomes nearly linear with the velocity.

Calibration of the SEN flow sensor has been performed using the same rotating disc of MCP-137. On the sensor head a piece of ceramic from a casting nozzle was mounted and therefore, the standoff distance from the sensor to the plate was constant 40 mm, see Fig. 31.



Fig. 31: Calibration of SEN flow sensor in the calibration rig (MEFOS)

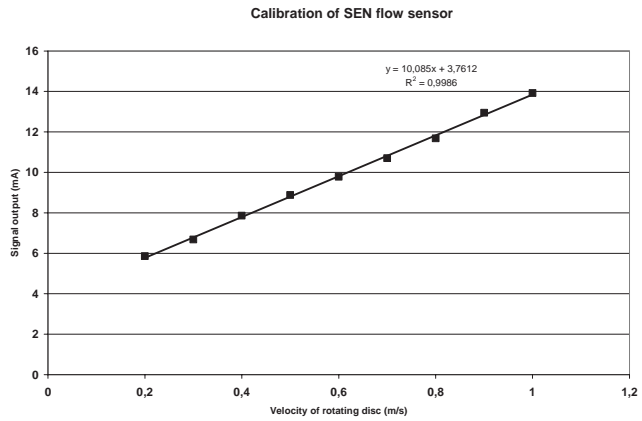


Fig. 32: Calibration of SEN flow sensor (MEFOS)

The output signal of the sensor as a function of the velocity of the rotating disc is shown in Fig. 32. The sensor gives a signal between 4-20 mA.

After the completion of the calibration, experiments in the physical model with the SEN flow sensor and meniscus velocity sensor were performed. The location of the different sensors in the physical model is shown in Fig. 33.

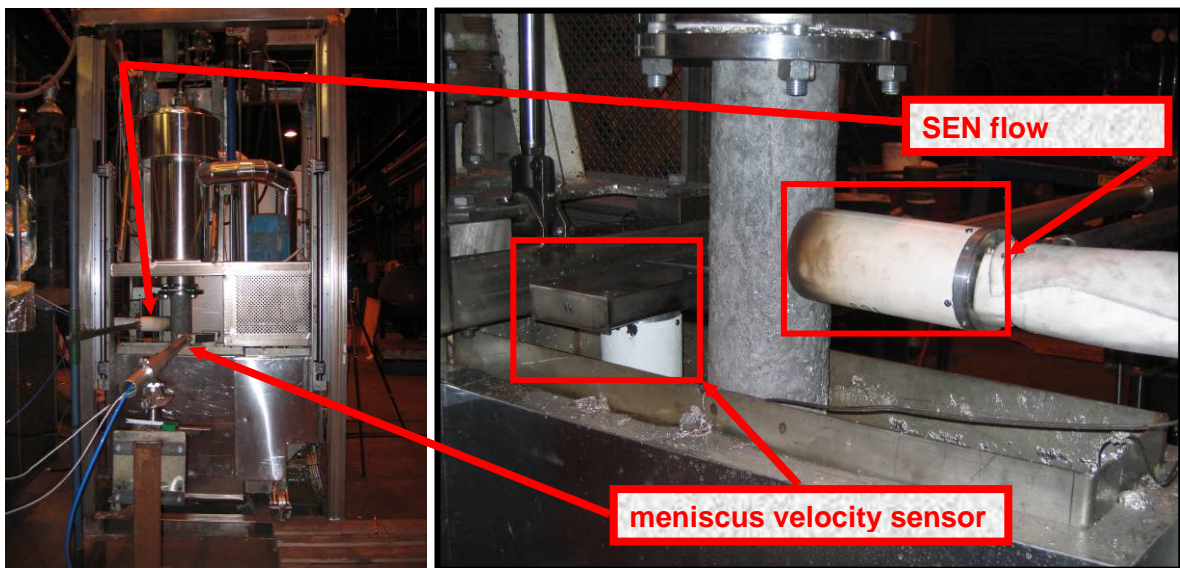


Fig. 33: Placement of the different sensors in the physical model (MEFOS)

In the physical model the meniscus velocity sensor gave a signal but the change in signal is insignificant when the metal flow in the model is increased as clearly shown in Fig. 34. From the figure it is also seen that the sensor was disconnected during the change of casting speed. The poor performance of the meniscus velocity sensor may be due to the formation of dross.

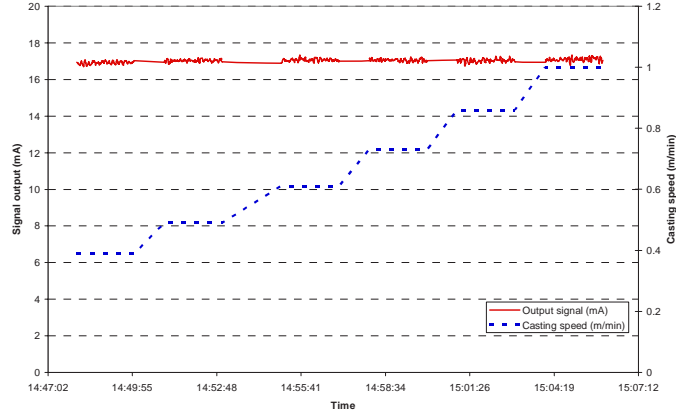


Fig 34: Signal output from the meniscus velocity sensor and casting speed as a function of time (MEFOS)

However, the results from the SEN flow sensor were more promising. The SEN flow sensor was located in the horizontal direction at a constant distance from the SEN, approximately 10 mm. During the trials three sequences with various casting speeds between 0.4-1.0 m/min were studied and the results are shown in Fig. 35.

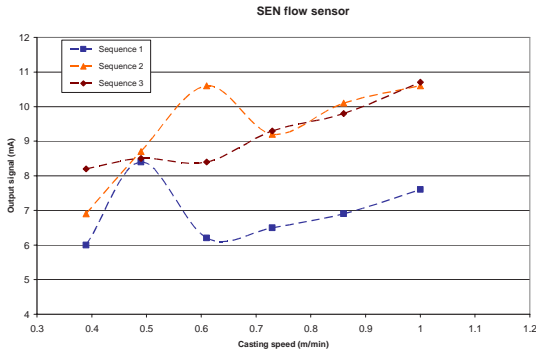


Fig. 35: Output signal of SEN flow sensor as a function of casting speed for three different sequences (MEFOS)

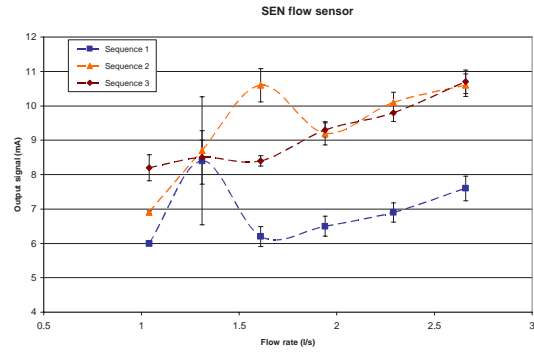


Fig. 36: Output signal of SEN flow sensor, including standard deviation for measured values as a function of metal flow rate (MEFOS)

As seen from the figure the signal is not linear at low casting speeds. One of the reasons may be that at lower casting speeds the casting nozzle is not full. At a casting speed higher than 0.6 m/min corresponding to a metal flow rate of 1.5 l/s the signal may be regarded as linear as shown in Figs. 35 and 36. During normal practice of casting slabs speeds below 0.6 m/min corresponding to low flow rates are not seen at steelworks. It is clearly seen that the signal output from the sensor is substantially lower for sequence 1 in comparison with sequence 2 and 3. MPC was not able to explain this observed phenomenon. One hypothesis is that the mechanical movement inside the sensor was improved during the uses of the sensor. However, as MPC did not provide any information related to the construction of the sensor it is most difficult for MEFOS to actually suggest any conclusions.

By combining the results from the calibration presented in Fig. 32 with the signal output from the different sequences, the velocity in the casting nozzle is known. As the volume flow of the fluid is known a theoretical velocity,  $\bar{v}$ , in the casting nozzle may be calculated according to:

$$\bar{v} = \frac{Q}{A} \quad (7)$$

$\bar{v}$  = velocity in casting nozzle (m/s)  
 $Q$  = volumetric flow of metal (m<sup>3</sup>/s)  
 $A$  = cross section area of casting nozzle, 0.0036 (m<sup>2</sup>)

In Fig. 37, the theoretical velocity is presented together with the velocities determined by the SEN flow sensor for the different sequences. As shown in the figure the theoretical velocity agrees with sequence 2 and 3 at higher flow rates. This implies that the suggested hypothesis of the mechanical movement in the sensor may have an influence regarding the discrepancy between sequence 1 and the two other sequences.

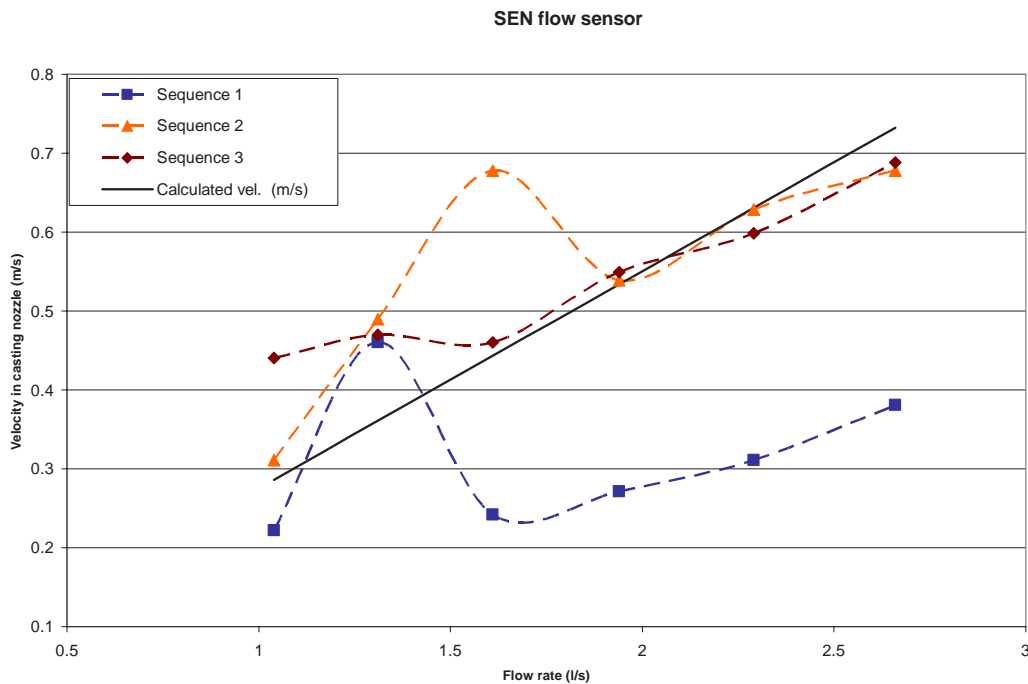


Fig. 37: Calculated velocity in casting nozzle compared with the output signal of SEN flow sensor as a function of metal flow rate (MEFOS)

### Campaign 3

During this campaign one of the main objectives was to improve results from the meniscus velocity sensor. As discussed earlier the formation of dross during the sequence of different casting speeds may have influenced the poor signal output of the sensor. It was determined that minimising the dross formation would be one of the focal points during campaign 3. Minimising the dross formation in combination with the most promising results from the second version of the SEN flow sensor used during campaign 2 would render the possibility to do simultaneous measurements with both sensors.

As discussed earlier, MEFOS addressed all different sources for dross formation and did extensive functional tests of the physical model. The final tests showed that the dross formation was reduced to extremely low levels. Even after running the physical model for several hours at constant casting speeds the total amount of dross did not exceed 2-3 kg. This facilitated excellent conditions for investigation of the different sensors.

MEFOS prepared the physical model for trials with both sensors from MPC and trials were planned to be executed. Unfortunately MPC informed MEFOS in short notice that it did not have the possibility to provide any sensors for the planned trials. The main reason for this may have been that MPC AB was purchased by Agellis AB thereby changing the commercial motivation in the development of the sensors. This resulted in that no results could be obtained during this campaign.

## **Work Package 2 - Plant Trials**

The objective of Work Package 2 was to carry out extensive production plant trials to gather data from all available sources.

### **Task 2.1 - Trials using electromagnetic sensor**

#### **Corus**

Trial using the electromagnetic SFV single and multiple frequency sensors were carried out on the slab caster at Corus Scunthorpe Works. Thirty-five sets of measurements were carried out in total, twenty-seven (82 ladles) using the single frequency and eight (30 ladles) using the multiple frequency devices. A summary of trials carried out at Corus is given in Table 2.

During trials sensor faults have occurred on a number of occasions in the single frequency sensor. In one set of measurements a total failure of the sensor occurred. The other faults resulted in the failure of one of the peripheral receiver coils. The central receiver that is directly opposite the transmitter and provides the majority of information remained operational and thus the trials were not significantly affected. The faults were traced and repaired. Minor modifications were made to reduce the risk of them reoccurring.

During the trials carried out using the multiple frequency sensor, the device operated as expected. The sensor outputs each are to be directly comparable to the output of the single frequency device.

The sensor signal data were combined with available plant casting data for analysis.

Several trials were significantly longer than previous experience<sup>(1)</sup>. Trials of up to 500 minutes in duration were successfully completed. The sensor performed correctly throughout these extended trials. The insulation survived intact with only some small degradation of the glass string holding it in place. Thermal stability during the trials was very good. Once thermal stability had been reached, approximately 7 minutes into the cast, coil temperature variation was within 2 °C for the majority of the trial.

During the trials carried out using the multiple frequency sensor the device operated as expected. The sensor outputs each appear to be directly comparable to the single frequency device.

Table 2: Summary of Corus trials (Corus)

Trial Number FLOWVIS	1	2	3	4	5	6	7
No. of Ladles	2	1	2	2	-	2	1**
Total Casting Time (mins)	200	65	130	144	-	116	115
Trial Number FLOWVIS	8	9	10	11	12	13	14
No. of Ladles	3	2	2**	2	7	4	1
Total Casting Time (mins)	180	12	222	120	500	279	67
Trial Number FLOWVIS	15	16	17	18	19	20	21
No. of Ladles	4	5	6	2	5	1	2
Total Casting Time (mins)	210	407	461	200	303	72	129
Trial Number FLOWVIS	22	23	24	25	26	27	28
No. of Ladles	4	2	6	2	7	5	4
Total Casting Time (mins)	264	126	316	115	350	287	215
Karmen Vortex Measurements			3	1	3	0	0
Trial Number FLOWVIS	29	30	31	32	33	34	35
No. of Ladles	2	3	4	2	4	2	4
Total Casting Time (mins)	113	161	237	115	250	105	220
Karmen Vortex Measurements	1	2	4		4	2	4

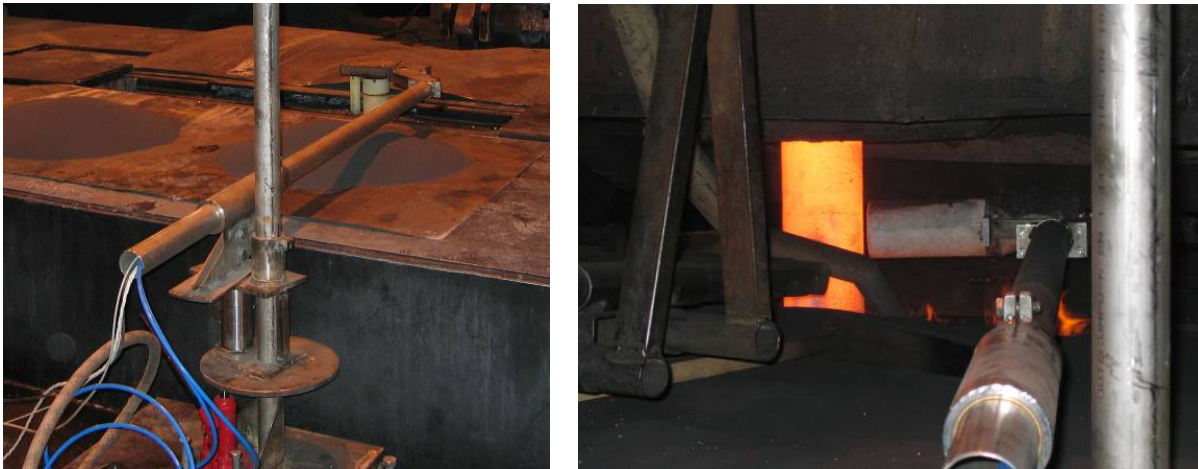
\*\*Strand failure resulted in entire cast being cast through one strand

## MEFOS

Originally it was planned to perform plant trials at SSAB Tunplåt in Luleå in conjunction with the different research campaigns in the physical model. As presented in Work Package 1 neither of the MPC electromagnetic sensors could provide any useful signal output during the first research campaign in the physical model and it was therefore decided that there would be no plant trials. The unavailability of sensors from MPC also meant that no trials were carried out in conjunction with the third campaign. However, in conjunction with the second research campaign the promising results from the SEN flow sensor led to plant trials at SSAB Tunplåt AB using both sensors.

During the industrial trials the casting speeds were varied between 0.99-1.2 m/min. Unfortunately, no simultaneous measurements using both electromagnetic sensors could be performed without severe interference with the operational practice at SSAB. A number of different ways to mount both sensors were investigated but it was not possible to find a suitable solution without disturbing the steel production.

The different sensors were mounted on mechanical arms rendering the possibility of easily removing the equipment if problems with the process were to arise. The assembly with the mechanical arms is illustrated in Figs. 38a and 38b for the meniscus velocity sensor and the SEN flow sensor respectively.



Figs. 38a and 38b: Mechanical arm with meniscus velocity sensor and SEN flow (MEFOS)

As mentioned above, plant trials with the SEN flow sensor were conducted in conjunction with the second research campaign in the physical model. The largest difference between the experimental set up between the physical model and plant trials was the amount of air flow through the sensor. The equipment was mounted at the caster between two different casting sequences. Unfortunately, the equipment did not record any signals from the sensor at the elevated temperatures that occurred during the plant trials. The SEN flow sensor was taken back to MPC. MPC performed fault tracing of the sensor and concluded that the cause of the absence of a signal was overheating of the sensor. MPC reported that the cooling effect of the air did not reach the bottom of the sensor. This resulted in overheating of the material in the sensor thereby hindering the motion of the magnet. MPC reported to MEFOS that it had addressed the cooling problems of the SEN flow sensor and would deliver it to MEFOS during the third campaign in the physical model. However, as mentioned earlier the purchase of MPC by Agellis may have changed the commercial focus in the development of the sensors and as a consequence no sensors could be delivered to MEFOS after these plant trials.

## Task 2.2 - Trials using ultrasonic sensor

### BFI/Saarstahl

The ultrasonic sensor system was applied to operational practice at one strand of a six-strand billet caster of SAG. An overview of the performed plant trials is given in Table 3. At the trials marked with grey no usable ultrasonic data could be gained. During the first four trial campaigns SENs with machined areas were used. The sound propagation through these SENs is different than the propagation through an unmodified SEN. Therefore these ultrasonic data could not be used for analysis. After the major redesign of the data acquisition system three additional measurement campaigns were needed to put the ultrasonic system back into operation. In total 10 sequences were measured, and a total of 40 ladles cast.

Table 3: Ultrasonic system - production plant hot metal trials (BFI/Saarstahl)

Seq. Nr.	Char. Nr.	Quality	Comment	Seq. Nr.	Char. Nr.	Quality	Comment
old system, machined SEN				10	29	C8C	
0	0	41 Cr			30	C8C	
1	1	30MnVS6			31	C10C	
	2	30MnVS6			32	C10C	
	3	30MnVS6			33	C10C	
2	4	37Cr4		11	34	C80	
	5	37Cr4			35	C80	
3	6	44SMn28			36	C80	
	7	44SMn28			37	C78	
					38	C78	
new system, tapered coupling rod				Installation of automatic data acquisition system			
4	8	20 MnCr 5	no coupling due to piece of fibre remained between coupling rod and SEN	n/a			broken sensor cable
	9	20 MnCr 5		n/a			insufficient coupling
	10	20 MnCr 5		n/a			no measurement data stored
	11	20 MnCr 5					
5	12	20MoCrS 4		12	39	C45E	
	13	20MoCrS 4			40	C45E	
6	14	25CrMoS 4	breakthrough during casting start		41	C45E	
	15	25CrMoS 4			13	42	23MnB 4
7	16	C60Pb			43	23MnB 4	
	17	C60Pb			44	23MnB 4	
	18	C60Pb			45	23MnB 4	
8	19	20 MnCr 5			46	23MnB 4	
	20	20 MnCr 5		14	47	C4C	
	21	20 MnCr 5			48	C8C	
9	22	C92D			49	C4C	
	23	C92D			50	C4C	
	24	C92D			51	C4C	
	25	C92D		15	52	20MnB 4	
	26	C92D			53	20MnB 4	
	27	C92D					
	28	C92D					

The mobile data acquisition system was used for the first plant trials and for the laboratory trials addressed in Work Package 3. During the project the mobile data acquisition system was replaced by an equivalent plant adapted permanent installed data acquisition system.

Trials with different steel grades were performed and correlated with actual casting conditions and the product quality in terms of cleanliness. These long-term operational trials lasting whole casting sequences were carried out throughout the entire proposed project time. Recorded data from these trials were applied to WP 3 - WP 6 in order to develop and improve the new on-line monitoring system at the caster and to verify the proposed process enhancements. Thereby, the work of BFI was mainly focused on data acquisition considering ultrasonic signals, steel grades and casting conditions whereas the work of SAG was mainly focused on collecting data of selected steel samples related to product quality in terms of cleanliness.

### **Task 2.3 - Trials using pressure sensor**

#### **Sidenor**

Thirty-five trials were carried out on the Basauri billet caster CCM2 using pressure sensors, a total of 122 heats. The trials using the pressure sensor had the following objectives:

- Corroborate the results obtained during the project 7215.PP/045<sup>(1)</sup> concerning the nozzle inner pressure characterisation as a function of some critical parameters such as air-tight condition of the stopper gas feeding circuit, gas flow rate and casting speed.
- Verify the correlation obtained in the previous project concerning the link between the nozzle inner pressure and clogging extent at nozzle exit.
- Investigate the effect of the nozzle inner pressure on the mould level stability.
- Further study of the influence of the nozzle inner pressure over the steel flow pattern through the nozzle and the analysis of possible reasons for changes in those steel flow conditions.

Due to the critical importance of the air-tight condition of the gas feeding circuit through the stopper for the reliability of the inner pressure measurements, an experimental pin-bolt stopper was used during these trials in order to guarantee an optimum tightness condition.

### **Task 2.4 - Trials using SEN thermocouples**

#### **Sidenor**

Thirteen trials were carried out using thermocouples for the characterisation of the nozzle surface temperature throughout casting time aimed to find correlation between nozzle surface temperature pattern and nozzle inner clogging. Additionally, hints concerning the characterisation of the steel flow patterns within the nozzle were also pursued to complement the information from the pressure trials and the trials using a mould monitored with thermocouples.

### **Task 2.5 - Trials using instrumented mould**

#### **Corus**

As detailed in Task 2.1 a number of trials have been carried out at Corus Scunthorpe Works slab caster using the electromagnetic SFV sensor. The slab caster at Scunthorpe has a thermocouple based Mould Thermal Monitoring system (MTM). The main function of this system is the automated detection of potential sticker breakouts by using an array of thermocouples embedded in the copper plates of the mould. A secondary function of this system uses temperatures measured in the end plates to give an index that indicates the degree of asymmetric or unstable flow in the mould. Where available, data from this system have been extracted for direct comparison with the output of the trial sensors.

#### **Sidenor**

The study of the relationship between pressure conditions in the steel flow jet and the meniscus thermal behaviour was carried out by means of using moulds monitored with thermocouples (IM). The inclusion of this technique in the industrial trials aimed to provide more information concerning the steel flow conditions aiming to correlate the steel duct inner pressure conditions and the in-mould solidification conditions, namely, mould thermal flux and meniscus thermal behaviour and stability. Fourteen trials were carried out which included forty-seven individual heats.

## Task 2.6 - Trials using mould flow sensor

### Corus

Measurements have been taken using the Karmen Vortex mould flow velocity sensors during thirteen of the casting trials carried out.

The probe consists of a refractory rod, which is dipped into the mould. During the measurement, the refractory is eroded by the action of liquid metal and mould powder limiting the measurement time to approximately 8 minutes. The probes are placed in pairs one on either side of the SEN allowing a direct comparison of mould surface flow velocity to be made. During the thirteen trials a total of thirty-three individual measurements were made.

### MEFOS

As reported above plant trials at SSAB Tunplåt in Luleå were performed in conjunction with the second research campaign in the physical model.

The meniscus velocity sensor was mounted during a repair stop at the caster. In contrast to the SEN flow sensor the level sensor used together with the meniscus velocity sensor needs to be calibrated in the mould before usage, see Fig. 39. The calibration of the equipment was performed by placing an aluminium plate at the top of the mould thereby fixing the position of the sensor relative to the mould. This is clearly shown in Fig. 38a which also shows the attachment of the mechanical arm.



Fig. 39: Calibration of the level sensor used together with the meniscus velocity sensor in the mould (MEFOS)

The meniscus velocity sensor was able to resist the elevated temperatures and it was possible to record signal output from the sensor during the duration of the plant trials. The results of the signal output from the sensor is presented in Fig. 40 together with the mean value of the actual casting speed from SSAB computer based control system as a function of time. The total time of the measurements presented in the figure was approximately one hour and the casting speed was varied in three different levels.

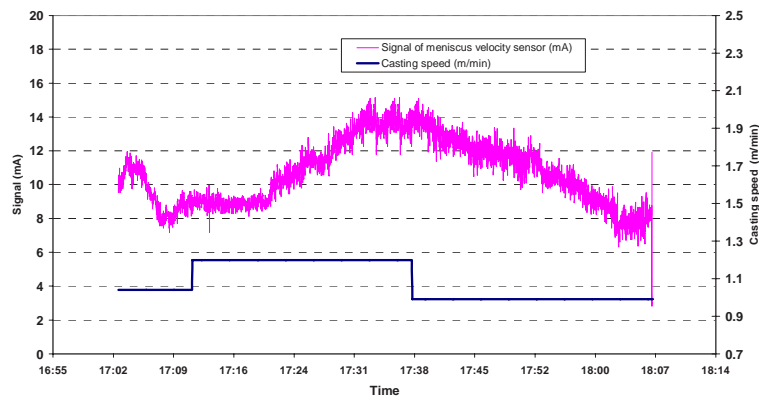


Fig. 40: Signal of the meniscus velocity sensor (MEFOS)

As seen from Fig. 40 it is very difficult to see any correlation between the recorded signal from the sensor and the change in casting speed. It may also be deduced from the figure that the signal seems to oscillate with time. However, it is difficult to provide any conclusions related to these small deviations of the signal output from the sensor.

Another observation from the plant trials was the attachment of casting powder on the, see Figs. 41a and 41b. The attachment of a magnetic material on the sensor housing may influence the extension of the magnetic field and thereby affecting the motion of the magnet.



Figs. 41a and 41b: Casting powder on the house of the meniscus velocity sensor (MEFOS)

### Work Package 3 - Assessment of Trial Data

The objective of Work Package 3 was to assess all trials data from diverse sources.

#### Task 3.1 - Product quality assessment - surface

##### Corus

In order to compare measured flow conditions with surface quality it was necessary to attempt to generate a link between casting conditions and actual product quality. Initially it was proposed that this could be done using automatic on-line strip surface quality measurements however due to circumstances beyond the control of the project it was not possible to carry out trials on the caster associated with strip production. As mentioned in Task 2.1 trials at Corus were carried out on the Scunthorpe slab caster.

It was proposed that the as-cast slab be inspected in the slab yard. A small number of slabs were inspected in this manner but it became quickly apparent that the logistics were difficult and results poor.

To generate more comprehensive data it was decided to consider data from down stream processing. A large proportion of the output of the slab caster is processed to plate at the Scunthorpe Heavy Plate Mill. Details have been obtained of all surface quality issues in finished plate which can be linked to casting defects which have led to the finished product being rejected or dressed for all trial casts processed at the plate mill.

Of the thirty-five trial casts at least partial plate quality data was obtained for twenty-one, of those data for the whole cast sequences were obtained for nine. It was decided to concentrate only on the complete sequences. The plate surface quality data identified individual plates, which exhibited surface defects that could be related to as-cast slab surface quality issues. Using as-cast slab length and casting speed, along with known slab cut positions it was possible to build up a map of periods of casting which led to defects in the finished plate which could be related back to the measurements taken by the electromagnetic steel flow visualisation sensor, and other process parameters. The main plate surface defects identified with as-cast surface features include transverse cracking, longitudinal cracking, spongy cracking and blister.

Figures 42 and 43 show examples of these defect maps.

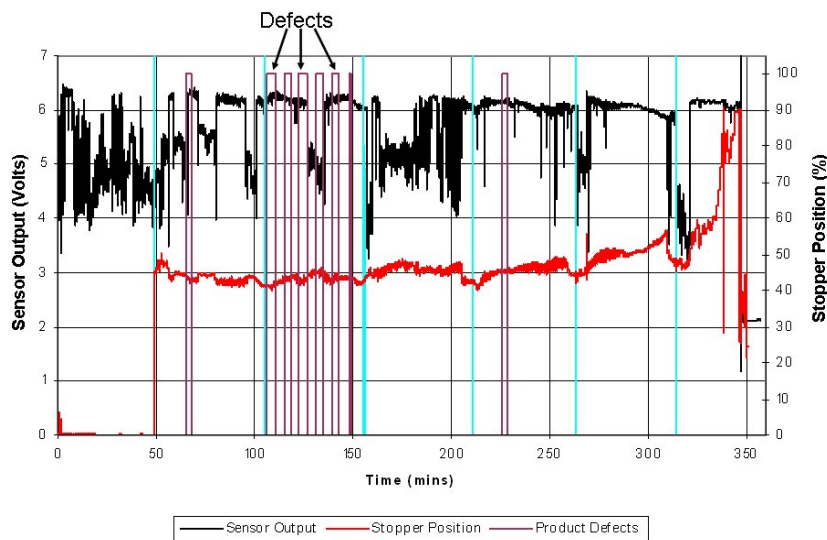


Fig. 42: Example of plate mill defect map against SFV measurements (Corus)

Preliminary examination of the defect maps with reference to measured data has highlighted no correlation between surface defects and SEN flow condition. It was expected that surface defects would be a function of stability of casting conditions. The more stable the casting conditions the better the surface quality. The most stable SEN flow condition would be to run full with a stable stopper position and minimal deviation in mould level. As can be seen in Fig. 42 this has been shown not necessarily to be the case. Defects can be found in material cast at what appear "optimum" very stable flow conditions and other periods which appear transient and unstable for significant durations have been found to be surface defect free.

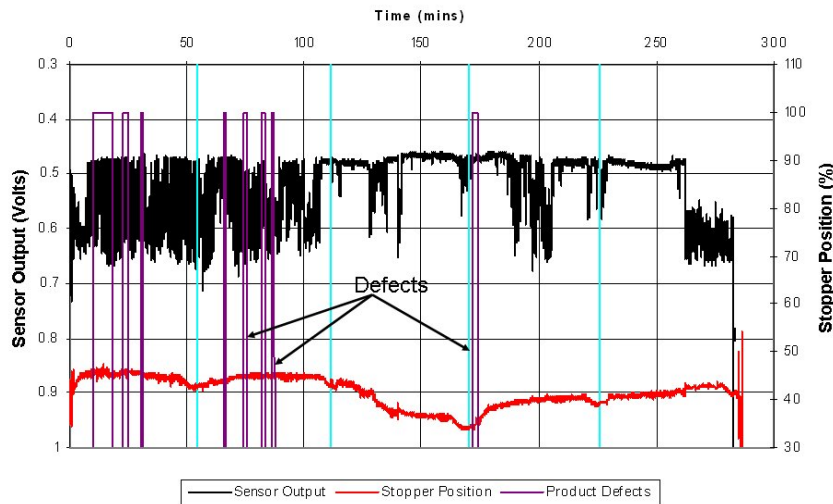


Fig. 43: Example of plate mill defect map against SFV measurements (Corus)

In Fig. 43 the majority of defects occur in the more unstable separated flow regime where large variations in steel level in the SEN are occurring over small time periods.

In total there were 66 rolled slabs that contained plates with defects. The defect maps were plotted relative to casting process variables. Defects that were produced during the major periods of transient operation, start up, ladle change and cap off were discounted leaving 50. A summary of the defect types is shown in Table 4.

Table 4: Defects Identified (Corus)

Defect Type	Total Defects	Defects without Transient Conditions
Blister	11	5
Transverse Crack	1	1
Longitudinal Crack	37	30
Spongy Crack	8	6
Longitudinal & Spongy Crack	3	3
Thermal Crack	3	3
Misc Crack and Dress	3	2
	<b>66</b>	<b>50</b>

The majority of defects appear to be produced during periods of stable stopper position. There is no apparent link between defects and stopper position.

With only one identified defect, there is insufficient data to correlate transverse cracking to process conditions. Thermal cracking occurred only in one cast as a group of three defects in one ladle. Again there was insufficient data to quantify a source of the defect.

There were a total of eleven blister defects detected. Of those six were at ladle change or capping off at the end of casting. The remaining five did not have consistent conditions in terms of the electromagnetic sensor signal or mould level. Historically blister defects are linked to mould powder issues which would be most likely under the transient conditions.

Spongy crack was identified on eleven plates. Two can be discounted through ladle change leaving nine. With reference to the SFV measurements these exhibit a range of flow conditions. Three where the SEN is running full, one half full, three where the level is varying rapidly over up to half the sensor field of view and two where there are transient changing conditions a step change up and a ramping down of the level. Again there is little evidence of a link between SEN flow condition and occurrence

of spongy crack. Spongy crack in slab is historically linked to sudden changes in heat transfer in the mould.

To prolong the life of the SEN, mould level is actively controlled to ramp up and down thus spreading wear caused by the interface between liquid metal surface and mould powder.

Of the fifty defects identified during normal casting, twenty-four were found to be on the up cycle, nine at the top peak, nine at the bottom peak and six on the down cycle. Of the thirty-three long cracks, sixteen were found to be on the up cycle, four at the top peak, seven at the bottom peak and four on the down cycle. Long crack is linked to the active mould level control occurring mainly when the meniscus is rising or at the extreme of the cycle. In these cases the slag line around the mould face is being entrapped or melted.

The thirty-three long cracks were considered relative to the electromagnetic sensor. Interpretation of the SFV signal is discussed in Task 5.1. The defect was found to be generated in the full range of identified SEN flow conditions: four full, nine include a step change (seven rising step changes, two decreasing step changes), two gradual rising SEN level, three gradual fall and thirteen stable level. The thirteen with stable level also varied from a small level variation or "noise" (2) through a less stable fluctuation where the level varied rapidly by between 0.25 and 0.5 of the detection range (8) and a number (3) where the variation or "noise" was greater than half the measurement range. Again no clear correlation.

The distribution of defects through a casting sequence was considered and it was noted that for longer casting sequences that the occurrence of surface defects tends to reduce as the cast with very few occurring beyond the third ladle. This can be seen in Table 5.

Table 5: Frequency of defects relative to cast length (Corus)

Cast Number	Number of Ladles	1	2	3	4	5	6	7
24	6	1	2	0	2	0	1	-
25	2	1	2	-	-	-	-	-
26	7	0	1	5	0	1	0	0
27	5	3	4	0	0	0	-	-
30	3	5	0	1	-	-	-	-
31	4	0	4	1	0	-	-	-
33	4	3	0	5	1	-	-	-
34	3	0	0	-	-	-	-	-
35	4	4	3	1	0	-	-	-

The instability of SEN flow conditions can be very large in the latter portions of cast sequences where the signal is indicating that the level in the SEN is switching between full and empty rapidly. In trial 35 (Fig. 44) the stability of SEN flow can be seen to be very poor. There is an associated degradation in mould level stability and stopper control. However there are no defects in the second half of the sequence apart from single plate with blister defect at the end of the cast. These blisters were seen on a number of casts and are linked to capping off. Note that as described previously the majority of defects are on the upwards ramp of the mould level cycle.

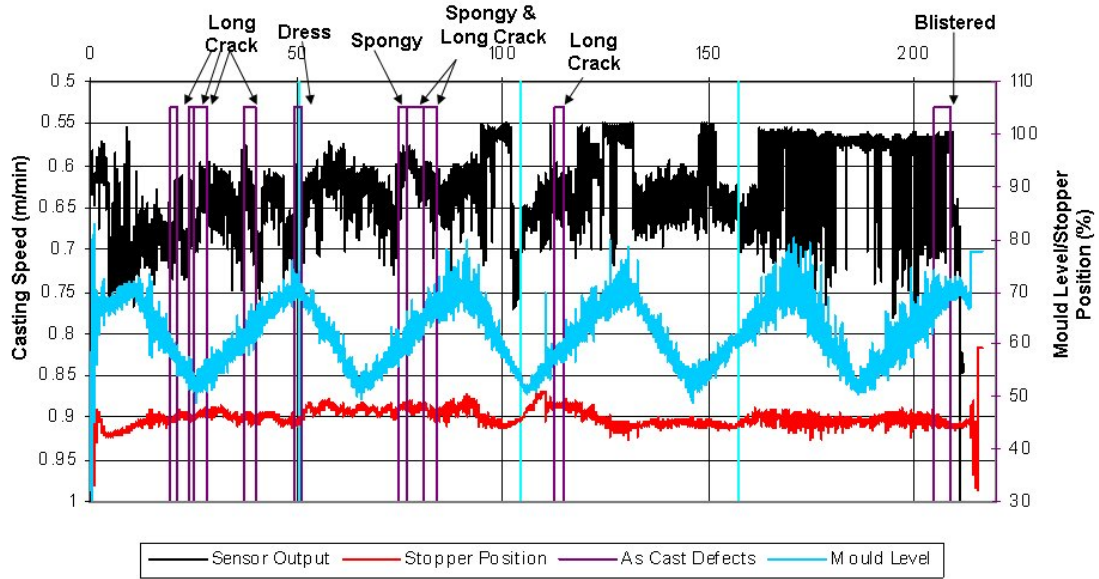


Fig. 44: Plate mill defect map against SFV measurements, stopper and mould level (Corus)

The limited nature of surface defect feedback meant that it was impossible to directly link specific casting events with defects and vice versa. The data could place a defect to within a single rolled slab approximately 1 m or slightly more than 1 minute of casting at the average casting speed. It has not been possible to find clear links between product defects and the trends in electromagnetic sensor output and other casting parameters other than the majority of long crack defects being generated during periods of controlled raising of the mould level.

### Task 3.2 - Product quality assessment - cleanness

#### Saarstahl

To provide the inclusion length values needed for the calibration and verification of the on-line signal analysis an extensive assessment of product quality concerning the cleanness in the semi-finished material has been done at Saarstahl.

Two methods were used, blue brittle and ultrasonic immersion technique. A comparison of both techniques found some significant differences. This might be caused by the fact that the blue brittle test is analysing a surface whereas the immersion technique relates to a volume. As the newly developed on-line ultrasonic system is measuring a volume, it was decided to use inclusion length values determined by ultrasonic immersion technique for the calibration of the PLS-algorithm (Task 3.4). For comparability the inclusion length value was not used directly but in a parameterised form. This was called the inclusion length index.

To test the reliability of data measured by ultrasonic immersion technique a comparison was made with cleanliness examinations on thirty-six more heats of the same steel grade, which were not investigated with the ultrasonic sensor during casting. The relative frequency distribution of the inclusion length indices of these heats (ultrasonic immersion inspection technique, one average index per heat, resulting from about six samples) is shown in Fig. 45. For comparison the average values for the sequences number 4 and number 8 are added. It can be seen that they are in the lower and middle range of the inclusion indices of these investigations, respectively.

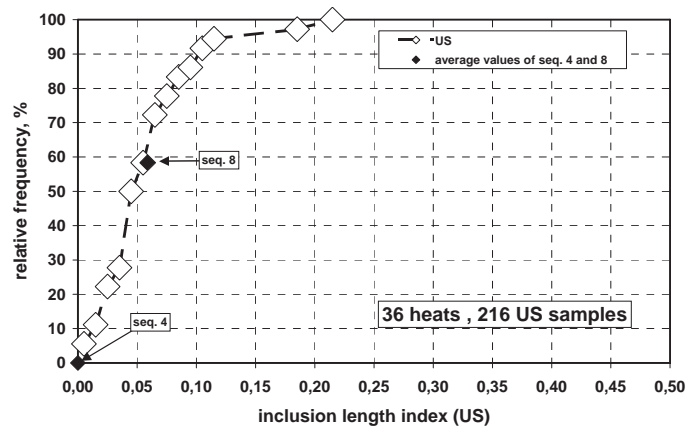


Fig. 45: Cleanliness of the semi finished product according to ultrasonic immersion inspection technique for forty-five heats of the same steel grade as sequences 4 and 8 (Saarstahl)

For the same steel grades inclusion analyses were made to obtain information concerning the inclusions passing BFI's ultrasonic sensors at the submerged entry nozzle and possibly influencing the measured signal. The resulting ternary systems for the inclusions at the end of ladle treatment in the liquid steel and in the finished products (wire) are shown in Figs. 46 and 47, respectively. As could be expected the inclusions in the liquid steel as well as the ones in the finished products are situated in the same area, ranging from the liquid calcium aluminates to the solid alumina phases and the MgO - Al<sub>2</sub>O<sub>3</sub> spinels. The sizes of the inclusions in the liquid phase relevant for the measurements are between 2 and 45 μm.

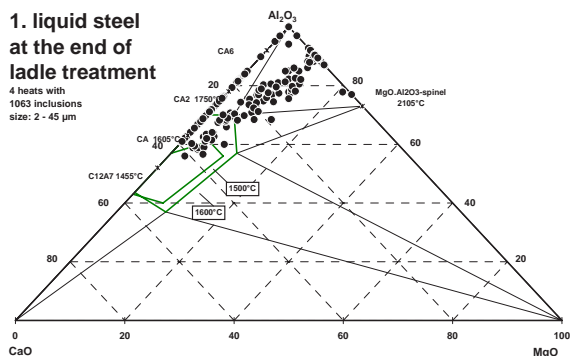


Fig.46: Position of the inclusion in the ternary system CaO - MgO - Al<sub>2</sub>O<sub>3</sub> in the liquid steel at the end of ladle treatment (Saarstahl)

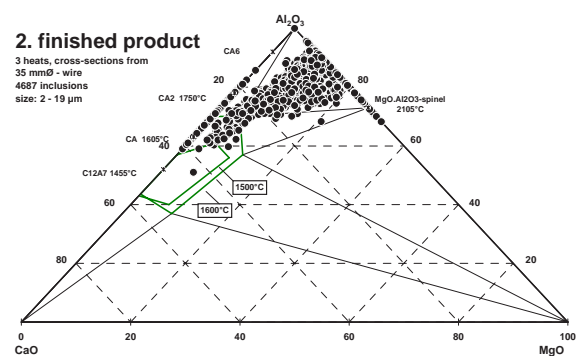


Fig. 47: Position of the inclusion in the ternary system CaO - MgO - Al<sub>2</sub>O<sub>3</sub> in the finished product (Saarstahl)

### Task 3.3 - Characterise steel flow pattern as a function of casting conditions

#### Sidenor

Below some key considerations are presented concerning the nozzle inner pressure characterisation at CCM2, and the influence of the stopper gas flow rate on that pressure condition.

- For the standard casting configuration used at CCM2 in Basauri Plant, under optimum gas feeding injection circuit conditions (air tightness quality), and without clogging, the relative pressure at the stopper rod tip (back-pressure of the stopper gas injection circuit) is around -0.45 bar (see Fig. 48, Trial 1). As explained earlier, both pressures, i.e. pressure at the stopper rod tip and back-pressure of the stopper gas injection circuit, can be considered as equal because of the big outlet diameter of the stopper (5 mm), and the low gas flow rates on use at CCM2 (<=0.8 l/min). This means that the normal relative pressure at the tundish nozzle inlet is -0.45 bar. This value is affected, on the one hand, by the operational parameters such as casting speed and gas flow rate; and, on the other

hand, it is also influenced by the clogging conditions at nozzle exit as it was discovered in the project 7215.PP/045<sup>(1)</sup>.

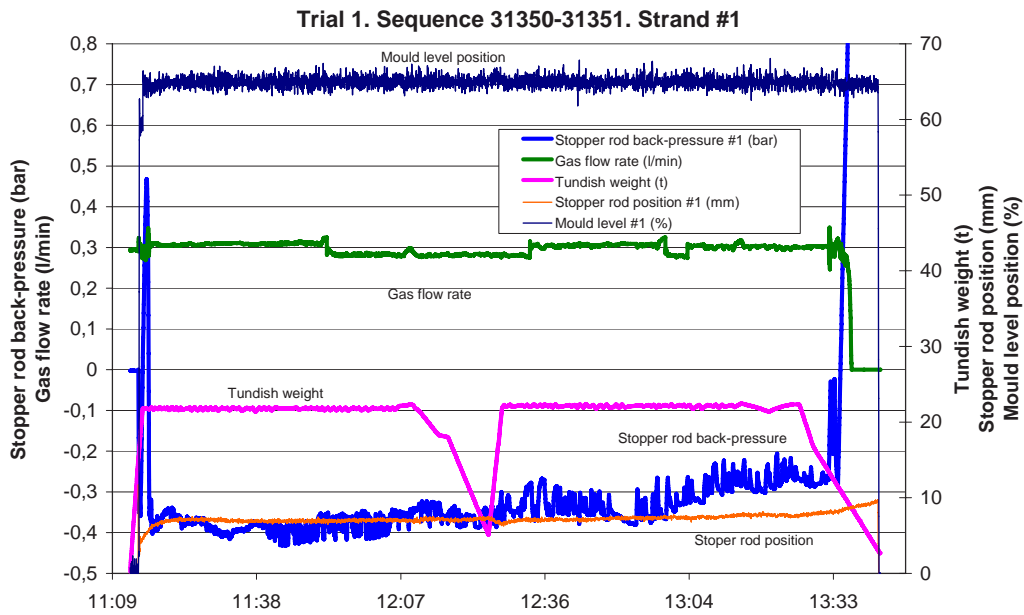


Fig. 48: (Trial 1). Pressure trial with stopper rod back-pressure measurement. Good air-tight condition. Sequence 31350-31351. Strand #1 (Sidenor)

- The effect of the gas flow rate on the gas feeding back-pressure, within the standard gas flow rate range at CCM2, is quite low if compared with the two other influential parameters. In this respect, Fig 49 shows how the reduction of the gas flow rate from 0.6 to 0.3 l/min produces a decrease in the stopper rod back-pressure from -0.34 to -0.37 bar. The higher the gas flow rate the larger the stopper rod back-pressure, that is to say, the lower the vacuum within the nozzle inner body.

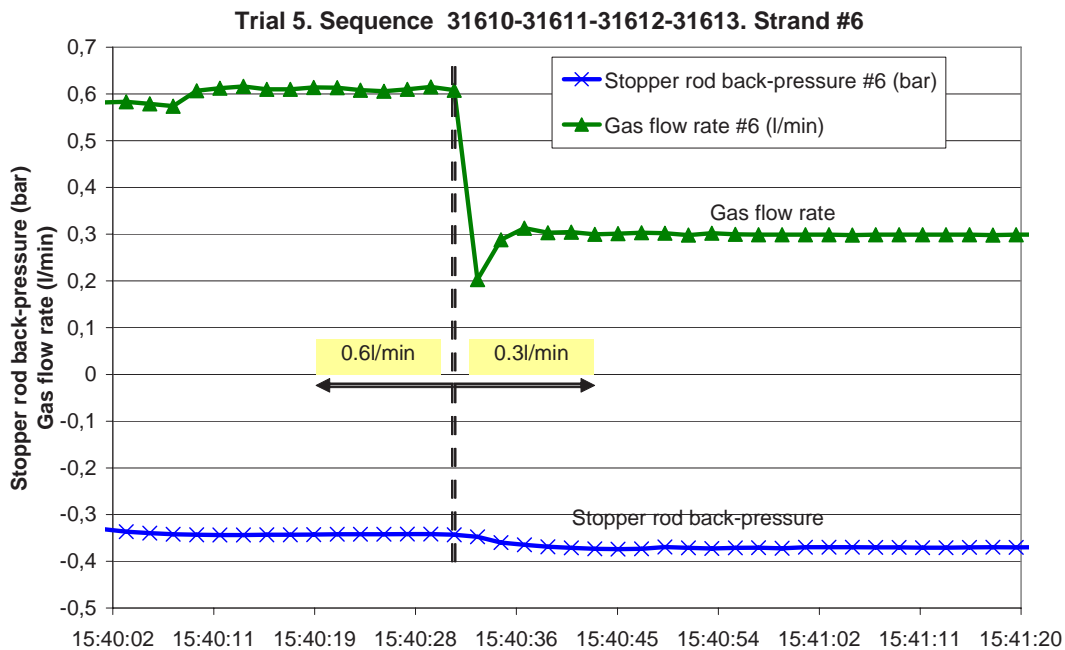


Fig. 49: (Trial 5). Influence of the stopper rod gas flow rate on the stopper rod gas feeding back-pressure. Sequence 31610-31611-31612-31613. Strand #6 (Sidenor)

Observations during the plant trials have confirmed the theory that the pouring duct between stopper rod tip and nozzle exit does not run full of steel, and that the "steel level" within the nozzle is determined by the inner pressure value. This pressure is the equilibrium between air infiltration, gas injection flow rate and the capability of steel to dissolve those gases. According to that theory, already presented in the project 7215.PP/045<sup>(1)</sup>, the tightness of the stopper rod gas injection circuit plays a critical role in the "steel level" value within the nozzle.

The evidence supporting that theory is the following:

- When using two thermocouples for the nozzle temperature characterisation, the difference between them in terms of rate of temperature increase just after the start of casting (see Fig. 50) seems to indicate that the nozzle is not full of steel and that the steel stream proximity to the either side of the nozzle could be responsible for the different thermal behaviour.

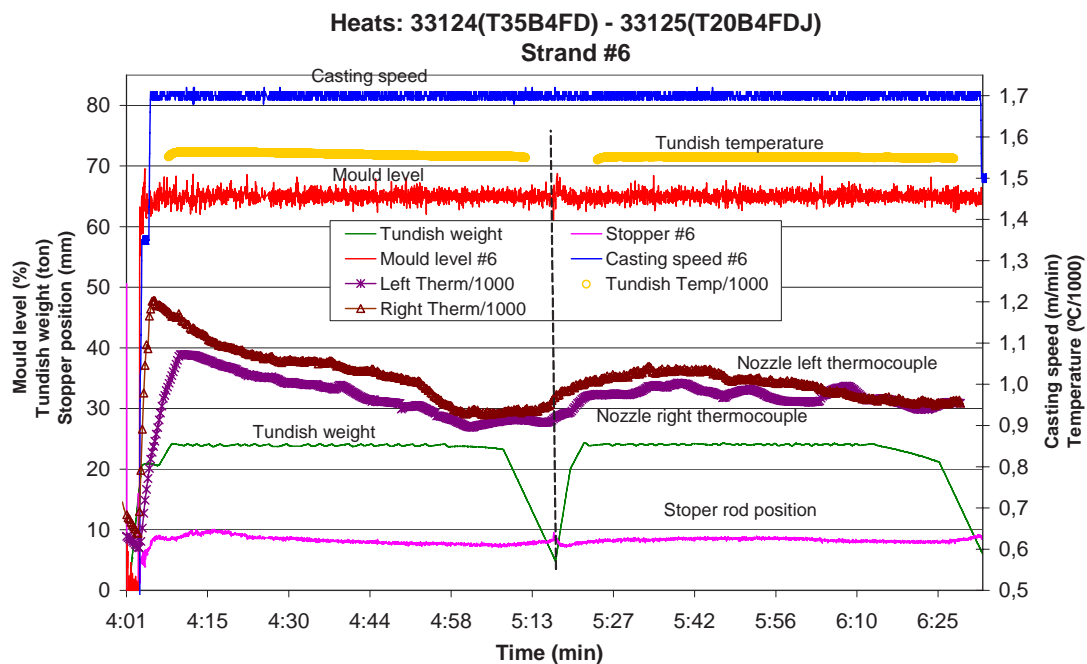


Fig. 50: (Trial 12). Example of trial using two thermocouples for the nozzle thermal characterisation. Difference between both thermocouples in terms of temperature increase slope just after cast beginning (Sidenor)

- Additionally, when using two thermocouples for the nozzle temperature characterisation, the frequent loss of parallelism between the temperatures also seems to indicate that the nozzle is not full of steel and the proximity of the steel stream to the either nozzle inner side could be responsible for that loss of thermal parallelism. (See Fig. 51).

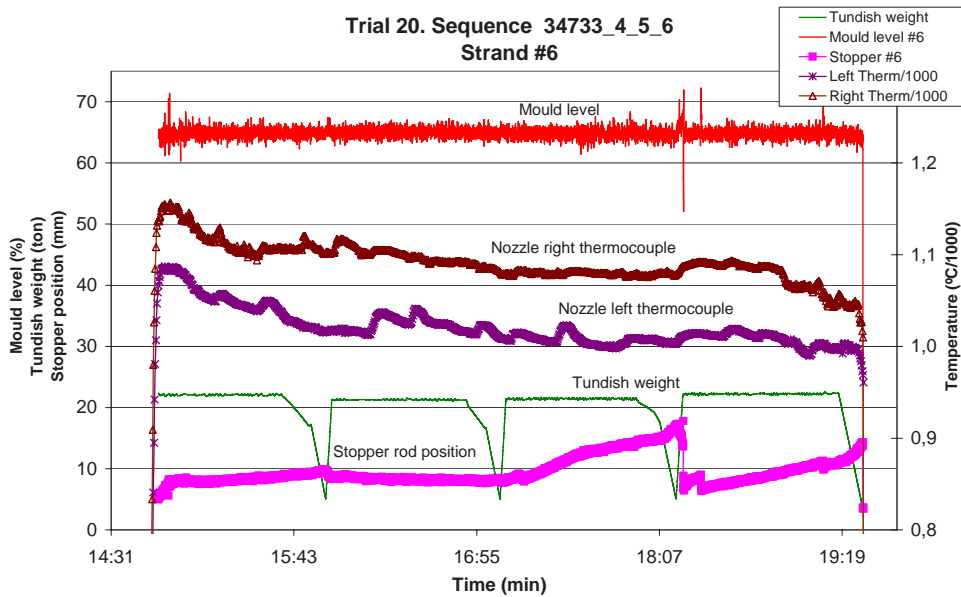


Fig. 51: (Trial 20). Example of trial using thermocouples for the nozzle thermal characterisation. Frequent loss of parallelism between the temperature of both thermocouples (Sidenor)

- Figure 52 shows a trial in which, at a controlled moment, the gas injection circuit was disconnected. From that moment on, air can enter freely through the stopper gas injection circuit and nozzle inner pressure becomes equal to atmospheric pressure. As a result, the nozzle inner pressure conditions changed suddenly, and it is possible to see that a corresponding sudden increase in the mould level position took place and the stopper had to react partly closing the gap between stopper tip and tundish nozzle to restore the normal mould level position. That mould level increase seems to be produced by a sudden discharge of the nozzle steel content into the mould when the nozzle inner pressure is made equal to atmospheric pressure. This example also suggests that there is a certain "steel level" within the nozzle, and that it is determined by the nozzle inner pressure.

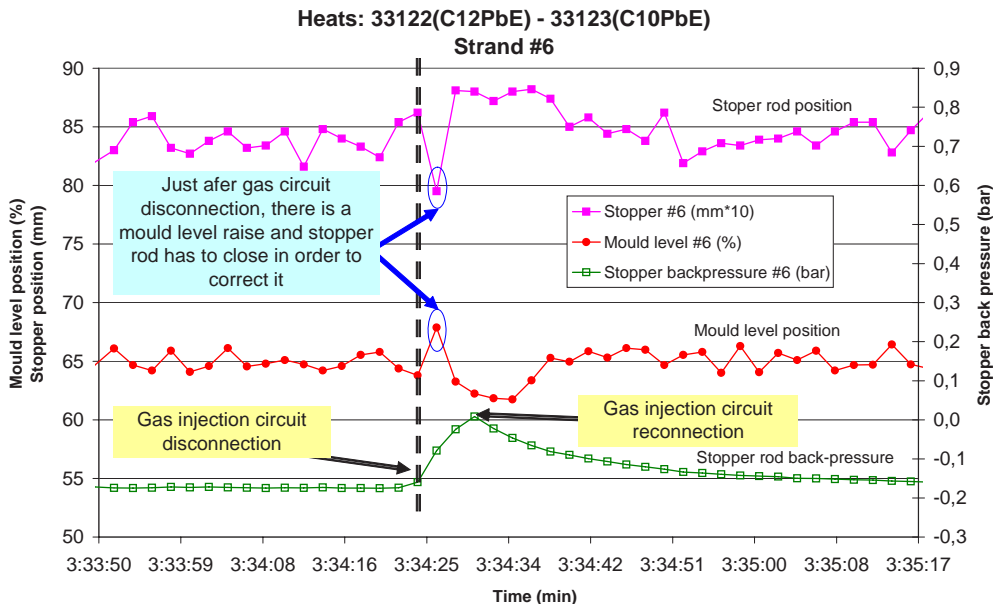


Fig 52: (Trial 11). Effect of gas circuit disconnection on mould level stability (Sidenor)

- Figure 53 shows another example supporting the theory that the nozzle doesn't run full of steel and that the "steel level" within the nozzle is determined by the nozzle inner pressure. In that example the nozzle inner vacuum was recovered spontaneously after a period with problems in terms of air tightness in the gas feeding circuit. In that figure it

is possible to see how the recovery of the normal vacuum conditions within the nozzle produced a sudden decrease in the mould level due to the recovery of the normal "steel level" within the nozzle.

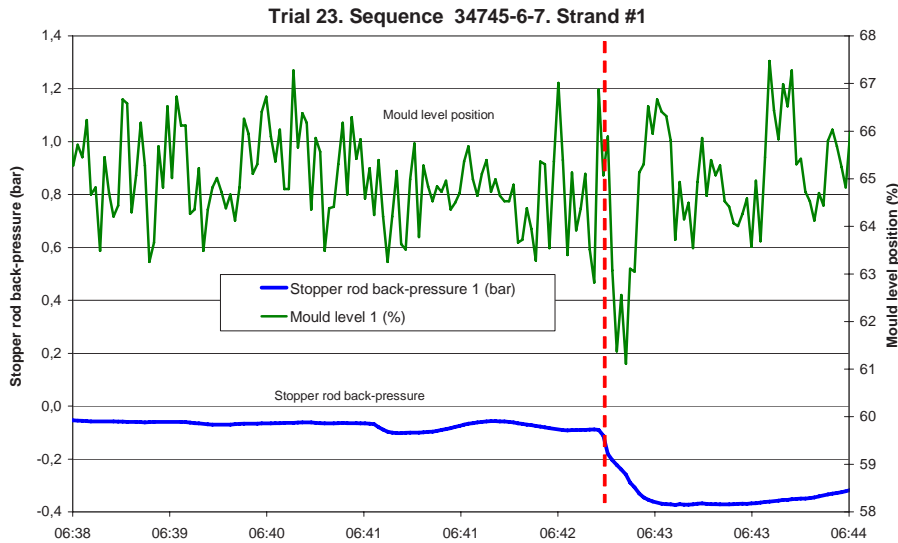


Fig. 53: (Trial 23). Effect of gas circuit disconnection on mould level stability (Sidenor)

Therefore, based on those facts, the following considerations about the steel flow pattern within the nozzle were drawn:

- The pouring duct between stopper rod tip and nozzle exit doesn't run full of steel, and the "steel level" within the nozzle is determined by the inner pressure value. That pressure is created as equilibrium between air infiltration, gas injection and the capability of steel to dissolve those gases.
- According to that theory, the tightness of the stopper rod gas injection circuit plays a critical role in the "steel level" value within the nozzle. That is to say, it could be possible to make a clear distinction between two extreme cases. Those cases would be the following:

#### Case A: Complete failure in the gas injection circuit tightness

In this case, a total failure in the gas injection circuit exists, and air intake is big enough to compensate completely the steel capability to dissolve the gases within the nozzle. Therefore the inner pressure will be equal to atmospheric pressure and "steel level" within the nozzle will be close to meniscus position. Figure 54 shows graphically those conditions. For a casting situation like that it is reasonable to conclude that steel within the nozzle is being contaminated to some extent by nitrogen and oxygen; leading to steel reoxidation and an increase in clogging. This has been corroborated in the industrial trials (see Task 5.2).

#### Case B: Correct tightness quality of the gas injection circuit

In this case, the good tightness quality almost completely avoids the intake of air, and just a small amount of air ingress takes place through nozzle refractory porosity. In those conditions, the nozzle inner pressure will be a function of the following parameters:

- air ingress quantity determined by the refractory porosity
- gas injection flow rate
- steel capability to dissolve the gases within the nozzle

According to the industrial trials, and for no clogging and no wear conditions, the inner pressure will be around 0.6 bar (stopper rod back-pressure around -0.45 bar of relative pressure). "Steel level" within the nozzle can be roughly estimated applying the continuity law for incompressible fluids between one

point located at the "steel level" surface within the nozzle and nozzle exit. As a result of that simplified calculation, the "steel level" would be around 580 mm above meniscus.

The higher the gas flow rate, the higher the back-pressure, that is to say, the lower the vacuum. Therefore, according to this theory, the larger the gas flow rate, the lower the "steel level" will be within the nozzle.

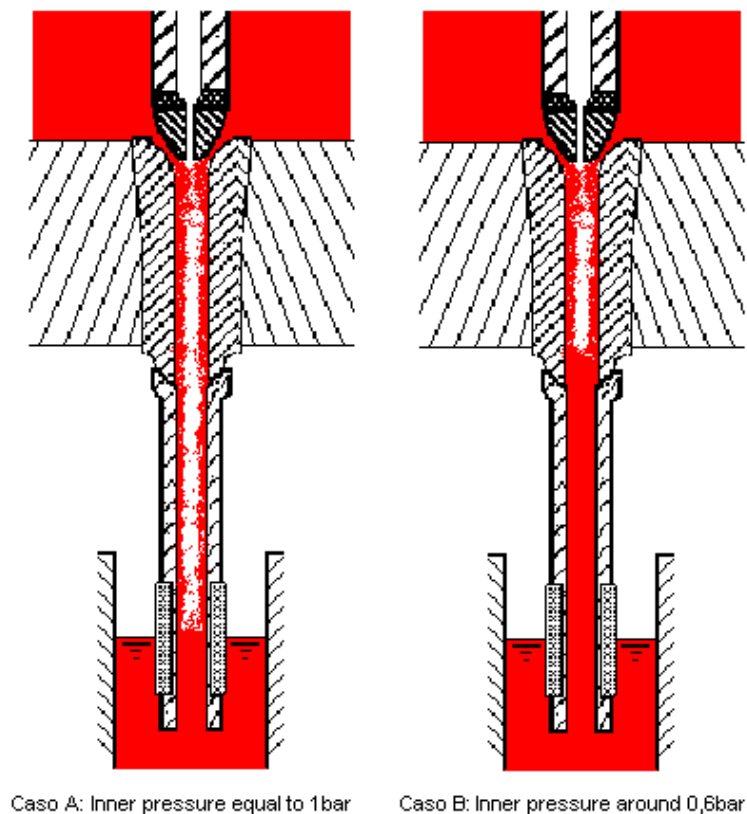


Fig. 54: Theory about "steel level" within the nozzle (Sidenor)

### Task 3.4 - Development of improved signal analysis

#### BFI

Recorded data of first production plant trials carried out in WP 2 were applied by BFI to develop an improved ultrasonic signal analysis with special regard to propagation time and phase shift of the ultrasonic pulses within the SEN system. The improved ultrasonic signal analysis was applied to WP 2 and WP 4 - WP 6. Furthermore, suitable criteria for continuous classification of ultrasonic data were defined, allowing efficient product quality data acquisition at selected samples carried out by SAG in WP 2.

Work by BFI on improvement of signal analysis was started with setting up a simple static water model in the laboratory for the test of the ultrasonic signal analysis. Figure 55 presents a photograph of the test rig. It consists of the two ultrasonic sensor heads inserted in holders which were fixed at a rectangular frame construction. Between the sensor heads a piece of an original SEN was located. The bottom of the SEN piece was closed by a rubber plug so that the inside could be filled with water.  $Al_2O_3$  particles with a diameter lower than  $100\ \mu m$  were introduced from the top into the water. Most of the particles fell through the measurement section. In Fig. 56 the ultrasonic RMS signal is plotted for three increasing amounts of  $Al_2O_3$  particles. There is a clear correlation of RMS signal and particle amount. The more particles were added the lower RMS-signal was observed.



Fig. 55: Simple static water model (BFI)

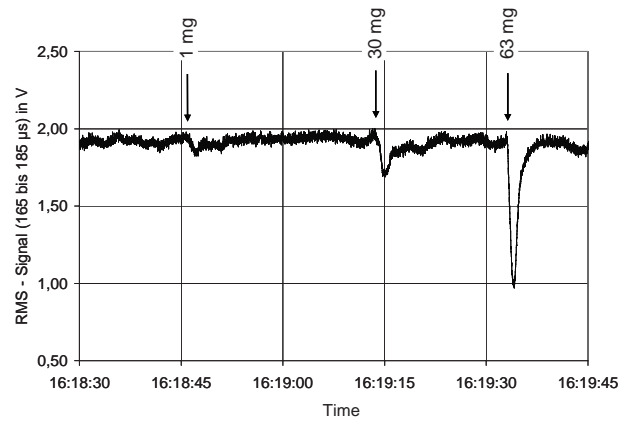


Fig. 56: Inclusion detection in water model trial (BFI)

It was identified during the plant trials that the coupling of the ultrasonic signal into and from the SEN was of high variability. The coupling has a direct influence on the detected ultrasonic RMS signal. Therefore, a simple observation of the RMS signal was not leading to the desired prediction of the steel cleanliness. Therefore, the acquired data were used to redesign and test the analysis routines off-line. A multivariate regression analysis approach was chosen in the form of a Partial Least Squares (PLS-) algorithm. Figure 57 gives a schematic overview of the operation of the PLS algorithm. There are two principal steps using PLS: A calibration step (marked grey) and a prediction step. During the calibration a numerical calibration model is built by the PLS using measured ultrasonic signals and the corresponding inclusion length values as reference. In the prediction step the PLS analyses newly measured ultrasonic signals using the numerical calibration model. The result is a prediction of the inclusion length for the volume of liquid steel scanned by the ultrasound.

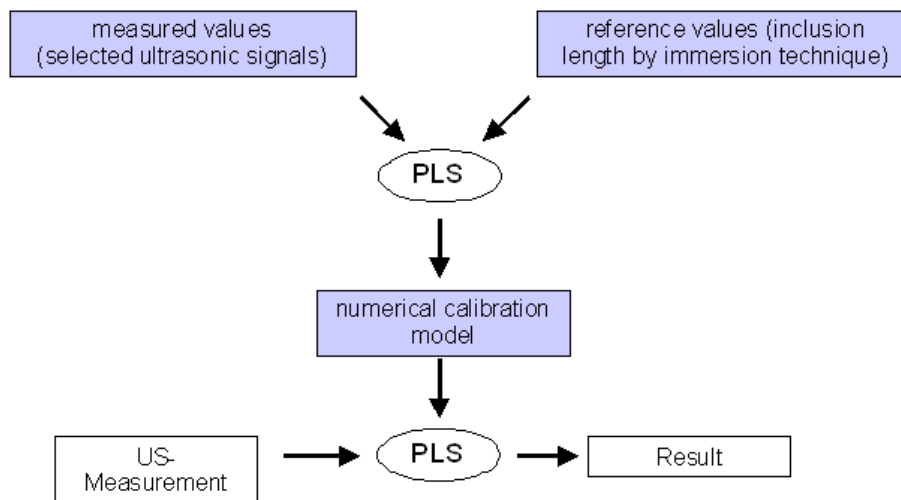


Fig. 57: Principal of partial least squares (PLS) algorithm (BFI)

#### Work Package 4 - Correlation with Existing Data, Product Grading Schemes and Product Quality

The objectives of Work Package 4 were to correlate measured data with cast product grading schemes and product quality. This included observations on how actual flow regimes compared with the established idealised situation.

## Task 4.1 - Correlation of measured data with product grading schemes

### Corus

Work to correlate measured data with product grading schemes had originally been planned for trials at Corus Port Talbot where quality critical grades are down graded in the event of deviations from expected casting conditions. As described in Task 3.1, all trials work during this project was carried out at Scunthorpe where no formal grading system was in place. The slab caster at Scunthorpe was scheduled for upgrading in 2006 as part of which it was planned to introduce a grading scheme. Work on the plant enhancement was completed in February 2007.

The slab tracking and grading scheme can be interrogated using a simple computer based system (example shown in Fig. 58). This shows periods of casting which exhibit casting behaviour outside set acceptable range. The deviations from normal operation which fall within the variables examined by this project are concerning casting speed and mould level.

Alarms are set for mould level deviation of 10 mm, 20 mm and 40 mm from set point also low casting speed. Plant data were obtained concerning this product grading scheme.



Fig. 58: Example of Scunthorpe slab grading screen (Corus)

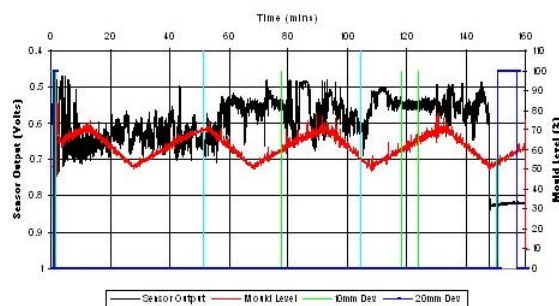


Fig. 59: Plot of grading events relative to SFV sensor output. (Corus)

From these data it was possible to plot the grading alarms relative to the measures electromagnetic SFV sensor data. Figure 59 shows an example of this kind of plot. There has been no evidence found linking the identified grading events with SFV data. Other than a strong indication that the majority of grading flags are related to ladle changes which are period of great instability.

In addition the connection between process variables and all measured trial values have been investigated including an in depth statistical study and comparison to defect location in the cast product. These are reported in detail in Tasks 3.1 and 5.1.

## Task 4.2 - Correlation of measured data with product quality

### BFI/Saarstahl

Based on the PLS algorithm developed in WP 3 a new process model for on-line prediction of product quality was developed. Data from production plant trials (WP 2) were applied to investigate the interactions between different continuous casting parameters and product quality, mainly in terms of cleanliness. Figure 60 shows as an example the comparison of on-line ultrasonic inclusion prediction with inclusion length measured by blue brittle test and measured by ultrasonic immersion technique together with the casting speed, the stopper rod position and the mould level. The measurement campaign comprises a sequence of five heats. The first two heats were of C8C whereas the other three heats were of C10C. The casting speed was changed four times during the sequence from 2.53 m/min up to 2.85 m/minute.

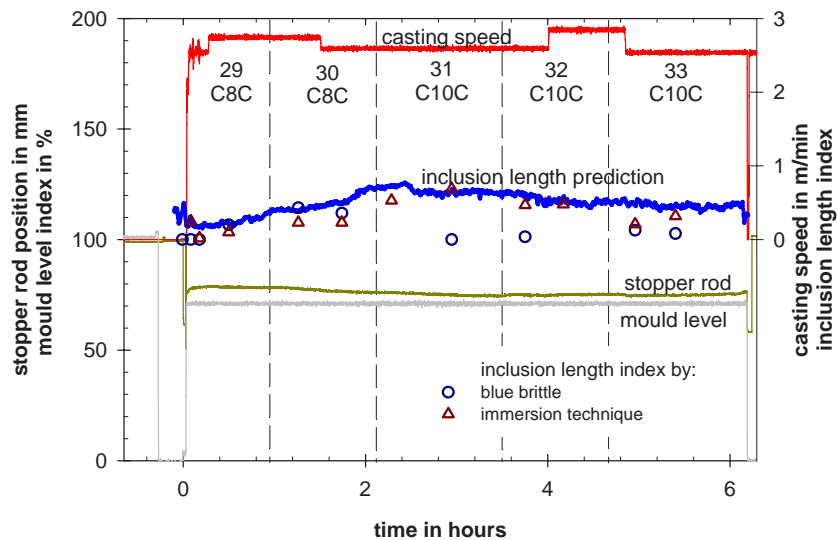


Fig. 60: Comparison of on-line ultrasonic inclusion length prediction with inclusion length measured by blue brittle test and measured by ultrasonic immersion technique for campaign no. 10 (BFI/Saarstahl)

Overall, a good agreement of the on-line ultrasonic inclusion length index prediction as measured during casting with the inclusion length index as measured by immersion technique at the semi finished product was observed. Some of the blue brittle values are showing a considerable aberration which was discussed earlier in WP 3. During the trials alteration of casting speed appeared to have no influence on the cleanliness in terms of inclusion length.

To correlate the on-line ultrasonic inclusion length prediction with inclusion length measured by ultrasonic immersion technique both values were plotted in Fig. 61. The linear correlation yields a regression coefficient  $r = 0.84$ . One inclusion length index value is not within the main collective. The value marked with \* was measured on-line directly after casting start when the thermal balance of the on-line ultrasonic system was not reached. Therefore, this value is not representative and was not included in the correlation.

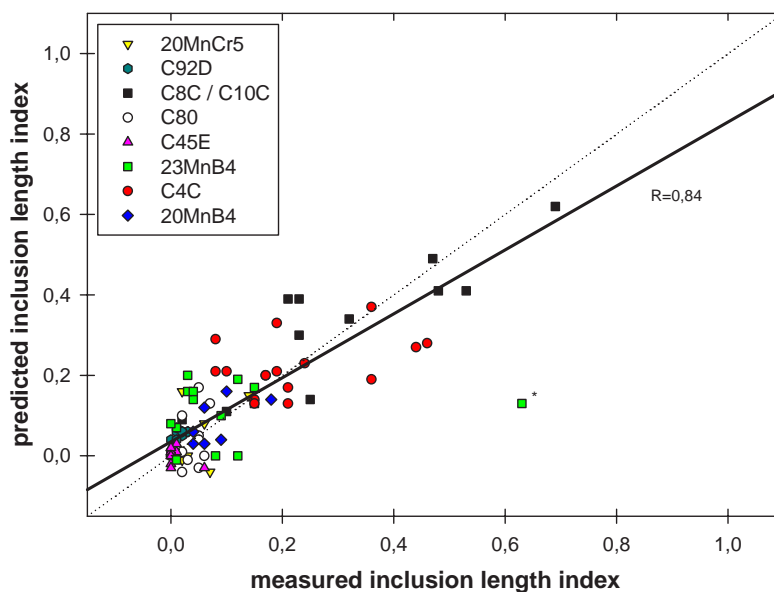


Fig. 61: Correlation of on-line ultrasonic inclusion length index prediction as measured during casting with inclusion length index as measured by ultrasonic immersion technique at the semi-finished product (BFI)

In the correlation plot the inclusion length indices were distinguished by steel quality. A clear dependency of inclusion length index on the steel quality was not observed for the qualities analysed. But it is evident that most of the inclusion length indices are very low (67% are below 0.1), i.e. the steel qualities cast are of high cleanliness in terms of inclusion length.

With regard to clogging a theoretical consideration of the steel flow through the air-tight casting system reveals a negative pressure at the stopper rod tip since the SEN's inner diameter is bigger than required for the actual steel flow<sup>(1)</sup>. This was also verified by measurements from Sidenor during this project. If clogging occurred, the outlet diameter of the SEN will be diminished and a back pressure will be built up which will reduce the negative pressure above. The change of the SEN's inner pressure may have an influence on the flow in the region of the on-line ultrasonic measurement which is located approximately in the middle between SEN inlet and SEN outlet.

The verification of whether there is an influence is not easy to gain since clogging occurred very seldom during the production plant trials. In Fig. 62 photographs of two SEN sections are shown in the on-line measurement region. On the left side the SEN of campaign no. 7 showed no clogging which was the normal case for all measurements. On the right side a SEN with light clogging is shown. This SEN was used prior to campaign no. 12 during the trial campaign at which no measurement data could be stored due to failure of the new permanent data acquisition system. But, at the on-line display no atypical signals or inclusion length predictions were observed during the measurement. This indicates that the occurrence of a light clogging has no influence on the flow condition inside the SEN.



Fig. 62: Clogging observed at the SEN: left: no clogging after casting of sequence no 7, right: light clogging after casting a sequence at which no measurement results could be received (BFI)

### **Task 4.3 - Assess influence of flow pattern on mould solidification**

#### **Sidenor**

Work concerning this task focused on the assessment of the effect of the steel flow patterns on the in-mould solidification, i.e. mould level stability, mould heat flux and friction between billet and mould because of their well-known influence on as-cast surface quality. In this way, the effect of those steel flow patterns on the surface quality of the as-cast product was pursued. To facilitate this some key criteria were defined, and they have been used in order to characterise the 'quality' of the in-mould solidification conditions. Those conditions are well known as not appropriate for obtaining a good as-cast product quality. They are the following:

- High mould level instability
- High mould thermocouples instability
- High or unstable billet/mould friction
- Non-regular billet solid shell growth (even leading to sticking breakouts)

Extensive industrial trials have been carried out and as explained previously, nozzle inner pressure trials have distinguished between two clearly different nozzle inner steel flow conditions, that is to say, 'Partly full nozzle' and 'Empty nozzle'. The first one is related to a high vacuum value within the nozzle, and the second one is obtained when no vacuum is obtained within the nozzle. Additionally, trials using thermocouples installed in the nozzle wall have also given valuable information concerning the steel flow jet position within the nozzle during casting.

The most relevant conclusions are presented:

- Effect of low stopper back-pressure values, i.e. high vacuum value (-0.5 bar ÷ -0.4 bar):  
A high vacuum level ('Partly full nozzle' but with a high level of steel within the nozzle) normally gives rise to an impaired mould level stability (see Fig. 63). It is well known that any increase of mould level instability gives rise to reduced stability of the in-mould solidification conditions, and this is clearly highlighted by an increase of the mould thermocouples instability mainly focused on the meniscus area.

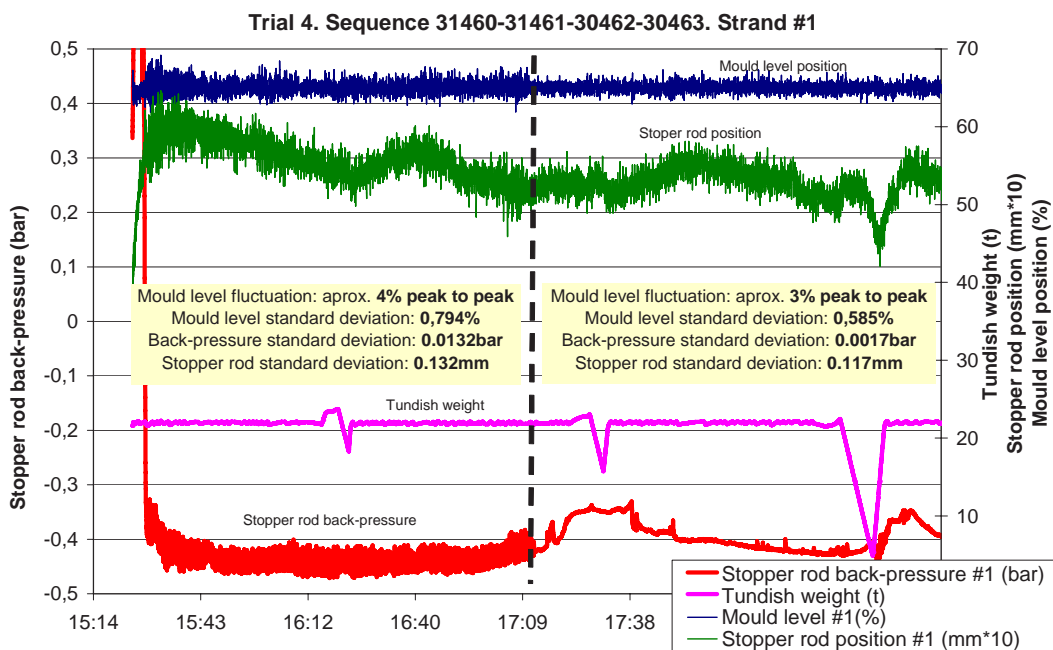


Fig. 63: (Trial 4). Example of abnormal mould level performance when having very low pressure level within the nozzle (Sidenor)

- Effect of steel flow pattern within the nozzle on in-mould conditions ('Partly full nozzle' vs. 'Empty nozzle'):
  - **Mould level:**  
Figure 64 shows the transition between a 'Partly full nozzle' and an 'Empty nozzle', obtained just by means of disconnecting the stopper gas feeding circuit. It is possible to see how a partly full nozzle gives rise to a significantly worse mould level stability (20% worse).

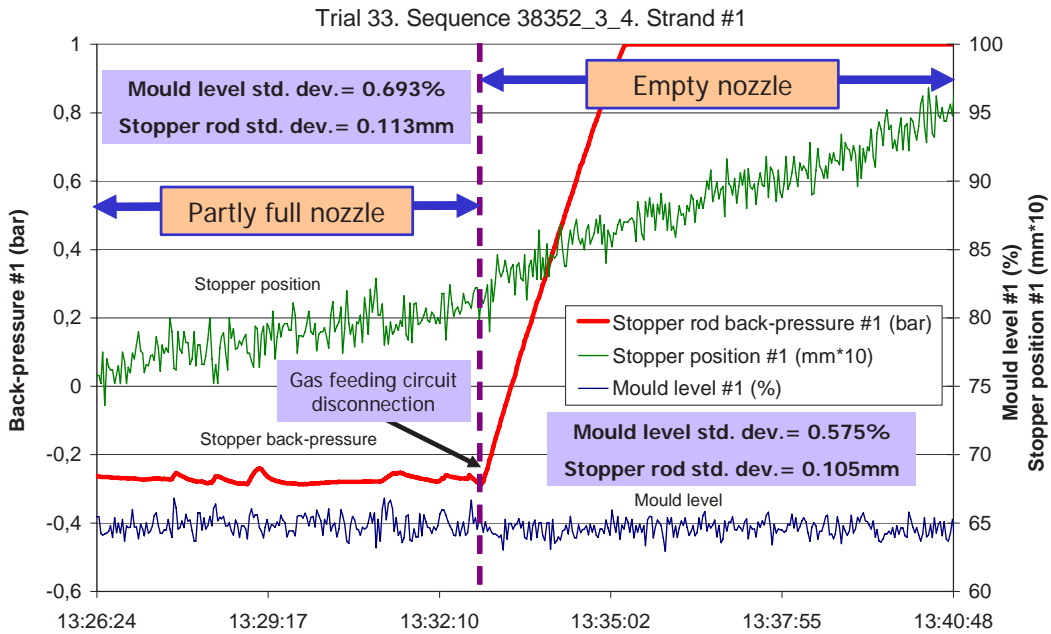


Fig. 64: (Trial 33). Example of slightly worse mould level performance when having a 'Partly full nozzle' (Sidenor)

○ **Mould thermal flux distribution:**

Additionally, a partly full nozzle gives rise to a lower heat flux at the top of the mould (see Fig. 65). The figure shows that when changing from a 'Partly full nozzle' to an 'Empty nozzle' the temperature at the upper part of the mould is greater, while in the rest of the mould there is a lower temperature. A possible explanation could be that the steel jet goes deeper inside the mould when having a 'Partly full nozzle'.

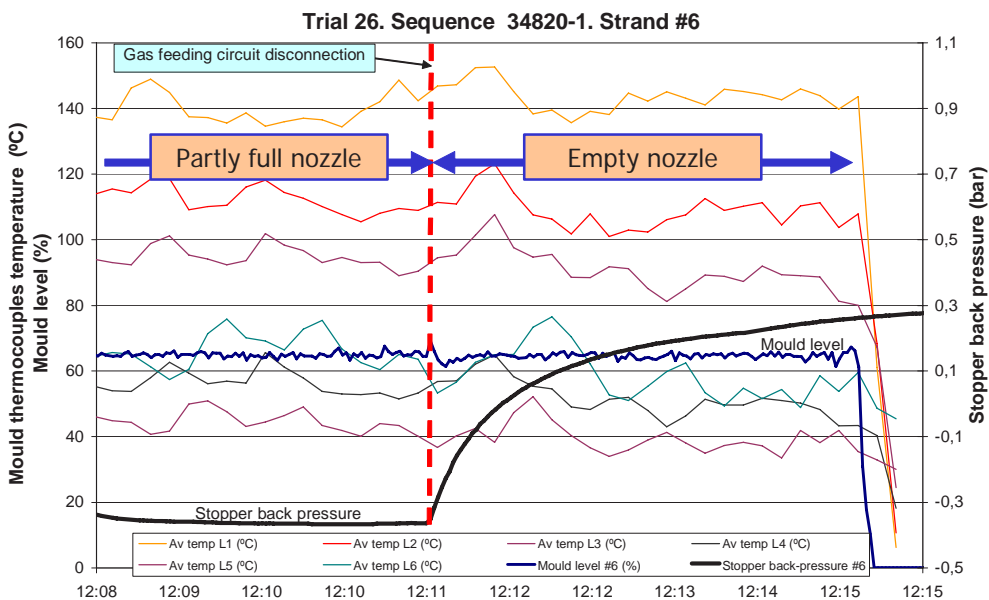


Fig. 65: (Trial 26). Example of lower thermal flux at the top of the mould when having a 'Partly full nozzle' (Sidenor)

○ **Mould thermal flux value:**

A 'Partly full nozzle', again in comparison with an 'Empty nozzle', gives rise to a lower thermal flux as it can be observed in Fig. 66. In this case the mould thermal flux has been obtained using the mould water temperature signal.

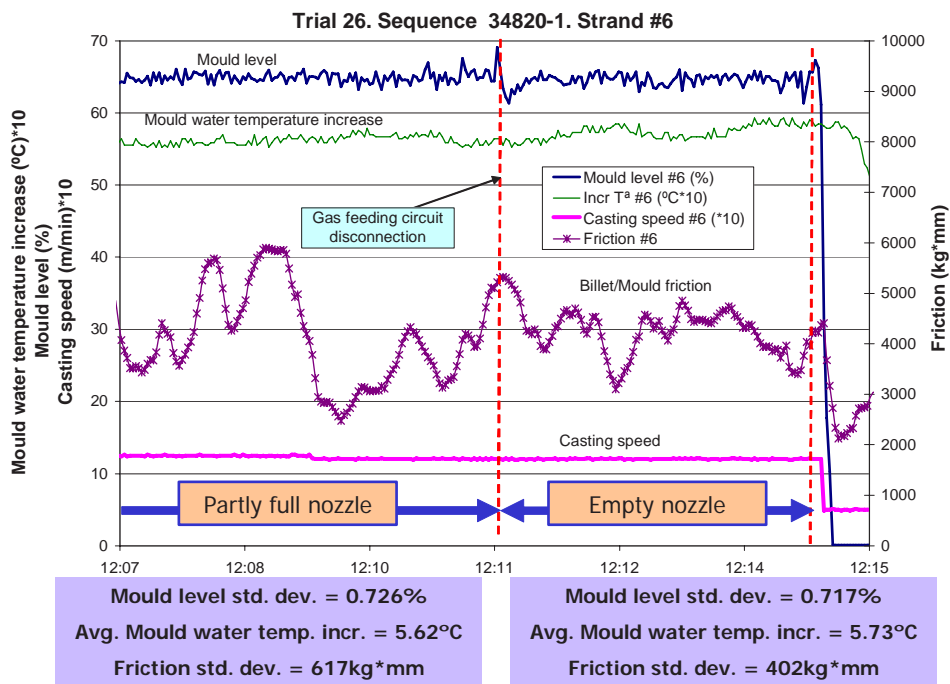


Fig. 66: (Trial 26). Example of lower mould thermal flux when having a 'Partly full nozzle' (Sidenor)

○ **Billet / Mould friction:**

Figure 66 also shows that a 'Partly full nozzle' gives rise to a friction with a similar average value, but less stable.

○ **Mould thermocouples stability:**

Finally, it has been also found that a 'Partly full nozzle' gives rise to a slightly worse stability in the mould thermocouples.

● Effect of the steel jet position within the nozzle on the in-mould conditions:

Trials using thermocouples at the nozzle outer face have shown that steel jet position within the nozzle varies throughout casting time. High casting speed was found to increase the variability of the steel jet position. Figure 67 shows clearly how a higher casting speed gives rise to a lower parallelism amongst the temperatures of the three mould faces and also a lower parallelism between the two nozzle thermocouples. This behaviour indicates that the changes in the steel jet within the nozzle give rise to changes in the steel flows within the mould and loss of parallelism between the mould face temperatures at meniscus, and they are more frequent at high casting speed.

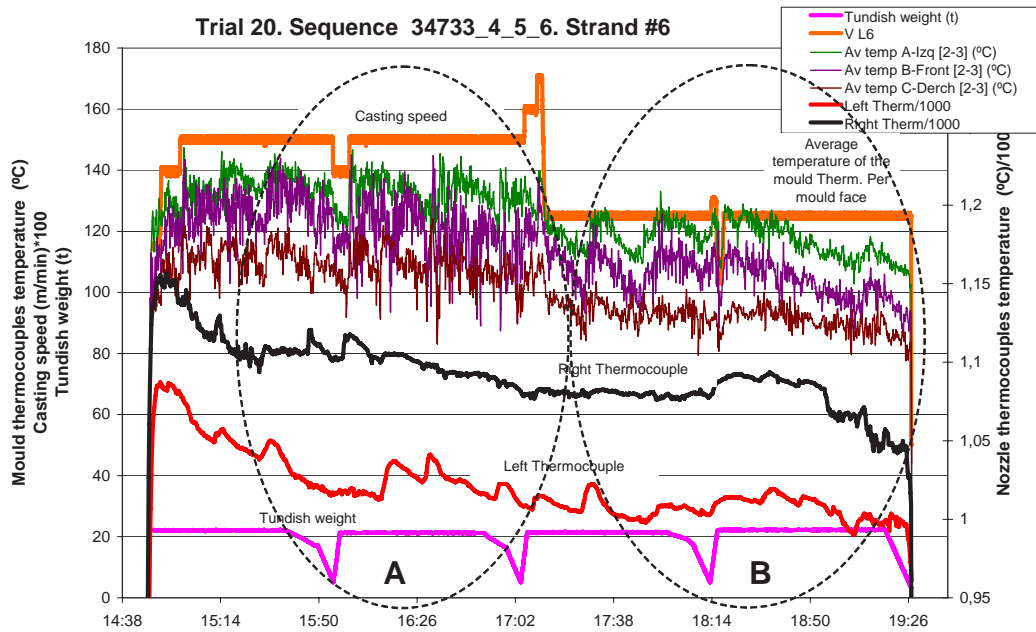


Fig. 67: (Trial 20). Correlation between the nozzle steel flow conditions and the mould thermal behaviour (Sidenor)

Taking these results into account, it could be stated that a 'Partly full nozzle' compared with an 'Empty nozzle' gives rise in general to worse in-mould solidification conditions, i.e.: worse mould level stability, worse mould thermocouples stability, lower thermal flux and less stable friction. Additionally, a high variability in the steel jet position gives rise to:

- Higher mould thermocouples variability (see Fig. 68). Peaks in the nozzle thermocouples correspond to changes in the proximity of the steel stream to the different inner sides of the nozzle. And, in that figure it is possible to see that many of the peaks in the mould thermocouples deviation are correlated to peaks in nozzle thermocouples; therefore, steel jet position within the nozzle affects in-mould solidification conditions.
- Higher mould thermal flux variability.
- Higher friction variability.

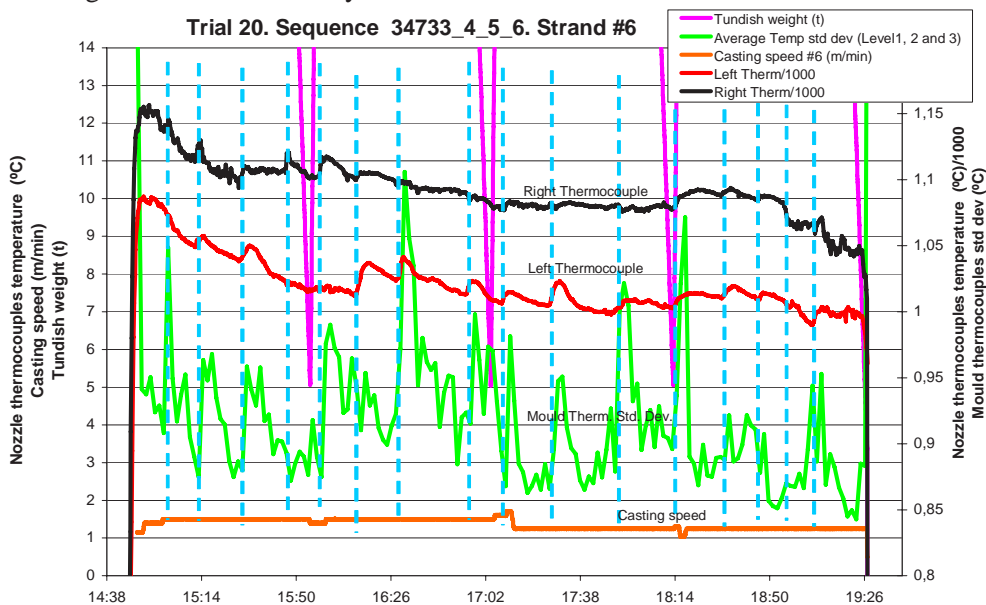


Fig. 68: (Trial 20). Example of higher mould thermocouples variability when having a high variability in the steel jet position (Sidenor)

## Work Package 5 - Reasons for Changes Observed in Flow Patterns

The objectives of Work Package 5 were to measure the degradation of flow patterns with time with the aim of correlation with casting nozzle condition and to assess the feasibility of developing criteria for changing the SEN during casting or on-line measurement, to indicate wear of refractory components.

### Task 5.1 - Determination of reasons for flow pattern changes during stable casting

#### Corus

##### *Electromagnetic Steel Flow Visualisation Sensor*

During the trials many different examples of casting behaviour were noted. Attempts have been made to associate electromagnetic SFV sensor signal variation with specific changes in measurable casting parameters in order to identify possible causes for changes in flow pattern.

During the first ten minutes of casting the sensor output was typically erratic with a very large variation, much larger than seen during normal operation. This is not fully understood and seemed to coincide with a negative stopper gas pressure and the ramping up of flow during start-up and persisted until steady state casting was established. This type of behaviour was evident during every trial for which the start up was logged.

The most obvious major casting event noted was ladle change. These can usually, although not always, be associated with significant signal drop as the steel level in the SEN reduced in line with the reduction in casting speed and tundish level. Measured flow pattern usually returned to normal operating level once the new ladle was opened. A clear example of this is shown in Fig. 69.

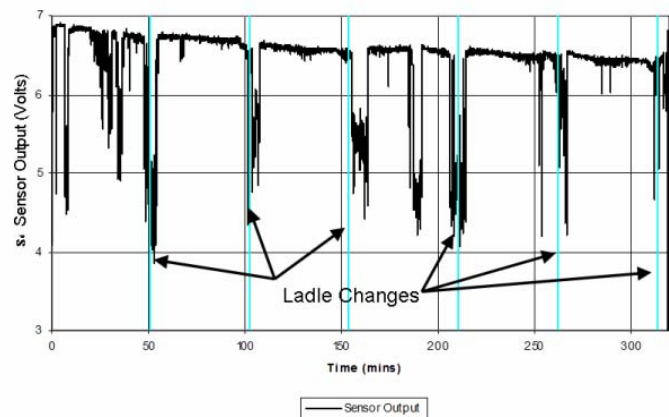


Fig. 69: Example of sensor output change at ladle change (Corus)

Examination of the relationships between flow patterns measured using the SFV sensor and casting variables have shown two basic flow states. The first is a "full" SEN where the metal level in the SEN is above the field of view of the sensor (Fig. 70). In this condition the sensor, which fundamentally detects a steel volume, is saturated giving a high stable signal disturbed only by small fluctuations caused by the rapid passage of dispersed argon bubbles from the stopper gas system. The alternative flow pattern is a "not full" flow characterised by a low variable signal and is made up of three components: The steel stream, the steel level in the SEN, if this is within the field of view, and a void comprising argon from the gas injection system and any other entrained gases.

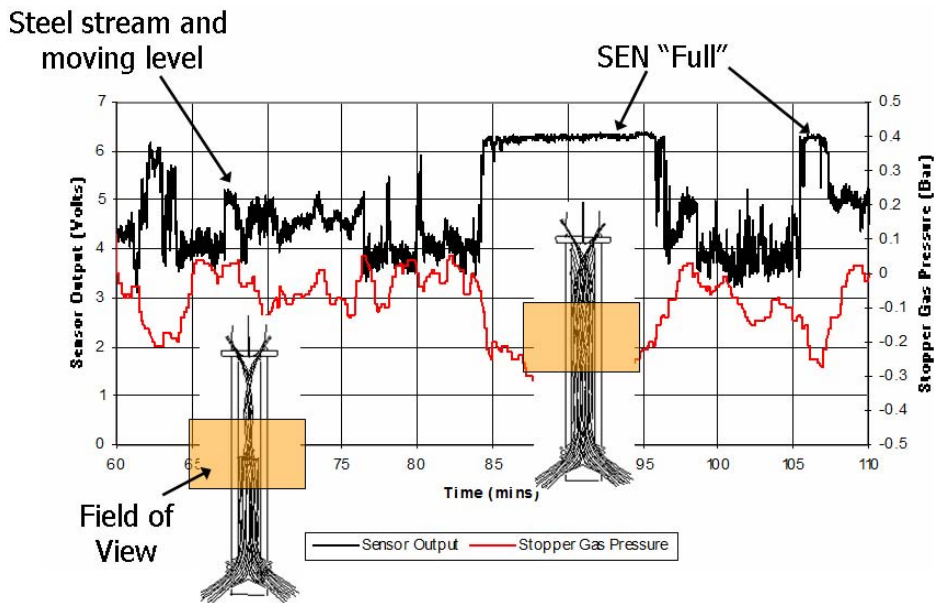


Fig. 70: Interpretation of SFV sensor signal (Corus)

The transition between the two main flow conditions is usually dramatic and sudden as shown in Fig. 70. The clearest visual correlation between casting variables and SFV sensor signal is related to these step changes indicating switch in flow pattern from an annular flow to full. Under normal casting conditions on this casting machine this transition appears to occur when the stopper gas pressure drops below -0.15 bar. This has been seen in almost all trials which show a flow phase transition and can be clearly seen in Fig. 71. The trigger pressure has apparently not changed regardless of other physical changes for example casting speed, mould width etc.

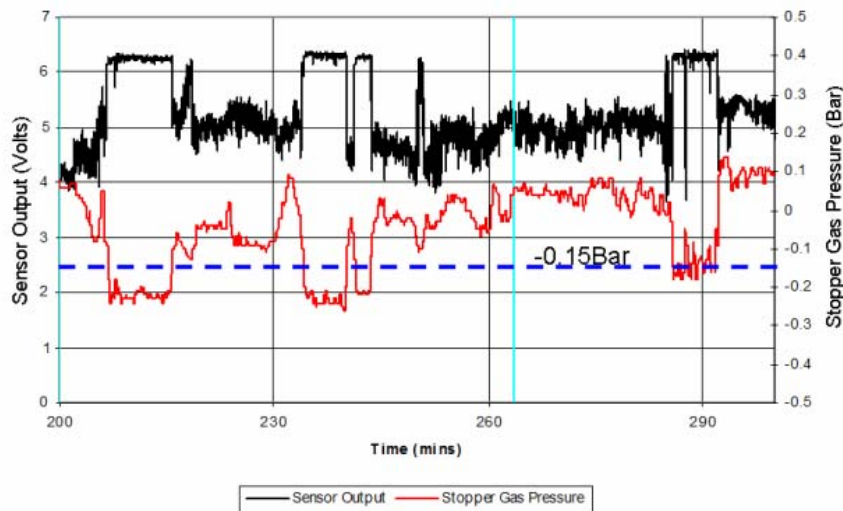


Fig. 71: Example of flow transition when stopper gas pressure <-0.15 bar (Corus)

Although there are many examples of switch over at -0.15 bar there are two exceptions to this observation. During the first ladle of a sequence the strength of the transition is lower with the level in the SEN spiking to full as can be seen in Fig. 72 below. The transition becomes much more stable once the cast is established. The other exception is that in a number of trials the switch has occurred at higher pressure. These have usually been the longer trials and exhibit rising trends in both stopper pressure and stopper position. This phenomenon is discussed in detail in Task 5.3 and may be related to build up of alumina accretions.

The stopper gas injection system on the slab caster at Scunthorpe uses a gas volume flow rate controller. The pressure finds its own level within the injection system and can vary greatly between positive and negative without changing the flow rate.

Usually during slab casting operations at Scunthorpe the stopper gas flow rate is fixed at 6 l/min. During Trial 13 (Fig. 72), for operational reasons, the stopper gas flow rate was altered during casting. During the first two ladles the SFV signal was very unstable with much switching between flow patterns. The gas pressure can be seen to increase just before the second ladle changed at around 120 minutes, which is in line with a step change in gas flow rate from 6.25 l/min to 6.33 l/min. This small change has a large effect on apparent flow pattern which becomes much more stable. See Figs. 72a and 72b. A further trial was carried out to attempt to exploit this phenomenon and is described in Task 6.3.

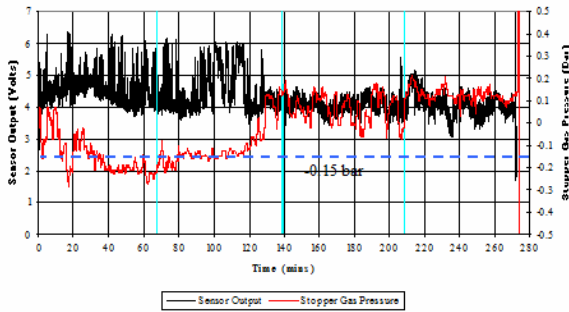


Fig. 72a: Output from sensor and stopper gas pressure during trial 13 (Corus)

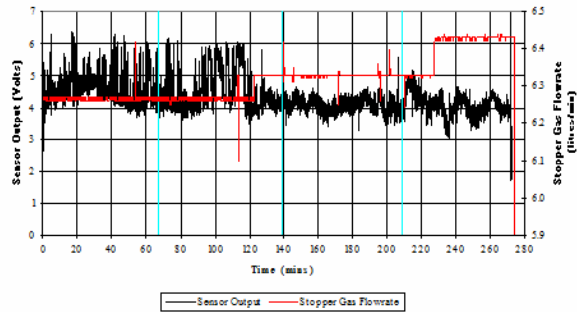


Fig. 72b: Output from sensor and stopper gas flow rate during trial 13 (Corus)

Connection between sensor signal and stopper gas pressure does not always show a direct correlation apart from the obvious switch in flow pattern. However, Fig. 73 shows a period of approximately 40 minutes around the third ladle change during trial 13 where the flow conditions are influenced by or influence the gas pressure. This kind of trend has been seen regularly in trials during periods of relatively stable annular flow.

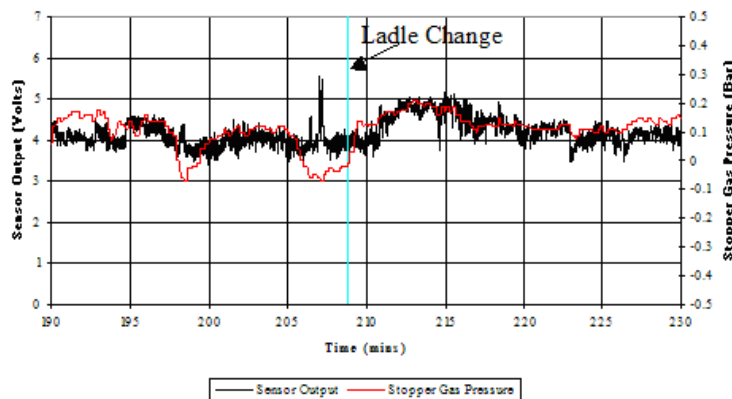


Fig. 73: Output from sensor and stopper gas pressure during trial 13 (Corus)

Clear indication of shifting flow conditions with respect to stopper position have been previously reported in the project 7215.PP/045<sup>(1)</sup>. The measurements during the first half of this project have shown similar phenomena especially linked to alumina flushes. When the stopper position rapidly closes due to the sudden increase of the size of the flow metering nozzle after large alumina accretions are washed away by the feed metal, the electromagnetic sensor will detect a change in the volume of steel in the SEN. Figure 74 shows an example of this during trial 1. The figure shows a period of approximately 10 minutes around a stopper flush. It can be clearly seen that the stopper position gradually increases to compensate for the loss of flow due to clogging. The electromagnetic signal

gradually decreases and becomes more unstable. When the flush occurs it can be clearly seen that the flow conditions in the SEN return to a similar condition to that before the blockage.

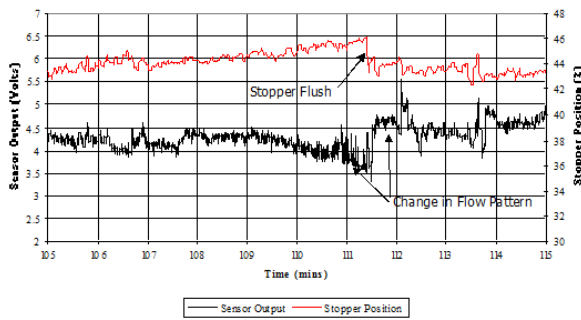


Fig. 74: Output from sensor and tundish stopper position during trial 1 (Corus)

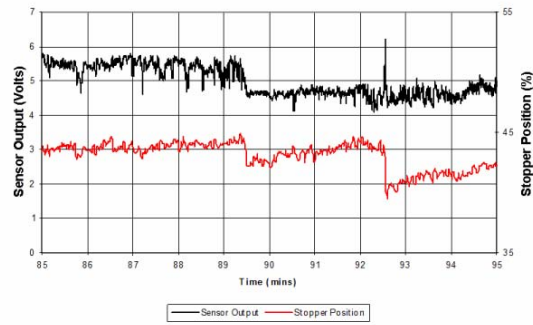


Fig. 75: Output from sensor and tundish stopper position during trial 21 (Corus)

It has also been seen that a stopper flush can be the trigger event for a longer term change in flow condition. In project 7215.PP/045<sup>(1)</sup> very clear step changes in flow pattern were observed related to stopper flushes. During this project this type of flow pattern transition has been limited. Very few examples have been apparent. One of these can be seen in Fig. 75. Two events can be seen. The first stopper change triggers a drop in level in the SEN. The second only causes a spike where the metal level in the SEN rises briefly but returns to the same level. The effect of the stopper position on the flow pattern appears to be significantly less than the stopper gas pressure.

Trial 18 was terminated when metal froze in the SEN. During the second ladle, low metal temperature prompted an increase in casting rate in an attempt to prevent freezing. This was however not successful and the cast was terminated at the end of the second ladle. Figure 76 shows a distinctive change in sensor signal due to the solidification of steel in the SEN. The electromagnetic properties of the solid material are very different from the liquid and produce a significantly higher signal response. The signal becomes much higher and stable as solidification takes place.

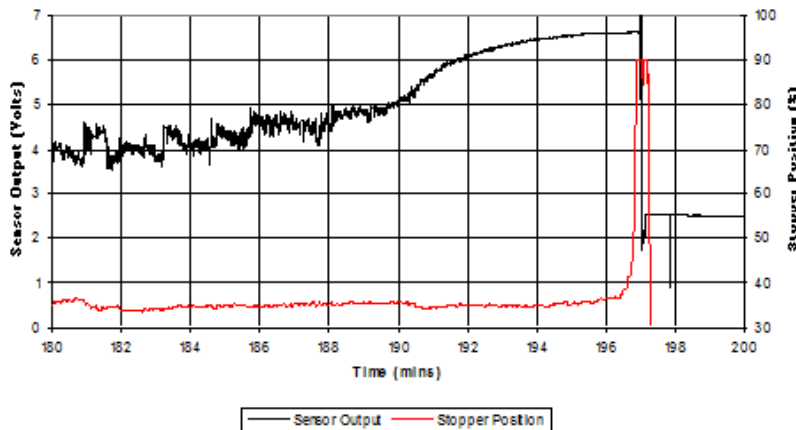


Fig 76: Output from sensor and stopper position during trial 18 (Corus)

During normal trials the SFV sensor was removed from the caster just prior to the end of casting. However, examination of data from other trials highlighted the same phenomenon, for example in trial 15. Although interesting this information could also be derived from other plant data.

#### Multiple frequency sensor

As described in Task 2.1 eight trials using the multiple frequency sensor have been carried out. Assessment of the logged data confirmed that the output from the sensor follows the same pattern as the output from the single frequency sensor. Figure 77 shows an example of the raw output data from the

multiple frequency sensor. The switch between empty and full SEN can be clearly seen when the stopper gas pressure drops below -0.15 bar. The overall trends of each sensor can be seen to be similar but small differences are apparent which may be usable to indicate lateral movement of flow stream in the SEN.

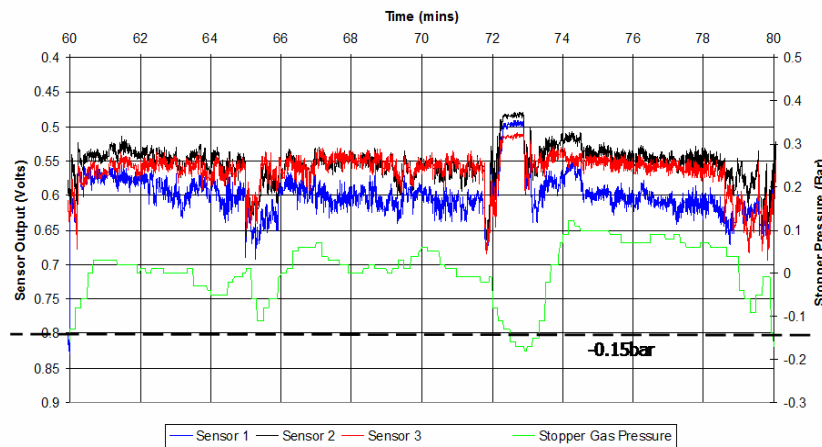


Fig. 77: Example of output from new multiple frequency electromagnetic sensor (Corus)

Interpretation of the signal differences is extremely difficult as the relationship between position of the steel stream relative to transmitter and receiver and signal output level is not linear. If the signal increases or decreases in all channels simultaneously the volume of steel in the field of view is increasing or decreasing. If there is a combination of increasing and decreasing signals a combination of change in flow and movement of the stream is the most likely explanation. An object of fixed size produces a minimum signal when in the centre, increasing to a maximum adjacent to both the transmitter and receiver. It is not possible to differentiate which of these the object (steel stream) is nearest to.

When compared to the original system the overall trend in the signal is directly comparable. The signal from the new sensor is inverted and the output voltages are significantly lower but the behaviour in terms of trends and reaction to changes in flow pattern are the same.

Because the three channels operate on different frequencies the response to an object can be different in terms of signal strength and range. An attempt was made to normalise the three signals by re-ranging them within common maximum and minimum limits. See Figs. 78a and 78b.

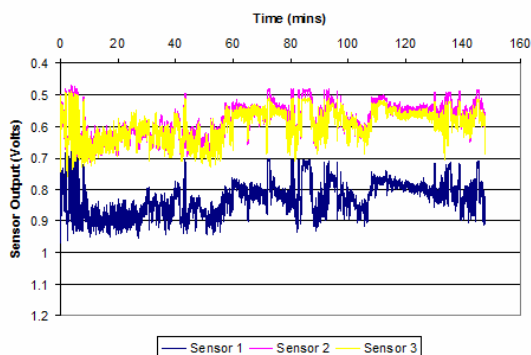


Fig 78a: Multi-frequency SFV sensor raw data (Corus)

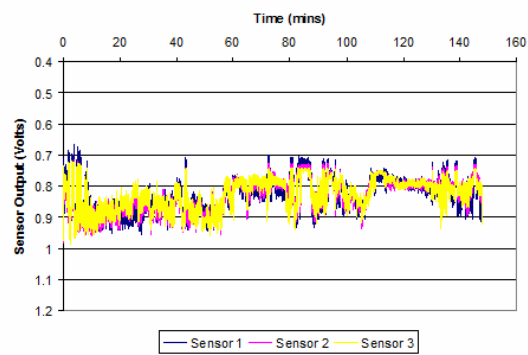


Fig 78b: Multi-frequency SFV sensor normalised data (Corus)

Taking the outputs from the two extreme sensor channels, sensor 1 (S1) and sensor 3 (S3), the difference between the two channels was plotted and compared to various plant parameters. Interpretation of these data is extremely difficult. As described in Task 1.1, the response of the sensor

to a metal object in its field of view is symmetrically related to distance from both transmitter and receiver with the largest response being when the object is in the middle. The difference between S1 and S3 therefore is at a minimum when either the SEN is full or the steel stream is exactly central and at a maximum when an object is close of one of the coils. However because of the symmetrical nature of the signal if an object moved from position 1 in Fig. 79 to position 2 or 3 the resultant signal on sensor 1 would be the same as the original on sensor 3.

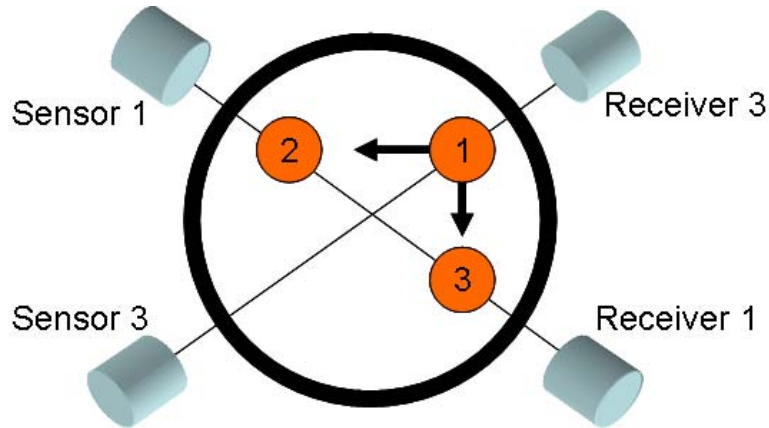


Fig. 79: Interpretation of the multiple frequency sensor (Corus)

Taking the difference between S1 and S3 will give an indication of a shift but its direction and when combined with the Sensor 2 output as shown in Fig. 80a, we get a graph showing steel volume and variability/stability of the stream.

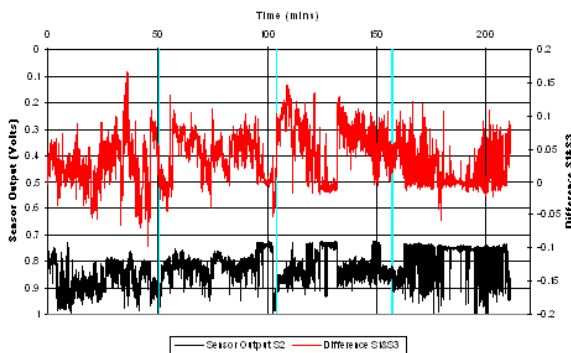


Fig. 80a: Graph showing Sensor 2 output and difference between sensor 1 and sensor 3 (Corus)

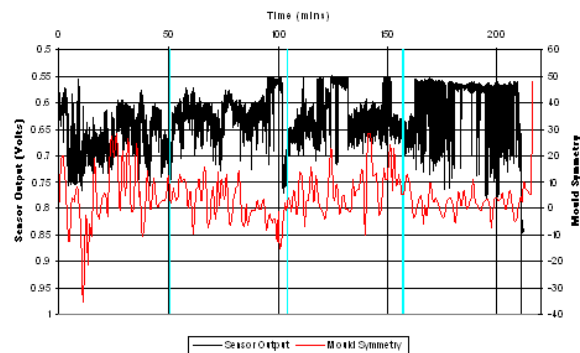


Fig. 80b: Graph showing Sensor 2 output and mould symmetry (Corus)

Although interesting this does not provide much additional information regarding the actual flow pattern than the signal "noise" or variability of a single channel. Figure 80b shows the mould symmetry plot for the same trial. There does not appear to be any easily discernable link between flow variation in the mould and flow variation in the SEN.

### Mould symmetry

The examination of data from the mould thermal monitoring system has been carried out with the aim of assessing whether asymmetry of flow within the mould may be linked to measured flow pattern in the SEN. The symmetry data are displayed as an index based on temperature measurements taken from thermocouples embedded in the slab mould end plates. The algorithm that generates the index is designed to highlight variability of temperatures both within each end plate and between the end plates. Symmetry data were available from eighteen of the plant trial sequences.

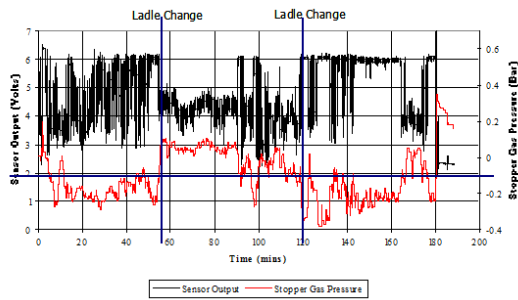


Fig. 81: Output from sensor and stopper gas pressure during trial 8 (Corus)

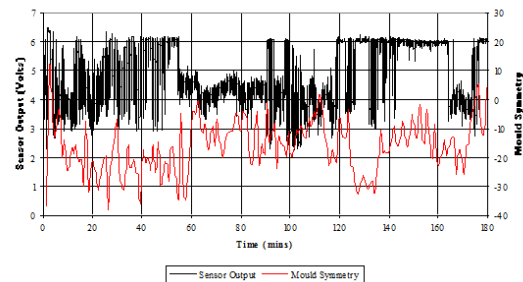


Fig. 82: Output from sensor and MTM mould symmetry during trial 8 (Corus)

As described earlier stopper pressure can be linked with gross flow patterns within the SEN. Another good example of this behaviour is seen in trial 8 (Fig. 81). During trial 8, three ladles were cast, each exhibiting significantly different flow conditions. During the first ladle the pressure is low, around -0.2 bar. The sensor signal is very erratic switching rapidly between full and not full, only stabilising for the last few minutes where the SEN is full. During the second ladle the pressure is mainly positive thus the SEN does not run full and the signal varies with other parameters, becoming erratic in a similar manner to the first ladle when the pressure dropped briefly. During the third ladle the SEN ran predominately full and was very stable. There are some indications that mould asymmetry may also have some connection to the flow pattern measured using the electromagnetic sensor although evidence is inconclusive. Figure 82 shows the symmetry index relative to the three ladles cast in trial 8 described above. There appears to be a shift in symmetry between the erratic first ladle and more stable second. However, the third ladle initially seems to follow the pattern of the first two.

Figure 83 shows that in trial 2 the symmetry varied significantly and yet there was no real effect on the measured flow pattern. Trial 9 shown in Fig. 83 displayed some regions where the symmetry appeared to loosely follow the flow pattern changes especially in the first 20 minutes. Unfortunately there is no gas pressure data for this trial so full comparison to operating parameters was not possible. Throughout the trial the stopper position was very stable. The stability of measured signal during the latter part of the trial cannot be explained, the symmetry appears just as variable as during the first 20 minutes.

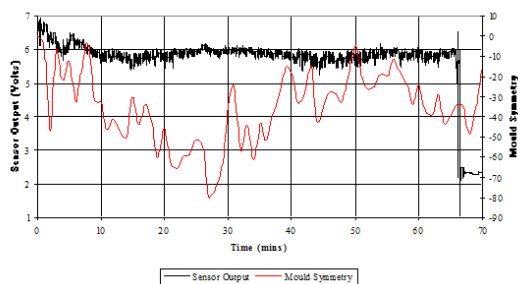


Fig. 83: Output from sensor and MTM mould symmetry during trial 2 (Corus)

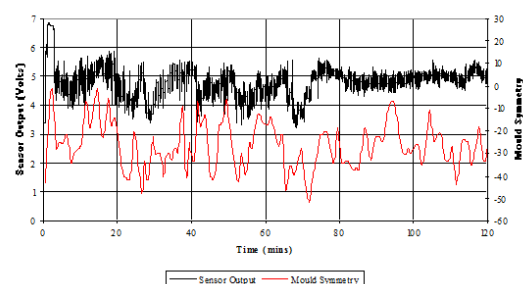


Fig. 84: Output from sensor and MTM mould symmetry during trial 9 (Corus)

A more in depth study of the symmetry index was made. Averages and standard deviations were calculated for periods of differing flow conditions. The first observation was that the index is negative for the majority of ladles examined and when positive the index is small. A negative index indicates that the east end plate is exhibiting greater unstable conditions and higher temperatures. This would suggest that the flow in the mould tends towards the east edge plate. The standard deviation when full or empty exhibits a range from 6 to 36 regardless of flow condition. There is no apparent link between the symmetry and SFV sensor measurements.

However observations have noted that conditions like trial 8 shown in Fig. 82, the shifts in symmetry are associated with major disturbances to stable casting e.g. ladle changes and large changes in casting speed. There are however, notable changes in symmetry which are not connected to such occurrence.

### *Karmen Vortex Mould Velocity Measurements*

Measurements using the Karmen Vortex mould surface flow velocity sensor were carried out to try and highlight any links between measured surface velocity and SFV SEN measurements or MTM symmetry data.

Thirty-three sets of measurements were carried out. On three of these one of the probes failed to operate correctly but single measurements were still made on one side of the mould. Table 6 shows a summary of all the results. In some cases where an obvious change in flow pattern has occurred during the trial measurement the result has been divided to allow any potential links between flow rate and SEN flow condition at the time to be studied.

Table 6: Karmen Vortex mould surface velocity measurements taken at Corus (Corus)

Trial No	Width (mm)	Casting Time (Mins)	Ladle No	Casting Speed (m/min)	West		East		Average Surface Velocity (cm/sec)	Difference in Average Velocity
					Average Velocity (cm/sec)	Std Dev	Average Velocity (cm/sec)	Std Dev		
12	1970	228-238	4	0.7	17.71	6.67	18.43	6.49	18.07	-0.72
		354-364	6	0.7	17.35	5.01	19.63	5.96	18.49	-2.28
13	1830	84-90	2	0.7	16.17	5.63	15.80	4.24	15.99	0.37
		228-235	4	0.7	18.66	5.94	17.01	5.52	17.84	1.65
16	1530	180-189	3	0.76	21.27	7.23	21.84	6.30	21.55	-0.57
		367-376	5	0.76	13.16	6.14	15.65	5.54	14.41	-2.49
17	1530	98-109	2	0.75	19.35	6.33	15.63	6.79	17.49	3.72
		351-362	5	0.75	15.18	6.75	14.48	7.49	15.31	0.7
19	1970	105-110	2	0.65	21.48	5.60	12.00	4.87	27.48	9.48
		111-113	2	0.6	22.35	7.07	11.92	4.90	17.14	10.43
		228-235	4	0.78	18.79	5.55	14.90	5.34	16.85	3.89
24	1970	131-137	3	0.91	21.67	7.77	-	-	-	-
		181-187	4	0.9	19.84	7.70	19.47	8.79	19.66	0.37
		286-293	6	0.91	20.22	7.88	16.71	7.48	18.47	3.51
25	1970	85.5-91	2	0.86	17.90	4.92	15.00	4.94	16.45	2.9
26	1830	82-88	2	0.9	20.90	7.47	18.64	6.49	19.77	2.26
		188-190	4	0.9	15.25	7.53	15.21	8.65	15.23	0.04
		190-193	4	0.9	18.97	7.77	18.16	7.84	18.57	0.81
		293-300	6	0.9	18.32	8.61	15.54	8.10	16.93	2.78
30	1970	80-84	2	0.9	17.81	6.90	17.81	7.47	17.81	0
		84-87	2	0.9	20.26	6.14	17.78	7.64	19.02	2.48
		135-144	3	0.9	20.89	6.94	16.02	7.31	18.46	4.87
31	1970	39-47	1	0.8	15.51	6.35	-	-	-	-
		102-110	2	0.9	15.92	7.04	17.27	6.94	16.60	-1.35
		156-166	3	0.9	17.89	8.23	16.23	6.93	17.06	1.66
		208-218	4	0.9	17.48	6.77	23.03	4.12	20.26	-5.55
33	1970	30-36	1	0.86	14.15	6.90	13.53	5.27	13.84	0.62
		95-102	2	0.91	17.88	5.24	15.04	5.83	16.46	2.84
		141-149	3	0.8	18.26	5.58	12.24	5.38	15.25	6.02
		220-231	4	0.91	10.71	4.97	17.53	6.90	14.12	-6.82
34	1970	25-31	1	0.85	17.51	5.62	19.88	7.54	18.70	-2.37
		87-94	2	0.85	14.92	6.03	-	-	-	-
35	1970	26-32	1	0.86	16.99	7.68	10.70	4.89	13.85	6.29
		82-89	2	0.85	15.98	6.74	15.78	6.74	15.88	0.2
		130-132	3	0.85	14.83	7.02	15.05	4.65	14.94	-0.22
		132-136	3	0.85	12.88	6.16	13.76	5.76	13.32	-0.88
		188-194	4	0.85	17.52	7.74	18.93	7.50	18.23	-1.41

It must be stated that the Karmen Vortex measurements indicate velocity only and not its direction. Hence it is not possible to link observations with the type of mould flow pattern occurring or if the velocity is reversing as asymmetry occurs. Twenty-two of the measurement periods indicate that there is an overall higher flow activity in the west side of the mould, i.e. the average surface velocity is

greater on the west side of the SEN. This could be linked to the mould symmetry measurements taken from the MTM system, which showed a tendency to be more unstable on the East side of the mould.

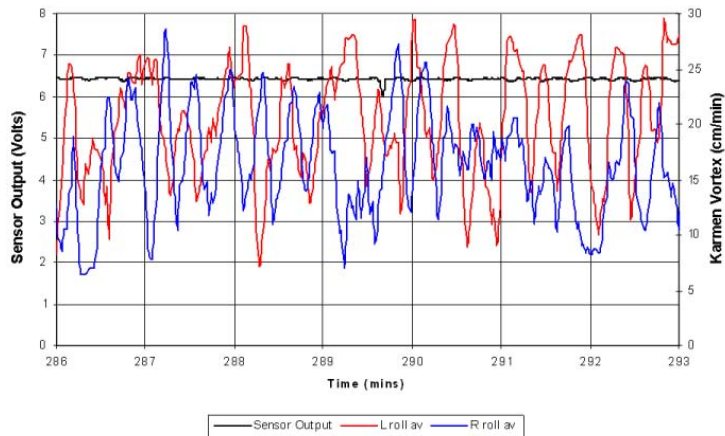


Fig 85: Example of Karmen Vortex flow measurement (Corus)

Figure 85 shows an example of the output from the Karmen Vortex sensor plotted together with the output of the electromagnetic sensor. The example is taken from a period where the SEN is running full. The first thing to note is the oscillatory nature of the measurement. In all surface flow measurements taken using this technique the velocity has been found to oscillate. The frequency and amplitude of the oscillations vary and are possibly linked to the occurrence of surface waves which can be seen in the mould. The peaks are regularly seen to be opposite as in the first half of this example. This suggests that the flow from the SEN “flip flops” side to side. This phenomenon has been shown to occur in physical modelling.

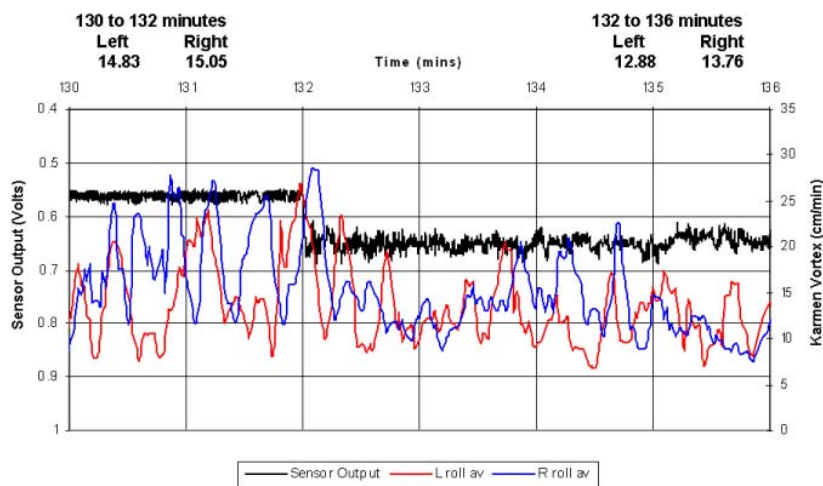


Fig. 86: Example of Karmen Vortex mould flow velocity measurements (Corus)

Figure 86 is an example of a measurement during which a change in flow pattern in the SEN has been detected by the SFV sensor. During the measurements a transition between "full" and "not full" occurred and the transition has a clear effect on the surface velocities measured. There is a significant drop in mould surface velocity on both sides of the SEN and although the standard deviation does not seem to change by much the variability of the signal does appear less.

This phenomenon has been seen during three sets of measurements, two where the transition has been from full to not full and one the other way. In all cases the surface velocity measured in the full condition is higher than the not full state which reflects the higher ferrostatic head driving flow in the

nozzle, whether the transition be upwards or downwards. This suggests that the flow pattern in the SEN is connected to the flow pattern in the mould.

The volume throughput remains constant so the change in velocity could mean that the type of vortex has changed. If the direction of roll reversed the surface velocity could drop even though the port exit velocity remains reasonably constant.

A study of the effect of casting speed was made following the caster enhancement which significantly increased the maximum casting speed. The surface velocities measured both before and after enhancement tend to be higher on the west side. Although the statistics are inconclusive studying the graphs the west end appears to be more erratic than the east. With the limited data available it is not possible to comment on whether casting speed has a significant effect on mould surface flows.

Clear links have been found between SFV measurement, Karmen Vortex surface flow and symmetry index for certain conditions or condition changes however the full picture cannot be generated without continuous flow measurement with flow direction as an element of the measurement.

#### *Statistical analysis of electromagnetic sensor signals*

It was decided that a more in depth statistical approach would be attempted to assess the connections between electromagnetic sensor signals and plant data. It was suggested that this may highlight connections which are not apparent to the naked eye. The statistical analysis was carried out on a number of trial data sets measured using the single frequency sensor.

In statistical terms the electromagnetic SFV sensor output voltage signal has a typical bimodal distribution with a 'narrow' distribution (low standard deviation) centred at higher voltage values and a 'broader' distribution (high standard deviation) centred at lower voltage values. The former distribution is associated with flow conditions in which the SEN is full of molten steel and the latter, when the SEN is only partially full with sub-optimum electromagnetic coupling occurring between the transmitter and receiver units in the sensor.

Multiple linear regression, time series analysis and other multivariate methods were applied to Corus plant trial data sets to investigate the possibility of building statistical models to predict the flow conditions in the SEN during continuous casting. The data sets included SFV sensor data, MTM (instrumented mould) data and logged casting parameters. Identification of a good model to predict onset of flow instability would be a valuable control tool for avoiding flow regimes associated with steel casts having quality issues. Linear models were investigated using stopper position, casting speed, mould level, stopper argon flow and stopper argon pressure as predictors for Flowvis sensor output voltages (S1, S2 and S3). The main findings of linear models and a range of multivariate techniques are summarised below:-

Stepwise linear models for S2 give a fair prediction of the measured S2 (and S3) output voltage, the most reliable models involving casting speed and stopper argon pressure. Predicted S2 values typically fall within  $\pm 20\%$  of measured observations and the distribution of percentage prediction errors has an interquartile range (IQR) of 12.44% (standard deviation = 16.92%) with adjusted correlation coefficient values ( $R_{adj}^2$ ) for typical models lying between 0.97-0.99. Nevertheless, the linear models were not found to be adequate for reliably relating process conditions to sensor output voltage during periods of flow instability.

Though univariate time series models give a much improved prediction, as evidenced by a percentage prediction error distribution of  $\pm 2\%$  of measured observations and an interquartile range (IQR) of 0.39% (standard deviation = 2.49%), extending the idea to a multivariate model was not successful due to the absence of consistent cross correlation spectra between sensor output voltage and process parameters.

Cluster and principal components methods were subsequently explored to see if better working models could be found. Two principal components (PC1, PC2) associated with argon pressure/flow conditions

and stopper position (casting speed) have been identified and typically account for 70% of the variance of the multidimensional process data sets. Both principal components explain a greater proportion of the variance than any of the individual process variables. Box plots of process variables and PC1 Vs PC2 plots, by cluster, have identified three distinct clusters associated with outliers. These are observations at start-up and end/run-down of trials, stopper closed position data and the largest cluster, containing observations which include the largest proportion of data from the two common distributions present in the output voltage data sets. Cluster analysis did not distinguish between the two output voltage distributions.

Histograms of stopper position and argon stopper pressure, differentiated by the two output voltage distributions suggest cut-off values for stopper position and argon pressure of 50 mm and 0.2 bar, respectively, above which stable flow appears to predominate. These observations were used to recode the sensor output voltage to binary form to investigate whether logistic regression could be used to predict the probability that SEN flow is stable or unstable. The SFV sensor voltage data is converted to binomial data by allocating 1 or 0 to the value above and below a cut-off value and the binomial distribution for this data can be written in the short hand form:

$$Y_i \sim B(n_i, p_i) \text{ for } i = 1, \dots, m, \quad (8)$$

Where:

$n_i$  is the number of Bernoulli experiments (e.g. an experiment with two possible outcomes, '1' for voltage value falling into stable flow distribution and '0' for a voltage value falling in the unstable flow distribution)

$p_i$  is the probability of success (voltage value associated with stable flow) and is unknown.

The model for the 'experiment' or trial can then be written in terms of a set of explanatory/predictor or independent variables that have an influence on the final event probability.

Logistic regression models equate the natural logarithm of the odds for a particular outcome with a linear function of the explanatory/'independent' variables and takes the general form:

$$\ln\left(\frac{p_i}{1-p_i}\right) = \beta_0 + \beta_1 x_{1,i} + \dots + \beta_k x_{k,i} \quad (9)$$

Where the  $\beta$ 's are model parameters and  $x_1 \dots x_k$  are the predictor/'independent' process variables used in the model.

The statistical parameters associated with the logistic regression model for unstable flow values ( $S2 < 5.8$  V), for the Flowvis 26 data set, is shown in Table 7 below.

Table 7: Summary of model parameter 'maximum likelihood' estimates (Corus)

Parameter	DF	Estimate	Standard Error	Chi-Square	Pr > ChiSq
Intercept	1	$(\beta_0)$ 2.8792	0.2311	155.272	<.0001
CasSpeed	1	$(\beta_1)$ -2.5115	0.1541	265.576	<.0001
MldLev	1	$(\beta_2)$ 0.0302	0.00254	141.8494	<.0001
StopPos	1	$(\beta_3)$ -0.0774	0.00146	2820.684	<.0001
StopArgPres	1	$(\beta_4)$ 3.5314	0.1126	983.9482	<.0001

From the tabulated model parameter estimates, the linear predictor related to the probability of an SFV sensor value falling in distribution 1, stable flow regime, is

$$\hat{\eta}_i = 2.8792 - 2.5115CasSpeed + 0.0302MldLev - 0.0774StopPos + 3.5315StopArg Pres \quad (10)$$

and for case 1, first line of data values in Table 7 we have:

$$\begin{aligned} \eta_i &= 2.8792 - (2.5115 \times 0.900656) + (0.0302 \times 52.762) - (0.0774 \times 43.1896) + (3.5314 \times (-0.27)) \\ &= 2.8792 - 2.262 + 1.5934 - 3.3429 - 0.9535 = -2.0858 \end{aligned}$$

And the probability associated with an unstable flow event is given by:

$$P_{case1} = \frac{e^{-2.0858}}{1 + e^{-2.0858}} = 0.1105 \quad (11)$$

If we take arbitrary values of <0.25 and >0.75 as strong indications that the flow is not unstable (is stable) and is unstable, respectively, we conclude that the case data used indicates a higher probability of stable flow. Note: Probabilities are opposite to what might have been expected because the model is for unstable flow to occur (distribution 2). Had the model been for stable flow the probabilities and interpretation would be reversed.

Associated with this type of model is an odds ratio table that shows how likely or less likely a process parameter influences the model outcome. For example, from the data in the Table 8 increasing average stopper argon pressure is thirty-four times more likely to result in an unstable flow regime and increasing casting speed is more likely to promote unstable flow. Stopper position is relatively less influential.

Table 8: Odds ratio estimates (Corus)

Effect	Point Estimate	95% Confidence Limits	
CasSpeed	0.081	0.06	0.11
MldLev	1.031	1.026	1.036
StopPos	0.926	0.923	0.928
StopArgPres	34.172	27.406	42.609

None of the models investigated were found to predict the onset of unstable flow conditions unequivocally and this indicates the need for a variable more closely associated with SEN steel level. The logistic model above should be validated further with other data sets. Two future options to help relate process conditions with the sensor output voltages associated with stable and unstable flow regimes include; acquiring data on an additional variable(s) more closely associated with molten steel level within the SEN (less stable flow conditions) and/or developing a hybrid variable from pertinent fluid flow theory.

The models developed are based purely on measured process parameters and there is no consideration of variations due to the effects of steel grade and time, thus SEN wear or clogging is not taken into account. There is clear evidence that as the outlets of the SEN begin to block during operation for longer trials there is a point where the ports are sufficiently constricted that the transition to the full flow condition occurs because of the increase in back pressure. The model at this point would not account for this.

The statistical analysis has confirmed the qualitative observations concerning the primary process variable effecting the stability of flow in the SEN being the stopper argon pressure and that stopper position (or casting speed at ladle changes where conditions are transient) has a secondary effect. Further, the logistic model analysis does actually quantify the relationship between process parameters and the sensor voltage (albeit it recorded to 0s and 1s for the two distributions) and allows the flow condition (stable or unstable) to be inferred.

## **Sidenor**

Research has corroborated that the nozzle inner pressure at CCM2 is a critical parameter influencing the steel flow pattern through the nozzle since it determines the working "steel level" within the nozzle. In this respect, a partial or complete loss of tightness in the gas feeding circuit gives rise to an important change in the steel flow conditions within the nozzle.

It has been observed that the most influential parameters over the steel flow pattern condition at CCM2 are the following:

- Air-tight condition of the gas injection circuit through the stopper. As presented in Task 3.3, a partial or complete loss of tightness in the gas feeding circuit produces a very important change in the steel flow conditions within the nozzle.
- Gas flow rate. The effect of this parameter is lower is more restricted within the standard gas flow rate range on use at CCM2 (0.3 - 0.8 l/min).
- The extent of clogging at the nozzle exit.
- Stopper rod position changes: It has been observed that the stopper rod movements due to changes in the casting speed, or due to clogging, give rise to changes in the nozzle thermocouple temperature, giving an indication that the steel jet pattern through the nozzle also changes.

## **Task 5.2 - Study of the influence of casting parameters on clogging/wear**

### **Sidenor**

Clogging and wear may lead to steel flow changes in the mould and to the subsequent inhomogeneous heat transfer in the mould, mould powder entrapment or defects in the cast product due to non-uniform shell growth. Therefore, accurate knowledge of both severity of clogging and nozzle inner wear, and the effects of a wide range of operational parameters on those phenomena can lead to the definition of guidelines for the optimisation of the metal delivery system aiming to improve the in-mould solidification process and the as-cast product quality.

Through the results of the industrial trials, it has been verified that the air-tight condition of the gas feeding circuit has a critical influence on the castability and extent of clogging. A failure of the tightness of the gas feeding circuit during casting time results in a significant air intake into the steel stream duct. It has been found that those conditions can have an adverse effect on castability due to steel reoxidation and the subsequent increase of accretions built up at the tundish nozzle inlet, leading to a progressive increase of the stopper rod position throughout the casting time. Figure 87 (Trial 10) shows an example in which strand #1 presented a poor air tightness quality and it exhibited a worse castability performance than strand #6. Steel reoxidation due to air intake through the gas injection circuit can also lead to an increase of the clogging at the SES nozzle inner body. In this respect, Fig. 88 (Trial 4) shows a comparison in terms of nozzle accretions between strand #1 and strand #6. In that case, strand #1 presented a correct gas feeding circuit tightness (back-pressure around -0.40 bar) meanwhile strand #6 had problems in that respect (back-pressure around -0.10 bar), leading to an appreciable worsening in terms of clogging conditions.

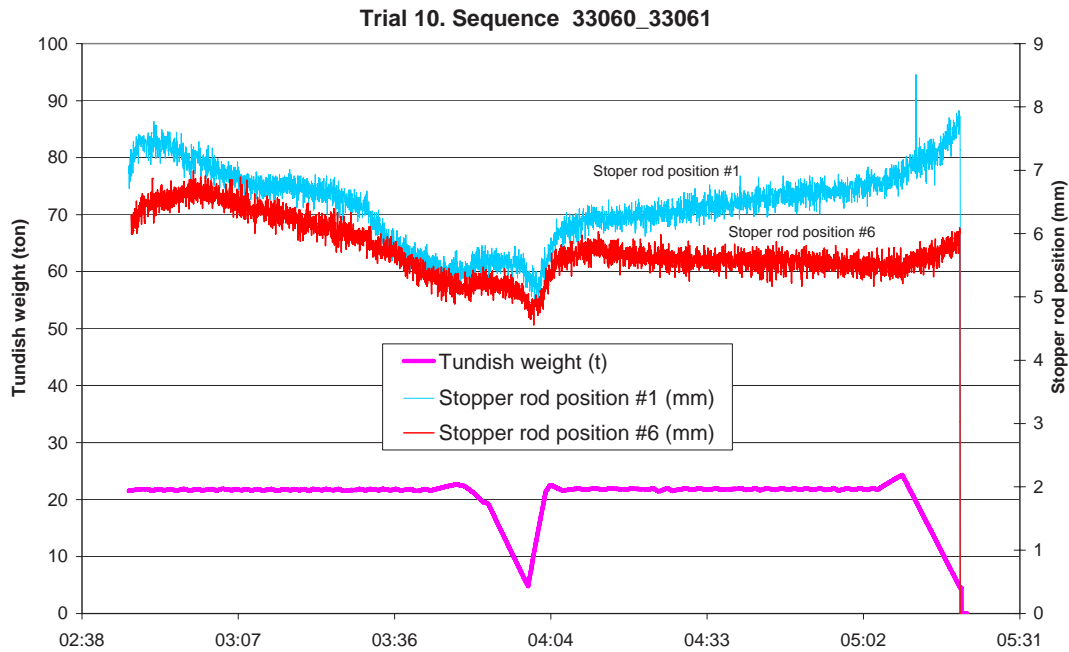


Fig. 87: (Trial 10). Example of relationship between stopper rod back-pressure and clogging at nozzle exit. Strand #6 had a good air-tight condition meanwhile in Strand #1 air-tight condition failed. Sequence 33060-33061 (Sidenor)

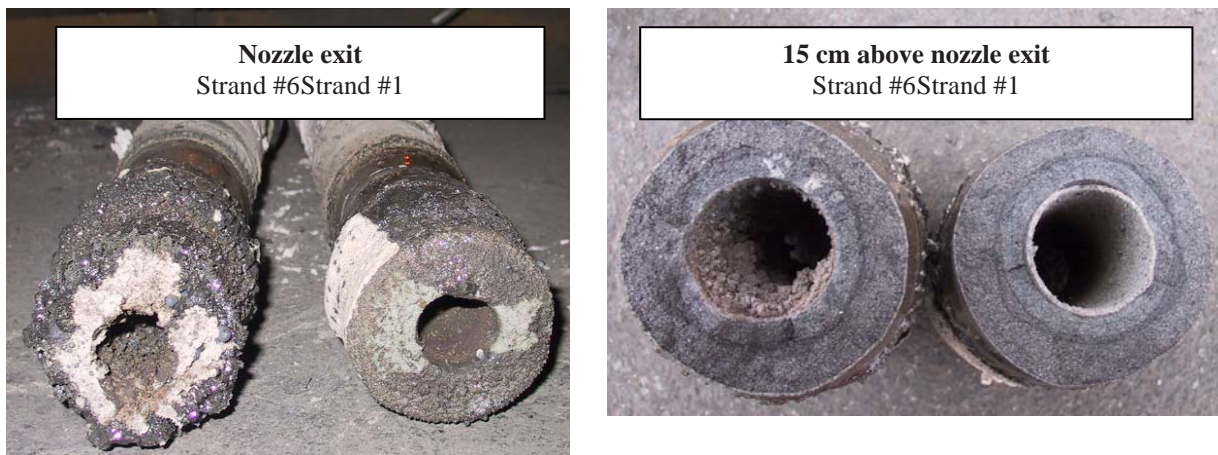


Fig. 88: (Trial 4). Comparison in terms of nozzle clogging extent between strand #1 and strand #6 based on the air-tight condition of the stopper rod gas feeding circuit. Strand #1 had a good air-tight condition meanwhile in Strand #6 air-tight condition failed (Sidenor)

Nozzle thermal characterisation by means of using thermocouples has turned out to be a method able to assess the extent of clogging at the nozzle inner body. Figures 89 and 90 show the result of two of the trials using thermocouples with a very different performance in terms of degree of clogging. Although in both trials the castability was very similar (see stopper rod trend throughout the casting time), nozzle inner clogging results were completely different. On the one hand, Trial 11 presented a thin inner alumina layer, and the thickness of the layer at the thermocouple position (340 mm from the nozzle exit) was very regular and around 1 mm thick. On the other hand, Trial 12 had a much thicker and irregular alumina layer of approximately 8 mm thick. Taking this into account, the following remarks could be made:

Trial 11: The similarity of thermocouple temperatures, together with the low rate of temperature drop throughout casting time are in good accordance with the clogging conditions at thermocouple position (uniform and 1 mm thick).

Trial 12: The large difference between the thermocouples and the significant temperature drop throughout casting time are also in good correlation with the clogging conditions (irregular and 8 mm thick)

Additionally, Trial 12 presented another hint that corroborates the good correlation between the thermocouple temperatures and the extent of clogging at the nozzle inner face. As the new ladle was opened (casting time 5:17) there was a significant increase in the thermocouple values. Taking into account that the tundish temperature is almost equal for both heats, that phenomenon could be explained as a partial washing away of the nozzle clogging when the new ladle was opened.

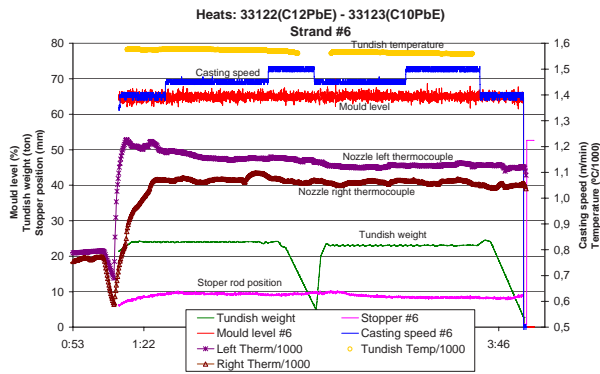


Fig. 89: (Trial 11). Example of trial using two thermocouples for the nozzle thermal characterisation. Almost non-existent clogging at nozzle body (Sidenor)

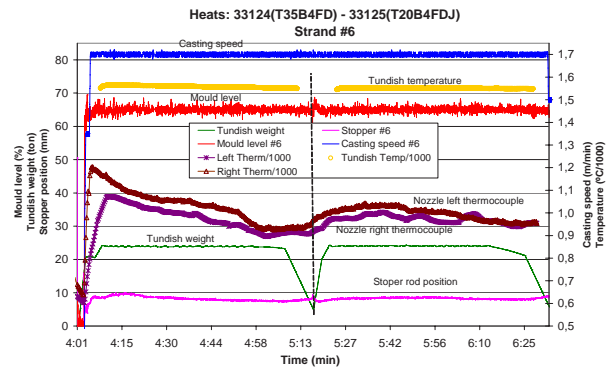


Fig. 90: (Trial 12). Example of trial using two thermocouples for the nozzle thermal characterisation. Clogging problems at nozzle body (Sidenor)

Additionally, as an outcome of the project 7215.PP/045<sup>(1)</sup> a good correlation was observed between stopper back-pressure variation (vacuum level) and nozzle outlet restriction due to clogging. In this way, the stopper rod back-pressure was shown to be a good index for the assessment of the clogging condition at the nozzle outlet. Pin-bolt stopper position gives a direct indication of how accretions are being built up at the tundish nozzle inlet and how stopper rod rises in order to provide a constant steel flow rate under constant casting speed conditions. However, information related to the stopper position is not as valid for the assessment of the clogging conditions at SES nozzle exit. When clogging appears it normally builds up at both, tundish nozzle inlet and nozzle exit. In normal casting practice, on the one hand, it is possible to find heats with severe clogging at tundish nozzle inlet and almost no accretions at SES nozzle inner body and exit; and on the other hand, it is also possible to face just the opposite situation. In Task 2.4 an example of this second situation was presented (Trial 12 presented significant clogging at SES nozzle exit while accretions at tundish nozzle inlet were almost nonexistent). Concerning the clogging at nozzle exit, it is a normal practice to use oversized nozzle bores, and this means that the stopper rod position is almost insensitive to the nozzle exit bore clogging process unless it becomes too severe. For this reason it would be very advantageous to develop a method for the on-line assessment of the extent of clogging at the nozzle exit. In this respect, in the project 7215.PP/045<sup>(1)</sup> a good correlation was found between stopper back-pressure variation (vacuum level variation) and nozzle outlet restriction due to clogging for the cases in which there was no failure of the air-tight conditions at the gas feeding circuit. Therefore, information from the industrial trials carried out during this project will be used to try to corroborate that finding (stopper back-pressure signal as a valid on-line indicator of how the nozzle outlet becomes more restricted due to the clogging accretions throughout casting time). In Table 6 both, the variation of the stopper rod back-pressure during the entire sequence and the evaluation of the nozzle exit diameter after sequence end are included. Figure 91 shows the result of the trials carried out so far in this respect, together with the results of the trials carried out in the project 7215.PP/045<sup>(1)</sup>, and it is possible to see that again a good correlation between both parameters is obtained.

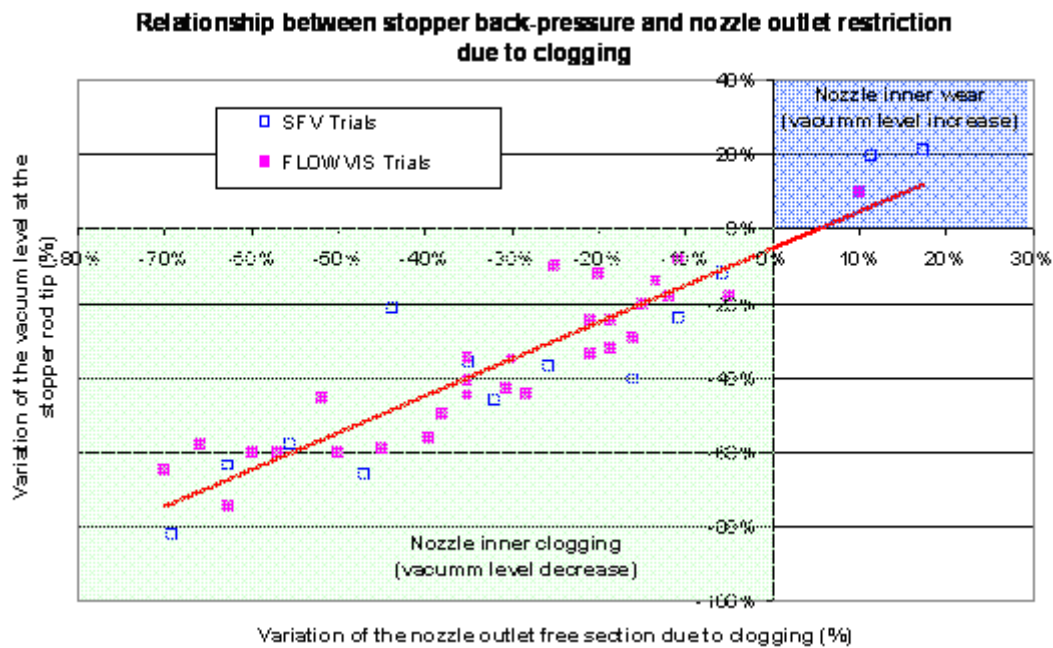


Fig. 91: Relationship between stopper back-pressure (vacuum level) and nozzle outlet restriction due to clogging phenomenon (Sidenor)

### Task 5.3 - Investigate criteria for changing casting nozzle during casting

#### Corus

As discussed previously when the project was proposed it was expected that part of the trial work would be carried out at Corus Port Talbot Works. The slab casting machines at Port Talbot all use a tube changing device to change the SEN. Although the slab caster at Scunthorpe uses a fixed SEN built into the tundish, data were collected concerning condition of the SEN at the end of a casting sequence which could be compared with the signal from the electromagnetic sensor.

The factors which limit the life of the SEN are:

- Inlet port size (clogging or wear)
- Outlet port size (clogging or wear)
- Internal bore (clogging or wear)
- Erosion at the mould meniscus

It is not possible to link erosion of the SEN at the meniscus to SFV signal or mould flow velocities. The expected life of an SEN in terms of erosion at the meniscus is well understood as excess erosion leads to failure of the nozzle and premature termination of casting. Any criteria for SEN changing which may be developed would be overridden by the maximum casting time allowable for the SEN. Clogging at the exit ports however will affect both flow inside the nozzle and how the metal feeds into the mould.

During plant trials where practical and safe to do so, an attempt was made to recover the SENs used. In total nine SENs were successfully retrieved which were free from solidified metal and it was thus possible to examine their condition.

Figure 92 shows the locations of measurements taken and Table 9 is a summary of measurements.

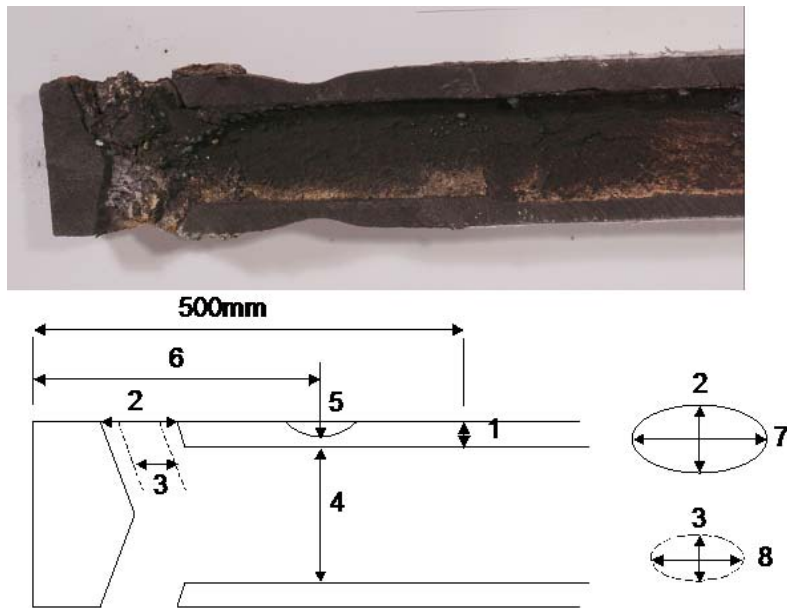


Fig. 92: SEN dimensions after use (Corus)

Table 9: Dimensions of used SENs (Corus)

Trial	Ladles Cast	1 (mm)	2 (mm)	3 (mm)	4 (mm)	5 (mm)	6 (mm)	7 (mm)	8 (mm)
Unused SEN	0	~22	70	70	74	23		70	70
FLOWVIS 14	1	-	70	51	73	N/A	-	60	50
FLOWVIS 16	5	20(-2)	71	36	91	12	170	65	40
FLOWVIS 17	6	19(-3)	70	30	74	13	193	60	40
FLOWVIS 22	4	-	70	45	-	N/A	-	60	60
FLOWVIS 24	6	21(-1)	70	58	75	N/A	183	68	60
FLOWVIS 25	2	19(-3)	76	70	82	N/A	220	72	70
FLOWVIS 29	2	22(0)	72	50	70	18	192	60	55
FLOWVIS 30	3	23(+1)	75	60	70	N/A	205	60	58
FLOWVIS 33	4	20(-2)	70	45	-	18	185	70	55

The SFV sensor is located approximately 500 mm from the bottom of the SEN in the operating position. As can be seen from Table 9 dimension 1, wear of SEN in this region is small and there is very little material deposited on the internal bore or worn away. Changes in the signal due to wear or clogging in the field of view of the sensor are not significant during the life of an SEN and therefore cannot be used as an indication of SEN condition.

A study of the effect of clogging on measured signals was carried out. A calculation of the change in exit port size was carried out. It was not possible to track the rate of change but a final figure was calculated for each SEN collected. See Table 10 and Fig. 93.

Table 10: Port sizes after casting. Degree of clogging (Corus)

Trial	Ladles Cast	Casting Time (mins)	2 (mm)	3 (mm)	7 (mm)	8 (mm)	Port Size (mm <sup>2</sup> )	Restricted/Clogged Port Size (mm <sup>2</sup> )	Reduction (%)
Unused SEN	0	-	70	70	70	-	3850	-	-
FLOWVIS 14	1	70	70	51	65	54	3575	2164	40
FLOWVIS 16	5	400	71	36	70	44	3905	1245	68
FLOWVIS 17	6	450	70	30	65	44	3575	1037	71
FLOWVIS 22	4	260	70	45	65	64	3575	2263	37
FLOWVIS 24	6	320	70	58	73	64	4026	2917	28
FLOWVIS 25	2	100	76	70	77	74	4478	4070	11
FLOWVIS 29	2	105	72	50	65	59	3677	2318	37
FLOWVIS 30	3	150	75	60	65	62	3830	2923	24
FLOWVIS 33	4	250	70	45	70	55	3850	1945	50

As expected the degree of clogging is clearly in general related to the total casting time. However certain grades are more susceptible than others, particularly those with a high aluminium content.

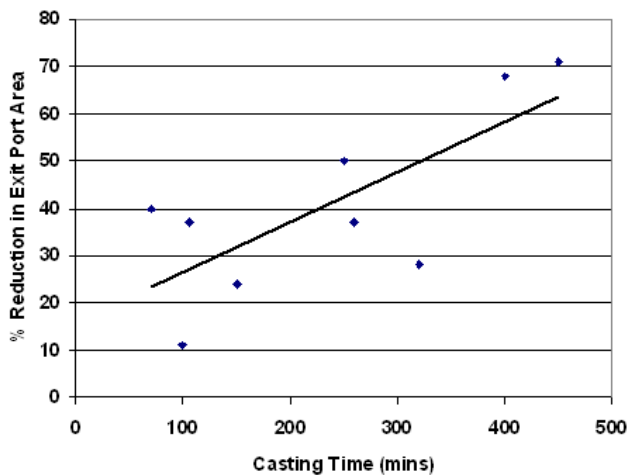


Fig. 93: Plot of casting time versus degree of SEN exit port clogging (Corus)



Fig. 94: SEN from trial 17 with 71% reduction in exit port size (Corus)

Examination of the electromagnetic SFV sensor signal has highlighted that for five of the nine casts the clogging had no visible effect upon the sensor signal other than normal variation expected relative to process variables (See Task 5.1). However, during three trials (Trials 16, 17 and 33) significant clogging was found, 68%, 71% and 50% reduction (see Fig. 94) in exit port size. Two of the trials were long with sequences of 5 and 6 ladles, 400 minutes and 430 minutes respectively. During the last ladle and a half of both trials the flow pattern was either full or tending towards full. This flow condition would usually be associated with a low stopper gas injection pressure; however both trials exhibited an increasing trend in stopper gas pressure that was significantly higher than the usual two-phase to full flow pattern transition. In these cases there must be another factor causing the SEN to fill. This would happen if there was a restriction at the SEN outlet. To maintain the mass throughput from the tundish to the SEN a greater driving head would be required at the exit ports which is generated by the increase in level in the SEN. The restriction would increase back pressure which leads to an increase in stopper in gas pressure required to depress the level in the SEN.

Trial 33 was shorter but approximately halfway through the fourth and final ladle an increase in speed from 0.85 m/min to 0.9 m/min triggered a switch to a full SEN with the same associated climbing stopper position noted in trials 16 and 17. The increase in speed was also accompanied by a stopper flush. The outlet ports were found to have a reduction in area of 50%.

Although the reduction in final cross-section is much less for trial 24 (only 28%) the flow behaviour in the SEN is very similar to that in trials 16 and 17. Trial 24, like trial 33, was carried out after the slab caster enhancement thus the operating speed was higher, 0.9 m/min as opposed to 0.75 m/min. As can be seen in Figs. 95a and 95b there was a "Full" SEN for the majority of the trial, but the transition to two phase flow from the "Full" condition can be clearly seen when the stopper gas pressure rises above -0.15 bar until approximately halfway through the penultimate ladle after which the SEN remains full despite the stopper gas pressure gradually increasing above the -0.15 bar level. This change in flow behaviour is caused by the accretions on the SEN outlet reaching the point where the port outlet size becomes the limiting factor on flow pattern change and not the stopper gas pressure. During this period the stopper position can also be seen to be steadily increasing. Although there is no evidence to support the theory the reduction in port area in this SEN may have been affected by the end of casting and partially washed clear.

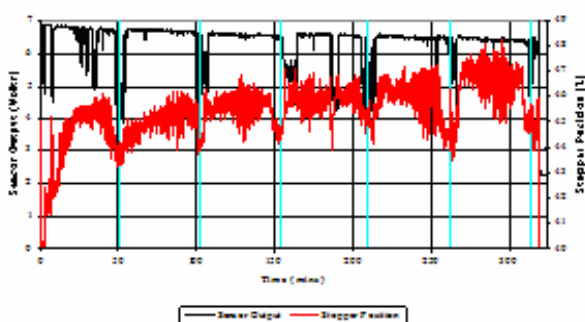


Fig. 95a: Trial 24 sensor output and stopper position (Corus)

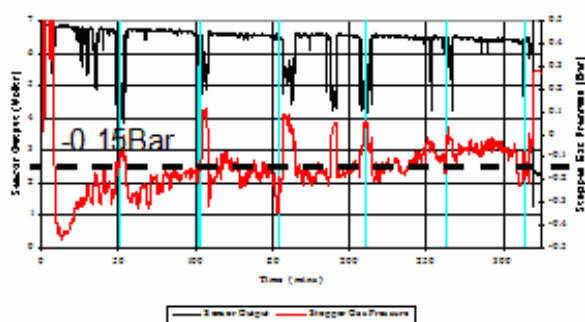


Fig. 95b: Trial 24 sensor output and stopper position (Corus)

From the evidence collected it is proposed that the exit ports interfere with the normal outflow of steel when they are reduced in area by greater than 50%. There does not appear to be any direct indication from the electromagnetic sensor to indicate whether the casting nozzle is not performing, and thus be in need of changing. The SFV sensor can only indicate that there is significant clogging when combined with other process parameters. There appears to be a link with stopper pressure and stopper position. It may be possible that a combination of the three may present an early warning. If the sensor shows the SEN is full while the pressure is high the exit ports of the SEN are becoming blocked. Also, when the SEN is full and the stopper is rising by a significant amount there is also a problem. This is an overcomplicated approach the problem. Task 5.2 has shown that clogging can be detected by monitoring the stopper gas pressure on the billet caster as described in the work carried out at Sidenor I+D. This may be transferable to the slab.

A second effect of the change in exit port size would be the velocity of steel exiting the port. During trials 16 and 17 two Karmen Vortex mould surface velocity measurements were taken. See Table 11. These were taken during periods of comparable casting conditions all at a casting speed of 0.75 m/min. In both cases during the second measurement the SEN was running mainly full (SFV sensor) and had raised stopper gas pressure indicating that the exit ports were significantly blocked.

Table 11: Variation in measured mould surface velocity (Corus)

Trial Number	Ladle Number	Casting Time (Mins approx)	Casting Speed (m/min)	Left		Right		Average Surface Velocity (cm/sec)
				Surface Velocity (cm/sec)	Std Dev	Surface Velocity (cm/sec)	Std Dev	
16	3	180-189	0.76	21.27	7.23	21.84	6.30	<b>21.55</b>
	5	367-376	0.76	13.16	6.14	15.65	5.54	<b>14.41</b>
17	2	98-109	0.75	19.35	6.33	15.63	6.79	<b>17.49</b>
	5	351-362	0.75	15.18	6.75	14.48	7.49	<b>15.31</b>
24	3	131-137	0.91	21.607	7.77	-	-	-
	4	181-185.5	0.9	19.84	7.70	19.47	8.79	<b>19.66</b>
	6	286-293	0.91	20.22	7.88	16.71	7.48	<b>18.47</b>
33	1	30-36	0.86	14.15	6.90	13.53	5.27	<b>13.84</b>
	2	95-102	0.91	17.88	5.24	15.04	5.83	<b>16.46</b>
	3	141-149	0.8	18.26	5.58	12.24	5.38	<b>15.25</b>
	4	220-231	0.91	10.71	4.97	17.53	6.90	<b>14.12</b>

The build up of alumina in the SEN exit ports is obviously changing the flow pattern within the mould. With a smaller exit port flow velocity will be faster for the same volume throughput however velocity at the mould surface is reduced. A change in flow pattern in the mould must result as an effect of reduction in port size with more of the flow penetrating deeper into the mould.

Karmen Vortex velocity measurements were also taken during trials 24 and 33 after the caster enhancement where the casting speed was increased to 0.9 m/min. Due to operational restrictions it was not possible to take measurements at the same casting speed in every ladle of a sequence however these two casts also exhibited the SFV and stopper gas conditions linked with clogging. Where the casting speed is consistent the surface velocity also shows a reduction during the later "clogged" ladles.

#### Task 5.4 - On-line evaluation of flow pattern, clogging and wear within SEN

##### BFI/Saarstahl

The on-line ultrasonic prediction of the inclusion length index is an indirect measure for flow pattern and alterations of the SEN since the ultrasonic data are dependent on the flow inside the SEN and the constitution of the SEN wall. For the individual evaluation of flow conditions the PLS algorithm had to be calibrated under well defined reference conditions. But these were hard to gain. Therefore, analysis was focused and refined on basis of the inclusion length index prediction. Moreover, the predicted inclusion length index has the benefit of being of direct interest for process control.

The results of the extensive plant trials showed stable casting conditions and very low inclusion length indices. This is a strong indication that no sudden changes of flow patterns had occurred.

#### Work Package 6 - Recommendations for Process Optimisation

The objective of Work Package 6 was to recommend criteria for optimisation of both nozzle design and casting parameters, based on the results of the research work.

##### Task 6.1 - Optimisation of casting parameters

##### Corus

Although there has been no strong evidence to indicate that product surface quality is affected by the flow pattern within the SEN, stable casting conditions are preferable. When designing the SEN and modelling the system both physically and using computing techniques the ideal flow condition is assumed to be with the SEN running full. The SEN full is the most stable condition as it removes the potential for transient conditions caused by fluctuation of steel level and steel stream position within the

SEN. The results of the trials at Corus have shown that the filling of the SEN is strongly related to the pressure of argon in the stopper injection circuit. In addition to observation of graphical data the relationship has been confirmed using statistical modelling. The modelling has not however been able to explain fully the relationship between process parameters and flow patterns. The real system is highly complex.

During trials it was observed that the transition in flow pattern could be triggered by changes in gas injection flow rate. This may be used to control the flow pattern in the SEN; however, care must be taken because gas flow rate is important to ensure that other factors in the casting process regarding clogging and flotation of inclusions in the mould are taken into account. Physical modelling has identified ideal injection rates to generate the desired flow pattern in the mould. A trial to demonstrate the potential for controlling flow pattern in the SEN is described in Task 6.3.

Trials to investigate surface defects have hinted that the occurrence of long crack in slab material is in part related to the active level control used to spread wear in the SEN by ramping mould level. The majority of defects occur in the region where mould level is rising or at the extremes of the cycle. The active ramping is employed to prolong SEN life and maximise casting time. However it is thought that a contributing factor to the surface defects is the movement of the meniscus relative to the mould plate causing lapping and melting of the slag rim generated by the mould powder. If the ramp is stopped the mould surface would cut through the SEN terminating the casting sequence in a relatively short time. This is not a satisfactory option.

In other casters around the world the method of spreading wear on the SEN is also to ramp the position of the tundish, meaning that meniscus level remains stable. This would require a significant investment as the tundish car is not designed to do this and is therefore not practical at this time.

In terms of casting setup generated by modelling neither solution is ideal as the act of ramping does not maintain the SEN at the optimum immersion depth.

## **BFI**

Inclusions show a very low level at Saarstahl steelworks and relevant clogging occurs very seldom. A potential for optimisation of the casting process at Saarstahl might be given in diminishing the outer diameter of the SEN which has a positive effect on the spatial conditions in the mould.

## **Sidenor**

The research carried out in the rest of Work-Packages has allowed to come up with a set of conclusions related to the optimisation of the casting parameters and conditions for the billet caster of Basauri Plant, and most of them are applicable for any caster. Those recommendations include the following subjects:

- Air-tight quality of the gas injection circuit through the stopper, and its influence on clogging-castability and mould level stability.
- Optimum nozzle immersion depth from the point of view of the effect of nozzle inner pressure on mould stability.
- Use of the stopper-gas injection back-pressure signal for the on-line assessment of the clogging at the nozzle exit.
- Use of thermocouples installed in the nozzle wall as a method for the on-line assessment of the extent of clogging at the nozzle inner body. This technique, due to its special arrangements is just recommendable in a trial basis and not for standard practice.

Below, a summary of the most remarkable guidelines, together with a brief explanation, is presented:

When using gas injection practice through the stopper, with low flow rates, the air-tight condition of the gas feeding circuit is a critical factor. To be precise, it has been found that it has a critical influence on castability and extent of clogging due to steel reoxidation because of the air infiltration into the steel

pouring line. That is to say, air tightness problems at the gas injection circuit through the stopper are generally associated with an impairing of clogging phenomenon.

Additionally, an unstable air-tight condition in the gas feeding circuit gives rise to mould level disturbances and also a worsening of in-mould solidification conditions. Figure 96 shows how a spontaneous sudden change of the air-tight condition of the gas injection circuit through the stopper is very harmful for the mould level stability because it gives rise to non-desirable mould level fluctuations. Therefore, the air tightness of this circuit has to be reliable enough in order to avoid this kind of unstable mould level condition.

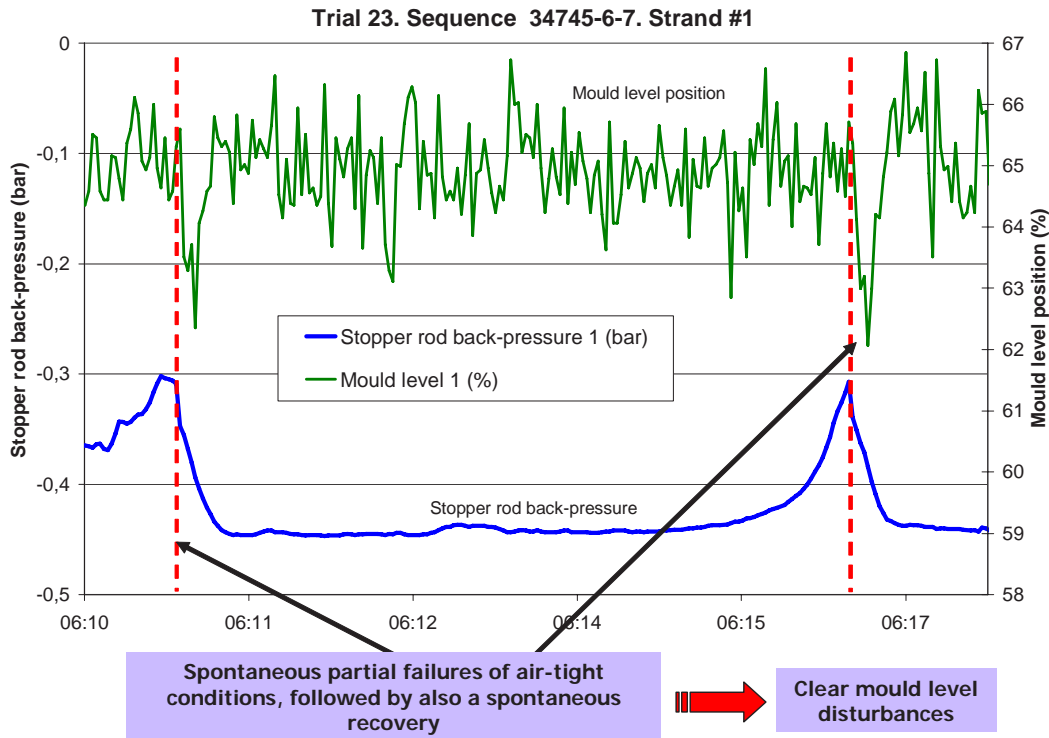


Fig. 96: (Trial 23). Effect of spontaneous sudden change of the air-tight condition of the gas injection circuit on the mould level stability (Sidenor)

Nevertheless, the outcome of the research has revealed that when having an airtight circuit through the stopper, a slight worsening of the in-mould solidification conditions was found, namely:

- Worse mould level stability
- Higher variability of the mould thermocouples
- Higher variability of the friction between billet and mould

Despite that, the benefits of a better castability and cleanliness clearly justify the interest of having an optimised gas injection circuit in terms of air-tight condition.

Additionally, it was been found that, taking into account the effect of stopper rod back-pressure on the mould level stability, the optimum nozzle immersion depth at the billet caster of Basauri plant is 115 mm instead of 105 mm. By means of this change, vacuum levels within the nozzle are lower and hence the risk of having an impairing of the mould level stability is significantly lower. Figure 97 shows a trial in which 115 mm was used instead of 105 mm, and it is possible to see how the mould level stability is quite stable throughout the sequence since stopper-rod back-pressure kept above -0.40 bar. In Work-Package No. 4 was demonstrated how the mould level stability clearly impairs when back-pressure makes lower than -0.40 bar.

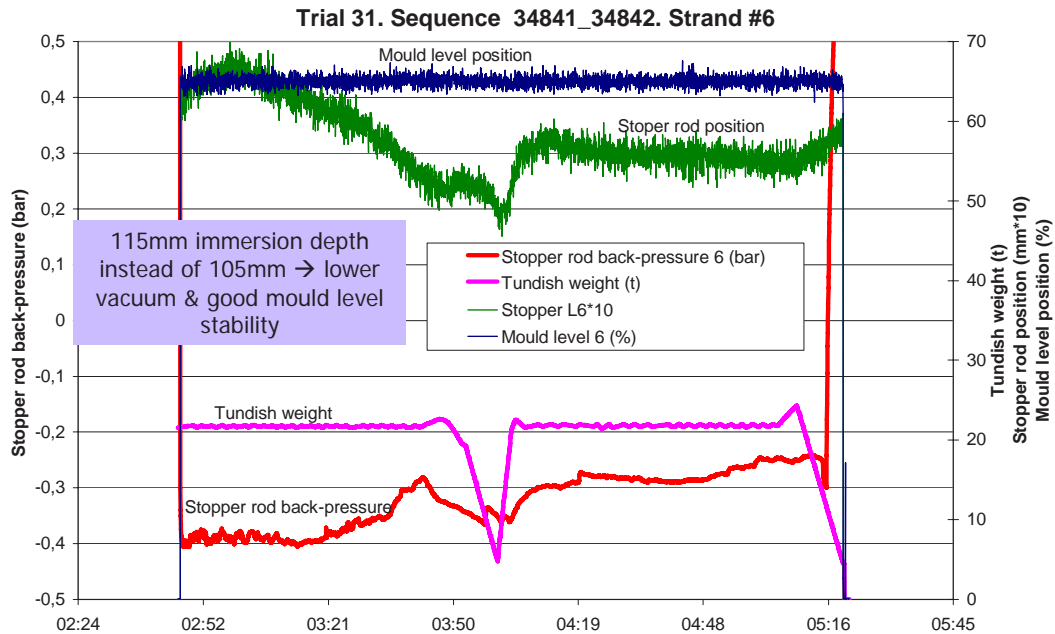


Fig. 97: (Trial 31). Trial using 115 mm of nozzle immersion depth instead of 105 mm. Stopper back-pressure is  $\geq -0.40$  bar (Sidenor)

As far as new techniques or signals able to give helpful information for the process control and optimisation, the most remarkable conclusions deal with the clogging phenomenon, and they are the following:

The nozzle thermal characterisation using thermocouples is a suitable method for the on-line assessment of the clogging extent at the nozzle inner body. But, it is only recommendable on a trial basis. This technique is not suitable for a standard casting practice because of the complexity of the thermocouple installation method.

The gas injection back-pressure signal has turned out to be a suitable signal for the on-line assessment of the clogging at the nozzle exit. A good correlation between stopper back-pressure variation (vacuum level) and nozzle outlet restriction due to clogging has been found. Figure 91 showed the result of the trials carried out till now in this respect, together with the results of the trials carried out in the project 7215.PP/045<sup>(1)</sup>, and it is possible to see that a good correlation between both parameters is obtained. In this respect, it is important to take into account that the stopper rod position and evolution throughout casting time gives a direct indication of the clogging extent at the nozzle inlet, but clogging at the nozzle exit could follow a different trend. Because of that reason, the use of this experimental technique can give additional information concerning the clogging behaviour focused on the nozzle exit.

## MEFOS

MEFOS has designed and constructed a physical model of the slab caster at SSAB Tunplåt AB in Luleå. A great effort has been undertaken to obtain a functional and accurate description of different phenomena during continuous casting using the physical model. The measurements with the SEN flow sensor gave promising results in the physical model as opposed to the meniscus velocity sensor which did not provide any useful information. The results regarding the measurements with the meniscus velocity sensor and SEN flow sensor provided by MPC were not satisfactory especially in relation to plant trials. This fact rendering it difficult for MEFOS to provide process optimisation suggestions based on the measurements with the different sensors.

From the theoretical view the most important factors affecting any electromagnetic sensor developed with the previous presented technique, e.g. Lorentz force, is the emitted magnetic field from the sensor combined with the distance between the sensor and the examined fluid as well as the velocity and

electric conductivity of the same. This was clearly illustrated in Fig. 15 and by Equations 1-3 (see Task 1.5). Bearing these fundamental facts in mind the performance of the different sensors may be discussed. As mentioned earlier the meniscus velocity sensor has earlier been used in an ECSC funded project<sup>(2)</sup> and one important task of the present project were to improve the signal output from this type of sensor.

The signal output from the meniscus velocity sensor may only be improved by either shortening the distance from the sensor to the meniscus or by enforcing the magnetic field emitted by the sensor. During the previous project the cooling of the sensor was thought to be the most important factor and one idea was to use a stronger magnet in the sensor thereby increasing the distance between the sensor and the meniscus as presented in Fig. 98. From the figure an estimated velocity in the meniscus of 0.3 m/s will lead to a decrease of the Lorentz force with a factor of 100 when the distance is increased by 0.07 m. The drastic decrease of the Lorentz force when the distance increases requires a most sensitive method to determine the force in the sensor and transform it to a signal output. Determination of these small forces  $\sim 0.001$  N in conjunction with the conditions during industrial continuous casting may raise some questions if these forces could ever be determined with any accuracy.

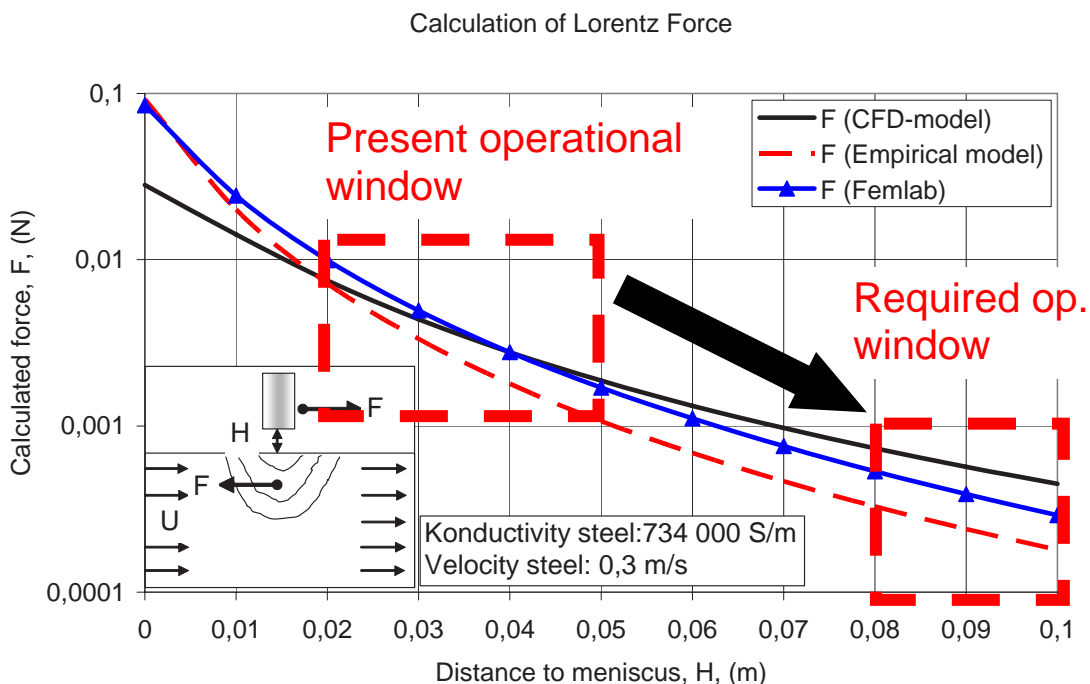


Fig. 98: Calculation of Lorentz force as a function of distance at a constant steel velocity at 0.3 m/s (MEFOS)

According to MPC it employed one of the strongest magnets available in the new meniscus velocity sensor. During the trials in the physical model dross formation may have affected the signal output from the sensor as the dross consists of approximately 90 percent metal. The dross is stagnant in the mould and would therefore hinder a motion of the magnetic material in the sensor which may explain the results presented in Fig. 40. This explanation may also be valid for the plant trials where the surface of the sensor was covered by iron dust, as shown in Figs. 41a and 41b. Thus, it needs to be pointed out that according to SSAB the iron content in the casting powder is less than 1 percent. This implies that even if the meniscus velocity sensor may withstand the elevated temperatures by using a strong magnet the sensor may not work due to pick up of iron dust from the casting powder.

MEFOS finalised the physical model hereby reducing the dross formation to negligible levels and it was planned to conduct a final measurement campaign at MEFOS as well as at SSAB. Unfortunately, no sensors were delivered by MPC to perform these last investigations. Even so, it is MEFOS opinion that the constraints related to the meniscus velocity sensor were too large to overcome using the present technique with electromagnetic sensors.

On the other hand, the second version of the SEN flow sensor delivered by MPC provided some interesting results in the physical model, as shown in Figs 35 to 37. It may be emphasised, that the comparison between the theoretical calculated velocity in the SEN and the measured velocity from the SEN flow sensor shows a very good agreement at higher casting speeds for two of the three measured sequences, as shown in Fig. 37. This implies that the sensor is actually measuring the velocity of the fluid in the physical model. Regrettably, the sensor could not operate at elevated temperatures during the plant trials. As mentioned earlier MPC performed a fault tracing investigation and found problem with the cooling system of the sensor. Similar to the meniscus velocity sensor a modified SEN flow sensor with a working cooling system should have been supplied by MPC.

The constraints related to the SEN flow sensor are easier to define than the constraints related to the meniscus velocity sensor. The distance between the flowing fluid and the sensor is constant given by the thickness of the submerged entry nozzle. A higher velocity of the fluid will lead to a higher force acting on the magnetic material in the sensor thereby facilitating an easier way of transforming the force to a signal output. The submerged entry nozzle will also protect the sensor from direct heat radiation from the liquid steel.

The fact of constant distance between the sensor and the flowing fluid may be used to identify any changes in the distance as this will directly affect the signal output if the velocity of the fluid is approximately the same. During normal operations at continuous casting the volume flow of steel may be assumed to be approximately constant with respect to time. By combining the facts of constant distance and an approximately constant velocity, problems with clogging should give an immediate response in the signal output. This could lead to a further application of the SEN flow sensor.

The promising results from the trials in the physical model imply that the SEN flow sensor could be developed to a working sensor at industrial conditions for velocity measurements as well as for determination of clogging problems.

Finally it may be concluded that the lack of results related to the electromagnetic sensors may have been a result of absence of funding for the development of the sensors to MPC in the current project. In retrospect MEFOS might have used MPC as a subcontractor in the project which could have prevented any change in focus related to development of the sensor when Agellis purchased MPC.

As a result of this no optimisation of casting parameters may be reported from MEFOS.

## **Task 6.2 - Optimisation of casting nozzle**

### **Corus**

There has been no strong evidence indicating that the flow condition within the SEN has an effect on product surface quality. As a result of trials using the electromagnetic sensor with mould flow measurements there are no recommendations for design changes in the casting nozzle.

### **Sidenor**

This task was scheduled in order to allocate some work in case it was decided to change the nozzle design as a part of the countermeasures in order to optimise the casting parameters aiming to improve the as-cast quality.

In Task 4.3. it has been highlighted that a big vacuum level can give rise to a clear worsening of the mould level stability. The main factors influencing the stopper-rod back-pressure are the following:

- Distance between the stopper rod tip position and the meniscus position
- Nozzle outlet section
- Gas flow rate
- Casting speed

Casting speed and gas flow rate are fixed because of productivity and quality reasons. In the case of gas flow rate, higher gas flow rates could give rise to pinhole problems. Therefore only the two first items are susceptible to be modified.

Concerning the nozzle outlet section, it plays an important role in the stopper back-pressure value in the sense that the bigger the outlet diameter, the bigger the vacuum within the nozzle. Therefore, the reduction of the nozzle outlet diameter could be one possible countermeasure in order to avoid an impairing of the mould level stability. Of course, this option is not recommended from the point of view of casting sequence length because a reduction of the nozzle outlet diameter diminishes the capability of the nozzle to allocate the clogging without having serious castability problems.

Therefore, in order to reduce the vacuum level within the nozzle, it was decided to increase the nozzle immersion depth (tundish in a lower position) instead of decreasing the nozzle outlet diameter. By means of this measure, the distance between the stopper rod tip position and the meniscus position is lowered, and stopper-rod back-pressure is kept within the safe range (back-pressure  $> -0.40$  bar). Therefore, problems concerning mould level stability impairing are avoided.

### Task 6.3 - Application and testing of optimisation criteria

#### Corus

As mentioned previously, during Semester 4, trial 13 it was noted that the transition from a "full" SEN to an annular or non-filled flow i.e. a steel stream in a partially filled SEN appeared to be stimulated by a small increase in argon flow rate. In the tundish mould set-up of the Scunthorpe slab caster this transition has already been clearly shown to relate to an argon pressure of  $-0.15$  bar. Below  $-0.15$  bar the SEN runs full and above this the flow pattern is annular or non-filled. The injection system used controls the flow rate of the argon allowing the pressure to vary freely.

To investigate this phenomenon a controlled trial was carried out where the stopper argon injection flow rate was increased in small increments over a two ladle casting sequence. The standard injection rate used at Scunthorpe slab caster is 6 l/min. Starting approximately 10 minutes into the cast (as can be seen below in Figs. 99a and 99b) the argon rate was reduced to 5.5 l/min. This was increased by steps of 0.1 l/min to a maximum of 6.9 l/min at the end of casting.

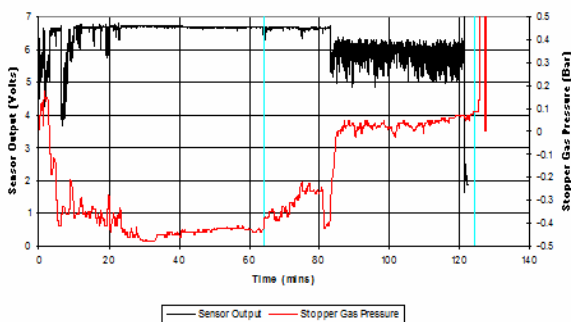


Fig. 99a: Output from sensor and stopper gas pressure during trial 23 (Corus)

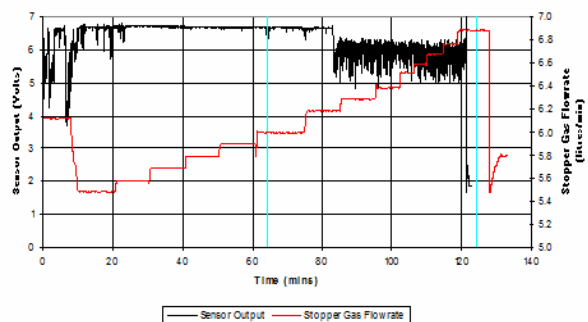


Fig. 99b: Output from sensor and stopper gas flow rate during trial 23 (Corus)

It can be clearly seen from Figs. 99a and 99b that there was a definite link between the changeover in flow pattern measured and stopper gas pressure which in itself appeared to be triggered by an increase in stopper gas flow rate. The transition occurred during the period where gas flow rate was 6.2 l/min just prior to increase to 6.3 l/min. During the original observation of this phenomenon in trial 13, the transition occurred in line with a step change in gas flow rate from 6.25 l/min to 6.33 l/min.

Further investigation of this change in flow pattern indicated that the transition was accompanied by a degradation of stability of both stopper position and mould level control. This can be clearly seen in Figs. 100a and 100b. Although not as obvious, a similar degradation occurred in trial 13.

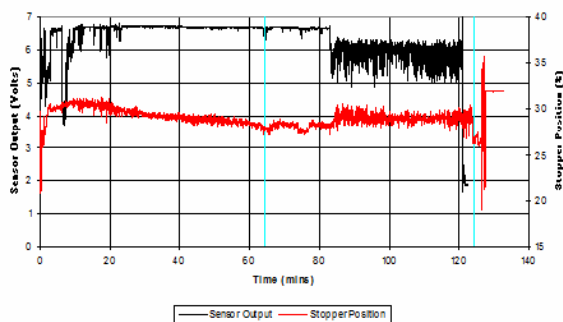


Fig. 100a: Output from sensor and stopper position during trial 23 (Corus)

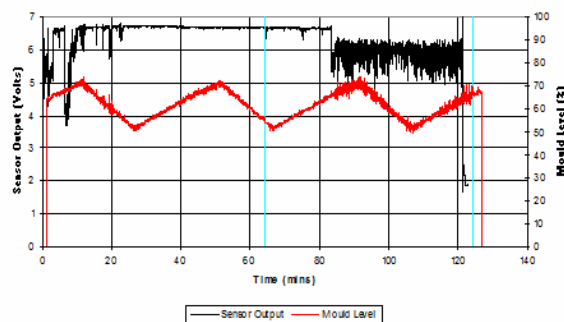


Fig. 100b: Output from sensor and mould level during trial 23 (Corus)

It must be remembered that the changes in stopper gas pressure, which trigger this kind of transition, are not always related to changes in argon flow rate. As stated previously the argon flow rate is controlled to a constant 6 l/min during standard operation. There are obviously other variables that trigger the transition. However it may be possible to use this phenomenon to control the flow pattern.

### BFI/Saarstahl

The results of this project demonstrate that the inner geometry of the pouring system of Saarstahl is near to the optimum with special regard to the cleanliness in terms of inclusion length. If the outer diameter of the SEN shall be reduced the only way is to diminish the wall thickness. But this is demanding to the mechanical stability, the chemical stability especially at the meniscus area and the air tightness since air ingress must be avoided, anyway. The design and application of a new SEN is far beyond the outline of this project since this will lead into questions regarding the inner structure of the refractory material.

### Sidenor

During the project, the recommendations and conclusions were properly tested at plant and applied to the industrial practice. In this respect, the following recommended practices have been already standardised at the CCM2 of Basauri Plant:

- Optimised stopper rods and gas injection circuit to provide an air-tight condition of the complete gas circuit between gas flow rate control valve and the exit at the stopper rod tip. This point has a critical influence over mould level stability, castability and extent of clogging due to steel reoxidation because of the air infiltration into the steel pouring line. The lower the flow rate the bigger the importance of this air-tight condition.
- Taking into account the effect of the stopper rod back-pressure on the mould level stability, it was found that the optimum nozzle immersion depth at the billet caster of Basauri plant was 115 mm instead of 105 mm. By means of this change, vacuum levels within the nozzle are lower and hence the risk of having a deterioration of the mould level stability is significantly lower. Due to that result, nowadays a nozzle immersion depth of 115 mm has been settled as standard practice at the billet caster of Basauri Plant. This decision was made after checking that there were no collateral problems either concerning meniscus lower temperature or mould powder performance when using 115 mm instead of 105 mm.
- Concerning the new techniques or signals able to give helpful information for the process control and optimisation:

- The nozzle thermal characterisation using thermocouples is a suitable method for the on-line assessment of the clogging extent at the nozzle inner body. This is only recommended on a trial basis because of the complexity of the thermocouples installation method.
- As explained previously, the gas injection back-pressure signal is suitable for the on-line assessment of the clogging at the nozzle exit. Once determined empirically the equation between stopper back-pressure variation (vacuum level) and nozzle outlet restriction due to clogging, may also be incorporated as a process control signal for the on-line assessment of the nozzle outlet restriction during casting.

## **MEFOS**

As previous mentioned, no application and testing of optimisation criteria may be reported from MEFOS.

### **Task 6.4 - Compare and contrast different measurement techniques**

In order to compare and contrast the different measurement techniques first we need to be clear what the different techniques are capable of, what their limitations are and how they interact with normal operation of a casting plant.

#### **Electromagnetic Steel Flow Visualisation sensor**

This sensor is a self contained non-contact device which gives a clear view of the overall flow pattern in the SEN. Although data is displayed in real time during casting the results are perhaps more meaningful when viewed in their entirety post cast. In order to interpret the results it is often necessary to combine the output with other plant data. It is unlikely that the sensor would be of significant benefit in day to day operation due to its complexity but is a useful diagnostic tool. The sensor has only been tested on slab casters but there is no reason why it could not be easily transferred to other types of caster.

It may be possible to develop a model which would predict the equivalent of the SFV signal from standard plant data using statistical methods but that would require huge effort. In that case the SFV sensor would be useful for calibration.

#### **Electromagnetic SEN flow velocity sensor.**

The SEN flow sensor again is a self contained non-contact device. Although the device was not successfully developed the potential was clear. Without a working prototype however it is difficult to say how useful the application of this tool would be.

#### **Nozzle Ultrasonic sensor.**

The on-line ultrasonic inclusion length index prediction shows good agreement with the product quality in terms of inclusion length. Extensive plant trials revealed the complexity of the application of the new measurement system to the production caster. The usage of the present system on a regular basis for all six strands seems not to be possible for the normal production team. However, on a measurement trial campaign basis the new ultrasonic measurement system is useful for a deeper look into the casting process especially for the verification of the effects of future alterations and optimisation.

#### **Nozzle Inner Pressure method**

The nozzle inner pressure technique is a clear and easy extension of existing plant technology. The facility to inject gas through the stopper is already in place on the majority of casting machines of all varieties and could be easily adapted to provide this output. The only potential drawback of this technique is the requirement for a gas-tight stopper gas injection system. This may require special stoppers etc. However, there is a secondary benefit that a gas-tight system would prevent air entrainment in the gas injection surface and reduce potential castability issues.

### **Nozzle Refractory Temperature method**

The use of thermocouples installed in the nozzle wall as a method for the on-line assessment of the extent of clogging at the nozzle inner body has been proven to be effective. This technique requires significant effort to prepare the SEN and as such is more appropriate for use on a trial basis. It would be impractical as a standard practice unless the SEN could be manufactured with the thermocouple already embedded. However the cost of such a nozzle will be high and would require justification.

### **Karmen Vortex Mould Surface velocity sensor**

The Karmen Vortex sensor gives good, clear, believable results concerning mould surface flow velocities. However, it is cumbersome time consuming and invasive when in use. The results are limited to 10 minute periods and there is no indication concerning direction of flow. The sensor probes are also expensive, labour intensive to refurbish and delicate. On the other hand the system is portable and can easily be adapted for use in almost any environment.

Other techniques have become available using similar disposable probes which would be also worth considering as an alternative to the Karmen vortex probe. A sensor based on measuring the angle of a freely moving probe has been shown to give both velocity and direction but it still has most of the other disadvantages.

### **Electromagnetic Meniscus Velocity sensor**

The meniscus velocity sensor again is a self contained non-contact device. The fitting of a device to detect flow velocity and direction in the mould could be combined with the standard mould level detector. Although the device was not successfully developed the potential was clear. Without a working prototype however it is difficult to say how useful the application of this tool would be.

### **Discussion**

The majority of techniques discussed show most potential for measurements designed on a campaign or trial basis. There is a clear use for the nozzle pressure technique in terms of process control and relatively small investment cost involved. This is probably the most generally useful and easily transferable technology. It should be mentioned that the results coming from the pressure trials have also been corroborated by the trials using thermocouples for the nozzle thermal pattern characterisation.

The ultrasonic technique is the only technique which provides a clear indication of product quality and could be directly used for product grading, and for tracking quality critical product for high grade application. It should be noted that the technique was developed for use on a caster which does not employ argon gas in the SEN. There are disadvantages in that it is quite invasive in terms of plant operation and requires significant effort to prepare.

The electromagnetic SFV sensor does provide a potential control signal for the SEN flow condition especially if it were decided to actively control the SEN to its "full" condition but there is a need to balance cost against benefit. If a calculated parameter could be used developed from trials using this technique perhaps it is worth considering although the development of such would be a large undertaking in itself.

The remaining techniques are useful diagnostic tools which are each useful in targeted specific requirements on a trial basis but it is unlikely that a permanent plant installation would be considered either in terms of cost or reliance as an ongoing plant control device.

## **Work Package 7 - Project Management, Meetings and Coordination**

The objective of this work package was to coordinate the project. This included coordination of project work, organisation and attendance of meetings and the production of reports.

### **Task 7.1 - Project management, coordination and reporting (All partners)**

During the course of the project, coordination meetings involving all partners were held each semester as planned. The meetings were held at the bases of operation of the partners in rotation. The meetings

were used to discuss the progress of the project and to agree the forward plan for each semester. In total six co-ordinating meetings were held.

Between meetings, contact between partners was maintained via regular electronic mail, telephone and other correspondence

#### 4. CONCLUSIONS

Detailed conclusions have been summarised mainly in the reporting of Work Package 6. However in this section a summary of the key conclusions will be given.

1. As a result of measurement trials recommendations have been made to improve steel surface and internal quality.
  - To maintain "ideal" SEN flow pattern on Corus Scunthorpe slab caster, stopper gas pressure should be maintained below -0.15 bar.
  - Surface defects on Corus Scunthorpe slab caster appear to be linked with active level control. Consideration should be given to alternative method of spreading SEN wear.
  - Recommendations for optimisation of the casting parameters and conditions for the billet caster of Basauri Plant are applicable for any caster these include:
    - Air-tight quality of the stopper gas injection circuit.
    - Optimum nozzle immersion depth.
    - Use of the stopper-gas back-pressure for on-line assessment of clogging at the nozzle exit.
    - Use of thermocouples as a method for the on-line assessment of the extent of clogging at the nozzle inner body.
2. The correlation of measured quantities within the tundish nozzle using the SFV sensor and in the casting mould with existing product grading schemes has been unsuccessful. The BFI/Saarstahl ultrasonic technique could be used to track product internal quality in terms of inclusions.
3. An ultrasonic on-line measurement system was developed and tested for monitoring the product quality in terms of cleanliness immediate during continuous casting. Based on the PLS-algorithm developed in Task 3.4 a new process model for on-line prediction of product quality was developed.
4. Measurement of the degradation of flow patterns with time has been studied.
  - The degree of clogging is directly related to the total casting time.
  - The SFV sensor can only indicate that there is significant clogging when combined with other process parameters.
  - The stopper back pressure method developed at Sidenor can detect clogging and wear in the SEN and could be used as an indicator.
5. New sensor developments were successfully completed, commissioned and used in experimental trials:
  - Multiple frequency electromagnetic Steel Flow Visualisation sensor.
  - Nozzle Ultrasonic sensor including remote data acquisition system which allows trials to be monitored from a different site.
  - Nozzle inner pressure method.
  - Nozzle refractory temperature method which allow up to 4 thermocouples to be embedded in the SEN.

New sensor developments were attempted but led to limited success:

- Electromagnetic SEN flow velocity sensor. Partial success but no plant results
- Meniscus velocity sensor.

6. A low temperature liquid metal model has been designed, manufactured and used.

## **5. EXPLOITATION AND IMPACT OF THE RESULTS**

*Actual applications:*

The majority of techniques applied during this project show most potential if applied on a trial campaign basis as tools to characterise and optimise plant performance.

The SFV and Karmen Vortex sensors have been used to assist in a process audit carried out on a Corus caster to assess the current status.

The ultrasonic technique has been used on campaign basis at one strand at Saarstahl.

The following recommended practices have been already standardised at the CCM2 of Basauri Plant:

- Optimised stopper rods and gas injection circuit.
- The nozzle immersion depth at the Basauri billet caster was increased from 105 mm to 115 mm.
- On-line assessment of the clogging at the nozzle exit has been incorporated as a process control signal.

## **6. TECHNICAL AND ECONOMIC POTENTIAL FOR THE USE OF THE RESULTS**

Clogging problems due to steel reoxidation between tundish and mould are a key point for fulfilling the most demanding steel applications. Otherwise, problems related to macro-inclusions can arise during client's operations or during final user utilisation with subsequent problems even in terms of personal safety for the most demanding applications. Also financial claims coming from final users have to be avoided.

On the other hand, as-cast surface quality is a critical point for the optimisation of the process yield, better conservation of resources, reduced use of process energy, and an improvement in overall lead time for delivery of finished product to the customer. Metallic losses due to rejections, coupled with the energy costs of the rectification and environmental aspects are critical. Poor surface quality on semi-finished products leads to a poor quality in the final rolled product, and when rectification is not an answer, only scrapping of the product will suffice. Under these circumstances the added value of the downstream processing is also lost. Moreover, in steel plants where direct charging is practised, the operators must have confidence that the surface quality of the semi is 'fit for purpose' as generally there is no opportunity to rectify the downstream product. An increase in hot charging capability will deliver energy savings and improve productivity.

Therefore, both aspects, cleanliness and surface quality, are key points for the steelmaker as part of global process optimisation, process sustainability and competitiveness. Nowadays, increasing competitiveness forces steel producers all around the world to meet continuously growing higher product quality standards.

During the project various techniques have been developed and tested. The majority of these techniques are more suited to use on a trial or campaign basis rather than an on-line constant measurement.

The on-line ultrasonic measurement device can be used on campaign basis for monitoring the stability of the casting process. Principally, it is possible to use the technique at other steelworks if the

calibration is adapted to the new casting machine. The ultrasonic technique is the only technique which provides a clear indication of product quality and could be directly used for on-line quality assessment with the associated benefits in terms of rejection and rework as the current cleanliness quality checks are time consuming and often take several weeks to receive the results. In the frame of future research the results of this project will be used to develop the on-line ultrasonic measurement technique for regular use at the continuous caster. Therefore, the potential of new contactless measurement techniques can be used in the future.

It has been demonstrated that it is preferable for the SEN to run "full" and that this condition is strongly linked to stopper gas pressure. The electromagnetic SFV sensor does provide a potential control signal for the SEN flow condition especially if it were decided to actively control the SEN to its "full" condition but there is a need to balance cost against benefit. Currently this is one of the techniques suitable for use on a trial basis but for use as a control either a permanent system would need to be developed or the feasibility of developing a calculated parameter examined. A calculated parameter to predict flow pattern would be a large undertaking.

There is a clear use for the nozzle pressure technique in terms of process control and relatively small investment cost involved. This is probably the most generally useful and easily transferable technology. It should be mentioned that the results coming from the pressure trials have also been corroborated by the trials using thermocouples during the nozzle thermal pattern characterisation.

The outcome of the research carried out by Sidenor in terms of conclusions related to the optimisation of casting parameters and facilities is potentially suitable for application for any billet caster. There are clear quality, and thus cost, benefits from improving air-tightness of the gas injection circuit through the stopper because of its influence on clogging-castability and mould level stability. Optimisation of nozzle immersion depth was shown to improve nozzle inner pressure stability and this was linked to mould stability. Since mould level stability has a big influence on as-cast surface quality, it could be stated that these recommendations are clearly related to the as-cast product quality as far as cleanliness and surface quality is concerned. Unfortunately it is very difficult to quantify the improvement of the semis quality derived from the guidelines defined as a result of this research.

There is potential to optimise the sequence length associated with an SEN by use of the stopper-gas injection back-pressure signal for the on-line assessment of the clogging at the nozzle exit. By monitoring the exit port size there may be potential for increasing sequence length which has obvious cost benefits.

The remaining techniques are useful diagnostic tools which are each useful in targeted specific requirements on a trial basis but it is unlikely that a permanent plant installation would be considered either in terms of cost or reliability as an ongoing plant control device.

## **7. PATENT FILING**

The supplier of the single frequency electromagnetic SFV sensor (MPC AB) holds a patent for the technology which predates the project. Corus has an agreement allowing use and development of the system.

No patents have been derived from the research in the case of Sidenor, BFI, Saarstahl and MEFOS.

## **8. PUBLICATIONS / CONFERENCE PRESENTATIONS RESULTING FROM THE PROJECT**

5<sup>th</sup> European Continuous Casting Conference, Nice, France. June 2005:

Visualisation of Steel Flow in the Continuous Casting Nozzle using an Electromagnetic Technique. S R Higson, P Drake (Corus R, D & T, UK), A Lyons (MPC AB, Sweden), A Peyton, B Lionheart (University of Manchester, UK)

2nd International Workshop on Measuring Techniques for Liquid Metal Flows, Dresden, Germany. April 2007:

An electromagnetic technique to measure steel flow patterns within the continuous casting nozzle. S R Higson, P Drake (Corus R, D & T, UK), A Lyons (MPC AB, Sweden), A Peyton (University of Manchester, UK)

Sensors for non-contact velocity measurements for continuous casting of steel. U Sjöström (MEFOS, Sweden)

5th World Congress on Industrial Process Tomography, Bergen, Norway. September 2007:

Developments of multiple frequency electromagnetic induction system for steel flow visualization. X Ma, A J Peyton (University of Manchester, UK), S R Higson, P Drake (Corus R, D & T, UK).

SMEA conference, Sheffield June 2007: Electromagnetic Visualisation of Steel Flow in Nozzles during Continuous Casting

A Peyton (University of Manchester, UK), S R Higson (Corus R, D & T, UK), A Lyons (AGELLIS Group AB Sweden)

No publications were made by Saarstahl, BFI Sidenor.

## 9. REFERENCES

1. Higson et al: 'Improvement in cast product quality by the visualisation and control of the steel flow pattern in the tundish pouring nozzle (SEN/SES)', ECSC Contract Number 7215.PP/045
2. Normanton et al: 'The detection and measurement of asymmetric flow in the mould and the assessment of its effect on product quality of continuously cast slabs', Final report ECSC Project 7210.PR/142
3. Yogeshwar el al: 'Criteria for water modelling of melt flow and inclusion removal in continuous casting tundishes', ISIJ International, vol. 36 (1996), No. 9, pp1166-117

## 10. LIST OF FIGURES AND TABLES

### *Figures*

- 1a New multi-frequency electromagnetic steel flow visualisation sensor (Corus)
- 1b New multi-frequency electromagnetic SFV sensor user interface screen (Corus)
- 2 Graphs showing sensor response to titanium bars for real and imaginary voltage (Corus)
- 3 Output from the new electromagnetic sensor during pilot plant trial (Corus)
- 4 New sensor support bracket (Corus)
- 5 Working principle of ultrasonic sensor system (BFI)
- 6 Numerical model trial of the new automated ultrasonic sensor system (BFI)
- 7a Sensor holder before tundish preheating (Saarstahl)
- 7b Measurement device during operation (BFI/Saarstahl)
- 8 Location of the pressure measuring points (Sidenor)
- 9 Pressure at the stopper rod tip. Back-pressure measuring procedure (Sidenor)
- 10 Pressure at the nozzle inner wall. Standard and experimental SES nozzle with a small hole (diameter: 2 mm) in the lateral wall for pressure measurements (Sidenor)
- 11 Nozzle inner pressure tests devices (Sidenor)
- 12 Experimental pin-bolt stopper for improved gas tightness (Sidenor)
- 13 Thermocouple location at the nozzle wall for the trials with two thermocouples (Sidenor)
- 14 New fixing method to guarantee a good contact between the thermocouples and the refractory nozzle body (Sidenor)
- 15 Theory of the electromagnetic sensors exemplified by a schematic description of the meniscus velocity sensor (MEFOS)
- 16 Calibration rig set up for calibration of the meniscus velocity sensor with a rotating disc of MCP-137 (MEFOS)
- 17 Difference in signal response between a rotating aluminium disc and a rotating disc of alloy MCP-137 (MEFOS)

- 18 Calibration of meniscus velocity sensor using a rotating plate of alloy MCP-137 in the calibration rig at MEFOS (MEFOS)
- 19a and 19b Original and enhanced meniscus velocity sensors (MEFOS)
- 20 Possible layouts of the ultrasonic sensor system (Saarstahl)
- 21 Data acquisition system (Saarstahl)
- 22 Physical model during construction (MEFOS)
- 23 Physical model. (MEFOS)
- 24a and 24b The inspection window of the casting nozzle without (8a) and with (8b) flowing water (MEFOS)
- 25 Volume flow rate of water in the model as a function of pump velocity (MEFOS)
- 26 Volume flow rate of the liquid alloy, MCP-137, in the model as a function of pump velocity (MEFOS)
- 27 Casting speed of the liquid alloy in the model as a function of pump velocity (MEFOS)
- 28 Schematic illustration of the manufactured stopper rod with the weak welding points marked as A and B (MEFOS)
- 29 Measured signal output from the CLV sensor as a function of the frequency at the casting speed of 0.8 m/min. (MEFOS)
- 30 The frequency of the maximum peak, as a function of casting speed, at the corrected signal from the flow with background noise excluded (MEFOS)
- 31 Calibration of SEN flow sensor in the calibration rig (MEFOS)
- 32 Calibration of SEN flow sensor (MEFOS)
- 33 Placement of the different sensors in the physical model (MEFOS)
- 34 Signal output from the meniscus velocity sensor and casting speed as a function of time (MEFOS)
- 35 Output signal of SEN flow sensor as a function of casting speed for three different sequences (MEFOS)
- 36 Output signal of SEN flow sensor, including standard deviation for measured values as a function of metal flow rate (MEFOS)
- 37 Calculated velocity in casting nozzle compared with the output signal of SEN flow sensor as a function of metal flow rate (MEFOS)
- 38a and 38b Mechanical arm with meniscus velocity sensor and SEN flow (MEFOS)
- 39 Calibration of the level sensor used together with the meniscus velocity sensor in the mould (MEFOS)
- 40 Signal of the meniscus velocity sensor (MEFOS)
- 41a and 41b Casting powder on the house of the meniscus velocity sensor (MEFOS)
- 42 Example of plate mill defect map against SFV measurements (Corus)
- 43 Example of plate mill defect map against SFV measurements (Corus)
- 44 Plate mill defect map against SFV measurements, stopper and mould level (Corus)
- 45 Cleanliness of the semi finished product according to ultrasonic immersion inspection technique for forty-five heats of the same steel grade as sequences 4 and 8 (Saarstahl)
- 46 Position of the inclusion in the ternary system CaO - MgO - Al<sub>2</sub>O<sub>3</sub> in the liquid steel at the end of ladle treatment (Saarstahl)
- 47 Position of the inclusion in the ternary system CaO - MgO - Al<sub>2</sub>O<sub>3</sub> in the finished product (Saarstahl)
- 48 Pressure trial with stopper rod back-pressure measurement. Good air-tight condition. Sequence 31350-31351. Strand #1 (Sidenor)
- 49 Influence of the stopper rod gas flow rate on the stopper rod gas feeding back-pressure. Sequence 31610-31611-31612-31613. Strand #6 (Sidenor)
- 50 Example of trial using two thermocouples for the nozzle thermal characterisation. Difference between both thermocouples in terms of temperature increase slope just after cast beginning (Sidenor)
- 51 Example of trial using thermocouples for the nozzle thermal characterisation. Frequent loss of parallelism between the temperature of both thermocouples (Sidenor)
- 52 Effect of gas circuit disconnection on mould level stability (Sidenor)
- 53 Effect of gas circuit disconnection on mould level stability (Sidenor)
- 54 Theory about "steel level" within the nozzle (Sidenor)
- 55 Simple static water model (BFI)

- 56 Inclusion detection in water model trial (BFI)
- 57 Principal of partial least squares (PLS) algorithm (BFI)
- 58 Example of Scunthorpe slab grading screen (Corus)
- 59 Plot of grading events relative to SFV sensor output. (Corus)
- 60 Comparison of on-line ultrasonic inclusion length prediction with inclusion length measured by blue brittle test and measured by ultrasonic immersion technique for campaign no. 10 (BFI/Saarstahl)
- 61 Correlation of on-line ultrasonic inclusion length index prediction as measured during casting with inclusion length index as measured by ultrasonic immersion technique at the semi-finished product (BFI)
- 62 Clogging observed at the SEN: left: no clogging after casting of sequence no 7, right: light clogging after casting a sequence at which no measurement results could be received (BFI)
- 63 Example of abnormal mould level performance when having very low pressure level within the nozzle (Sidenor)
- 64 Example of slightly worse mould level performance when having a 'Partly full nozzle' (Sidenor)
- 65 Example of lower thermal flux at the top of the mould when having a 'Partly full nozzle' (Sidenor)
- 66 Example of lower mould thermal flux when having a 'Partly full nozzle' (Sidenor)
- 67 Correlation between the nozzle steel flow conditions and the mould thermal behaviour (Sidenor)
- 68 Example of higher mould thermocouples variability when having a high variability in the steel jet position (Sidenor)
- 69 Example of sensor output change at ladle change (Corus)
- 70 Interpretation of SFV sensor signal (Corus)
- 71 Example of flow transition when stopper gas pressure  $< -0.15$  bar (Corus)
- 72a Output from sensor and stopper gas pressure during trial 13 (Corus)
- 72b Output from sensor and stopper gas flow rate during trial 13 (Corus)
- 73 Output from sensor and stopper gas pressure during trial 13 (Corus)
- 74 Output from sensor and tundish stopper position during trial 1 (Corus)
- 75 Output from sensor and tundish stopper position during trial 21 (Corus)
- 76 Output from sensor and stopper position during trial 18 (Corus)
- 77 Example of output from new multiple frequency electromagnetic sensor (Corus)
- 78a Multi-frequency SFV sensor raw data (Corus)
- 78b Multi-frequency SFV sensor normalised data (Corus)
- 79 Interpretation of the multiple frequency sensor (Corus)
- 80a Graph showing Sensor 2 output and difference between sensor 1 and sensor 3 (Corus)
- 80b Graph showing Sensor 2 output and mould symmetry (Corus)
- 81 Output from sensor and stopper gas pressure during trial 8 (Corus)
- 82 Output from sensor and MTM mould symmetry during trial 8 (Corus)
- 83 Output from sensor and MTM mould symmetry during trial 2 (Corus)
- 84 Output from sensor and MTM mould symmetry during trial 9 (Corus)
- 85 Example of Karmen Vortex flow measurement (Corus)
- 86 Example of Karmen Vortex mould flow velocity measurements (Corus)
- 87 Example of relationship between stopper rod back-pressure and clogging at nozzle exit. Strand #6 had a good air-tight condition meanwhile in Strand #1 air-tight condition failed. Sequence 33060-33061 (Sidenor)
- 88 Comparison in terms of nozzle clogging extent between strand #1 and strand #6 based on the air-tight condition of the stopper rod gas feeding circuit. Strand #1 had a good air-tight condition meanwhile in Strand #6 air-tight condition failed (Sidenor)
- 89 Example of trial using thermocouples for the nozzle thermal characterisation. Almost non-existent clogging at nozzle body (Sidenor)
- 90 Example of trial using two thermocouples for the nozzle thermal characterisation. Clogging problems at nozzle body (Sidenor)
- 91 Relationship between stopper back-pressure (vacuum level) and nozzle outlet restriction due to clogging phenomenon (Sidenor)

92	SEN dimensions after use (Corus)
93	Plot of casting time verses degree of SEN exit port clogging (Corus)
94	SEN from trial 17 with 71% reduction in exit port size (Corus)
95a	Trial 24 sensor output and stopper position (Corus)
95b	Trial 24 sensor output and stopper position (Corus)
96	Effect of spontaneous sudden change of the air-tight condition of the gas injection circuit on the mould level stability (Sidenor)
97	Trial using 115 mm of nozzle immersion depth instead of 105 mm. Stopper back-pressure is $\geq -0.40$ bar (Sidenor)
98	Calculation of Lorentz force as a function of distance at a constant steel velocity at 0.3 m/s (MEFOS)
99a	Output from sensor and stopper gas pressure during trial 23 (Corus)
99b	Output from sensor and stopper gas flow rate during trial 23 (Corus)
100a	Output from sensor and stopper position during trial 23 (Corus)
100b	Output from sensor and mould level during trial 23 (Corus)

*Tables*

1	Electrical conductivity (MEFOS)
2	Summary of Corus trials (Corus)
3	Ultrasonic system - production plant hot metal trials (BFI/Saarstahl)
4	Defects Identified (Corus)
5	Frequency of defects relative to cast length (Corus)
6	Karmen Vortex mould surface velocity measurements taken at Corus (Corus)
7	Summary of model parameter 'maximum likelihood' estimates (Corus)
8	Odds ratio estimates (Corus)
9	Dimensions of used SENs (Corus)
10	Port sizes after casting. Degree of clogging (Corus)
11	Variation in measured mould surface velocity (Corus)

European Commission

**EUR 24205 — Flowvis: measurement, prediction and control of steel flows in the casting nozzle and mould**

*S. R. Higson, P. Drake, M. Lewus, T. Lamp, H. Köchner, P. Valentin, C. Bruch, J. Ciriza, J. J. Lauraudogoitia, J. Björkvall, L. Bergman*

Luxembourg: Publications Office of the European Union

2010 — 102 pp. — 21 × 29.7 cm

Research Fund for Coal and Steel series

ISBN 978-92-79-14429-5

doi:10.2777/85987

ISSN 1018-5593

Price (excluding VAT) in Luxembourg: EUR 7